QUANTUM RANDOMNESS AND QUANTUM MEASUREMENT IN A UNITARY SETTING

ÓSCAR EDUARDO RODRÍGUEZ VILLALBA

UNIVERSIDAD NACIONAL DE COLOMBIA
FACULTAD DE CIENCIAS
DEPARTAMENTO DE FÍSICA
BOGOTÁ, D.C.
2023

QUANTUM RANDOMNESS AND QUANTUM MEASUREMENT IN A UNITARY SETTING

ÓSCAR EDUARDO RODRÍGUEZ VILLALBA

submitted for the degree of doctor of philosophy
Doctorado en Ciencias - Física

Advisor
PROF. DR. THOMAS DITTRICH

Research group
caos y complejidad

UNIVERSIDAD NACIONAL DE COLOMBIA
FACULTAD DE CIENCIAS
DEPARTAMENTO DE FÍSICA
BOGOTÁ, D.C.
2023

Title in English

Quantum randomness and quantum measurement in a unitary setting

Título en español

Aletoriedad cuántica y medición cuántica desde un enfoque unitario

Abstract: In this thesis a novel approach towards quantum measurement and quantum randomness, within the framework of unitary time evolution, is proposed. Spin measurements are simulated by coupling the spin to an environment modeled as a heat bath comprising a finite number of boson modes with initial states represented in terms of coherent states. The time evolution of the entire system is achieved by means of the multi-Davydov ansatz. In order to simulate measurements with equally likely outcomes, the spin is prepared in a neutral polarized state prior the measurement. The uncontrollable nature of the environment is captured in its initial state by preparing each mode in a coherent state sampled from a random distribution. An environment that does not introduce a deliberate bias is set by centering the random distribution in the origin of the phase space. Before considering unbiased measurements, the most appropriate parameters of the model are identified by means of simulations with intermediate initial conditions between the ground state and thermal states compatible with the time evolution method. Different measurement protocols are modeled by turning on and off the self-energy of the spin and the coupling with the environment with time-dependent modulations. The outcome of the measurement is assessed by the long-term behavior of the spin. Due to its interaction with the environment, the spin gets entangled with it losing its coherence, thus reproducing the "first state vector collapse". Quantum randomness is observed as the tendency of the final state to approach either one of two possible eigenstates of the spin measured operator, recovering an almost pure state. The entire process is characterized by the exchange of energy and entropy between the spin and the environment. It leads to the observation of a prominent role of low-frequency modes in the long-term behavior of the spin. The measurement process is also analyzed from the information theory perspective. The information dynamics during the entire process is followed using the partial entropy of the spin. A round trip of the spin state from a pure state through a mixed state back to a final state close to a pure state is identified. With this approach the entire measurement process is reproduced in an approximate way.

Resumen: En esta tesis se propone un enfoque novedoso hacia la medición cuántica y la aleatoriedad cuántica, en el marco de la evolución temporal unitaria. Las mediciones de espín se simulan acoplando el espín a un entorno modelado como un baño de calor que comprende un número finito de modos bosónicos con estados iniciales representados en términos de estados coherentes. La evolución temporal de todo el sistema se logra mediante el multi-Davydov ansatz. Para simular mediciones con resultados igualmente probables, el espín se prepara en un estado polarizado neutral antes de la medición. La naturaleza incontrolable del entorno se captura en su estado inicial al preparar cada modo en un estado coherente muestreado a partir de una distribución aleatoria. Un entorno que no introduce un sesgo deliberado se establece centrando la distribución aleatoria en el origen del espacio de fase. Antes de considerar medidas no sesgadas, se identifican los parámetros más apropiados del modelo mediante simulaciones con condiciones iniciales intermedias entre el estado fundamental y los estados térmicos compatibles con el

método de evolución temporal. Se modelan diferentes protocolos de medición activando y desactivando la autoenergía del espín y el acoplamiento con el entorno con modulaciones dependientes del tiempo. El resultado de la medición se evalúa por el comportamiento a largo plazo del espín. Debido a su interacción con el entorno, el espín se enreda con él perdiendo su coherencia, reproduciendo así el "primer colapso del vector de estado". La aleatoriedad cuántica se observa como la tendencia del estado final a acercarse a uno de los dos posibles estados propios del operador medido de espín, recuperando un estado casi puro. Todo el proceso se caracteriza por el intercambio de energía y entropía entre el espín y el entorno. Esto conduce a la observación de un papel destacado de los modos de baja frecuencia en el comportamiento a largo plazo del espín. El proceso de medición también se analiza desde la perspectiva de la teoría de la información. Se sigue la dinámica de la información durante todo el proceso utilizando la entropía parcial del espín. Se identifica un viaje de ida y vuelta del estado de espín desde un estado puro a través de un estado mixto hasta un estado final cercano a un estado puro. Con este enfoque, todo el proceso de medición se reproduce de forma aproximada.

Keywords: Randomness, quantum measurement, unitary time-evolution, spin-boson model

Palabras clave: Aleatoriedad, medición cuántica, evolución temporal unitaria, sistema espín-bosón

A mis padres, Lucila y Luis: porque en la dinámica de mi vida siempre me han brindado las mejores condiciones iniciales

Acknowledgments

This work highlights the role of the environment in the development of a single system and how depending on multiple interactions a definite result is reached. It is difficult to resist the temptation of drawing a connection with the process leading to the completion of this work in order to acknowledge the many interactions that have guided me through this path that has come to an end. Being immersed in pursuing a PhD involves an intricate and complex interplay with many people where it is difficult to give the right place to each interaction when pondering them. Even a "small" interaction at the appropriate moment can have a huge impact on the fate of the system and, considering the analogy, in my life. Nevertheless, in these few lines I can only mention those interactions that were more vivid and present during this phase in my life.

In first place I would like to thank Prof. Thomas for the guidance he has provided me during the years I have been part of the group Caos y Complejidad. Not only when navigating the beautiful and chaotic sea of physics explored by the group but also with the subtleties of the academic career. I have enjoyed learning from you about physics but also about your point of view of the world. I am also grateful for your support when my studies were at stake. My transit in the university was not easy from the beginning but you were there offering your help to find a solution. Finally, I thank you for the invitation to be part of this project as a PhD student. I really appreciate the opportunity of doing research in this kind of topic that I find intriguing and exciting, which I am passionate about.

For me it was clear I wanted to be part of the group Caos y Complejidad since I enrolled in my graduate studies but finding such an encouraging and supporting environment was a fortune. I thank all my friends and colleagues of the group. The time I spent with you discussing physics and the many facets of life drinking a couple of beers and/or a bottle of wine is invaluable. I thank Prof. Carlos Viviescas for the many clarifying discussions and the challenging questions posed by you during the groups seminars where you have taken the time to participate, keeping the space alive.

Different interactions could lead you to a position you never imagined. For me that meant traveling and getting to know people far away from my usual environment. I would like to thank the hospitality the TU Dresden extended to me during my stay. I thank Prof. Frank Grossmann for kindly sharing with me his expertise with coherent states and the time evolution of many-body systems. I also thank his former students, Michael Werther and Sreeja Loho Choudhury, for many inspiring discussions and for teaching me about the multi-Davydov ansatz method, without this powerful method the present work had not be done. I am grateful to Prof. Walter Strunz and his students of the theoretical quantum optics group, in particular, Konstantin Beyer, for sharing their arguments and concerns

about this project. Have had the opportunity of presenting the ideas behind this project in the group seminar have definitively enriched them and changed them when was necessary.

There are interactions that, once they were established, remain during time providing permanent and valuable feedback in any moment of time. I thank my friends Cubos, Freedy, Jeicot and Laura for being part of many moments in my life (in particular, this one) and for allowing me to share so much fun with you. I have learned a lot from you that makes me a better person and I apologize (for the past and in advance) for the direct and sparing way I express myself and for teasing you (I will keep doing it anyway). Even at the distance you are at this moment, Jeicot, knowing that I can rely on your advice with academic as well as personal affairs is encouraging. It makes me think of the quantum nature of friendship: once correlations are established, they persist even over long distances. A big part of this work was done during the lockdown due to the COVID pandemic. A situation that was easier to cope with thanks to your company, Laura.

Sometimes two systems are close but never interact directly. It seems that this happens only at the right moment and place. It started weakly but it has rapidly grown to establish a new bond. This unexpected interaction has completely widened my view of the world, making it brighter and more colorful. It also has made me reflect about myself and has moved me from lethargy in some respects in my life, giving me courage to explore this new landscape. Thank you, Farly, for being part of this process. Your friendship is a treasure I did not expect to find along this path.

Some interactions have been always present, guiding me in every moment in my life. In any endeavor I have tackled you have always given me your support and trust. Taking care of me in the first steps but giving me the freedom to choose my own path and encouraging me to follow it. Inspiring me with your tenacity of keeping going forward despite the adversities and showing me with your example how to stand up again when life takes you down. Showing me what really matters in order to construct a significant life. For always providing me with the best initial conditions for pursuing what really fills my heart and nurtures my soul I thank my mom, Lucila, my father, Luis and my brother, Javier. I apologize for not being there at many important moments. The way I found to do this PhD absorbed me in many ways and made me pause many facets in my life. A brighter person could find a more balanced way of doing it, I could not.

For all those uncountable and invaluable interactions that have affected my life, leading me to this point, thank you.

Contents

Contents **II**

List of Figures **IV**

Introduction **IX**

1. Measurement and randomness in quantum mechanics **1**

1.1 The measurement postulate 2

1.2 Measurement as a process in time 4

1.2.1 Interaction between object and meter 4

1.2.2 Partial trace 6

1.2.3 Environment-induced superselection 6

1.3 The EPR experiment 9

1.4 Stern–Gerlach experiment 10

1.5 Quantum randomness 11

2. Dynamics of a system coupled to an environment **15**

2.1 Two different routes 16

2.1.1 Statistical approach 17

2.1.2 Unitary approach 19

2.2 Feynmann-Vernon and Caldeira-Leggett models 21

2.3 Finite-bath models 23

2.4 Multi-Davydov ansatz 24

3. A model for spin measurements **27**

3.1 Constructing the model 27

3.2 Dynamics of the spin-boson model: from $N = 1$ to $N \to \infty$ 29

3.3 Parameters of the model 31

3.4 Symmetry properties 32
3.5 Initial states of the object and the environment 33
3.6 Initial superposition of states 35

4. Polarized initial conditions **37**
4.1 Thermal equilibrium and polarized initial conditions 37
4.2 Localization of the spin state 39
4.3 Reflected polarized initial conditions 41
4.4 Out-of-equilibrium initial conditions 42

5. Simulation of spin measurements **44**
5.1 Selecting unbiased initial states 45
5.2 Spin dynamics with unbiased initial states 48
5.2.1 Constant modulations 49
5.2.2 Time-dependent modulations 50
5.2.3 Final state of the environment 51
5.2.4 Energy dynamics 52
5.3 Redundant measurements 56
5.4 Linear superpositions of initial states 57

6. Information dynamics of spin measurements **60**
6.1 Quantification of the knowledge about a system 61
6.2 Information transfer in quantum measurement 62

A. D2-ansatz for the spin-boson model **66**

Conclusions **69**

List of Figures

1 Measurement as a black box. The initial state $|\psi_{\text{ini}}\rangle$ is transformed into the eigenstate $|s_k\rangle$ of the measured observable $\hat{S}$. The outcome is the corresponding eigenvalue s_k. Quantum mechanics tells us the possible outcomes of future measurements and the probability of obtaining them. It also indicates the final state after measurement. Nevertheless, how this occurs is not contemplated by the postulate. X

1.1 Spin measurement according to the decoherence program. The entire system composed of the object, the meter and the environment evolve unitarily. At the level of the object, its initial pure state becomes a mixed state due to the interaction with the meter. The environment preserves the correlations between both subsystems and defines clearly the pointer states in the measurement. How the object collapses onto one of the possible eigenstates of the measured observable (second state vector collapse), recovering a pure state, is not considered in this approach. 8

1.2 Random number sequences generated using spin measurements. It is believed that quantum phenomena constitute an improved source of random numbers since randomness in quantum mechanics seems to be an intrinsic property. 13

2.1 The time evolution of the central system can be obtained following two different routes. In the first route, the initial state of the central system is evolved to its final state at time t by means of a dynamical map. In the second route, the time evolution of the entire system is obtained first, then the state of the central system is extracted from this state via the partial trace. Adapted from [55]. 17

2.2 Spectral density function $J'(\omega') = J(\omega)/\omega_c$ with $\omega' = \omega/\omega_c$ and an exponential cutoff function. Depending on the value of the exponent s, the spectral density function emphasizes the low-frequency modes (subohmic) or the high-frequency modes (superohmic) with respect to the ohmic case. . 22

2.3 Approach to decoherence and dissipation in harmonic oscillator coupled linearly to a heat bath comprising a finite number of boson modes, for increasing mode number N. (a) Semilogarithmic plot of the purity of the reduced density operator for the central oscillator, as function of time. (b) Mean energy of the central oscillator vs. time. Color and symbol codes for $N = 0, 1, 10, 20, 50, 100, 500$ in the insets. Reproduced from [10]. 23

3.1 Simulation of spin measurements under well-defined symmetry conditions concerning parity $P_z : z \to -z$, Eq. (3.16). Panels show the time evolution of the components a_x (blue), a_y (green) and a_z (red), of the Bloch vector representing the state of the measured spin, prepared initially in the symmetric state $|\psi_{\rm O}(0)\rangle = |+_x\rangle \in \mathcal{H}_{+,{\rm O}}$, as function of scaled time $\omega_1 t$ under Hamiltonian (3.7) with a single boson mode, with particular initial states of the harmonic oscillator as follows: (a) ground state $|0_1\rangle$, (b) superposition of even Fock states $|2n_1\rangle$, $n_1 \in \mathbb{N}$ (element of the symmetric subspace $\mathcal{H}_{+,{\rm E}}$), (c) superposition of odd Fock states $|2n_1 + 1\rangle$ (element of the antisymmetric subspace $\mathcal{H}_{-,{\rm E}}$), (d) superposition of even and odd Fock states (no specific parity). Parameter values are $\omega_0/\omega_1 = 4$ and $g_1/\omega_0 = 2$. 33

4.1 Magnitude of the initial displacements (4.4) defined by the initial state (4.5) for ohmic and subohmic environments with 150 modes. Different values of the cutoff frequency, in (a) $\omega_c/\omega_0 = 10$ and in (b) $\omega_c/\omega_0 = 2$, do not change the magnitude of the displacements. 38

4.2 Time evolution of the Bloch vector with polarized initial conditions for the environment and a spin prepared initially in the state $|\psi_{\rm O}(0)\rangle = |+_x\rangle$ for (a) ohmic and (b) subohmic regimes. Time is scaled in terms of the cutoff frequency $\omega_c = 2\omega_0$. Localization of the a_z component is enhanced in the latter case. The number of modes was $N = 150$ and the multiplicity of the method was $M = 10$. Further parameters are $\alpha = 0.3$ and $s = 0.25$ for the subohmic environment. 39

4.3 Behavior of the a_z component for different values of (a) the cutoff frequency ω_c, (b) the exponent s and (c) the Kondo parameter α for a subohmic environment with polarized initial conditions. Further parameters as in Fig. 4.2. 40

4.4 Dynamics of the Bloch vector with reflected initial conditions 4.6. The parameter values are the same as used in Figure 4.2b. 41

4.5 Dynamics of the Bloch vector component a_z with out-of-equilibrium initial conditions for different values of μ. Localization is observed for all the values shown but the closest asymptotic corresponds to $\mu = 1$. Parameters of the simulation are $\alpha = 0.3$, $s = 0.25$, $\omega_c = 2\omega_0$, $N = 150$ and $M = 10$. 42

5.1 Examples of random ensembles of initial coherent states of the heath bath modes, distributed according to Eqs. (5.1) (panels a, b, c) and (5.5) (panels d, e, f). Blue dots mark the centroids of 150 coherent states in dimensionless phase space coordinates $\mathrm{Re}(\gamma) = \sqrt{m\omega/2\hbar}q$, $\mathrm{Im}(\gamma) = p/\sqrt{2\hbar m\omega}$. Parameter values are $k_B T = 0.2\hbar\omega_0$ and $\omega_c = 2\omega_0$. 45

5.2 Continuous probability functions for $\mathrm{Re}(\gamma_n)$ obtained by binning the phase-space region where the displacements, generated using Eqs. (5.1) and (5.5), are found. Displacements and probability density function values are normalized to facilitate the comparison. The number of samples used to produce the probability density in (a) was $N = 10000$. The logarithmic scale in the vertical axis of plot (b) demonstrates the quadratic dependence of the argument of the exponential function in the Gaussian distribution and the deviation of the probability density function corresponding to the displacements of the P-function from this behavior. 47

5.3 Simulations of measurements of the polarization of the spin, with unbiased initial state $|\psi_{\mathrm{O}}(0)\rangle = |+_x\rangle$ of the spin and random initial conditions of meter and environment Eq. (5.5), modeled by the Hamiltonian (3.6) with time-independent modulations $f_{\mathrm{O}}(t) = \text{const}$ and $f_{\mathrm{OE}}(t) = \text{const}$. Panels (a) to (f) show the three components $a_x(t)$ (blue), $a_y(t)$ (green), and $a_z(t)$ (red) of the Bloch vector vs. time for different specific initial conditions of the environment. Time scaled as $\omega_c t$, with the cutoff frequency ω_c of the environment spectrum, see Eq. (2.28). Parameter values are $N = 150$, $M = 10$, $\alpha = 0.3$, $k_{\mathrm{B}}T = 0.2\hbar\omega_0$, $\omega_c = 2\omega_0$. 49

5.4 Distribution of long-time asymptotes $a_z(t)$ for $t \gg 2\pi/\omega_c$, counting only those 41 simulations among a sample of 100 runs that converge to a stable long-time localized states. Parameter values as in Fig. 5.3. 50

5.5 Simulation of measurements of the polarization of the spin, with unbiased initial state $|\psi_{\mathrm{O}}(0)\rangle = |+_x\rangle$ of the spin and random initial conditions of meter and environment, Eq. (5.5), modelled by the Hamiltonian (3.6) with time-dependent modulations $f_{\mathrm{O}}(t)$ and $f_{\mathrm{OE}}(t)$ as shown Fig. cite. Panels (a) to (f) show the three components $a_x(t)$ (blue), $a_y(t)$ (green) and $a_z(t)$ (red) of the Bloch vector vs. time for different specific initial conditions of the environment. Time is scaled as $\omega_c t$. The number of boson modes is $N = 300$, the Kondo parameter α varies with $f_{\mathrm{OE}}(t)$, reaching a maximum of $\alpha = 2$. Other parameter values are as in Fig. 5.3. 51

5.6 (**a**) Modulating functions $f_{\mathrm{O}}(t)$ (blue) and $f_{\mathrm{OE}}(t)$ (red) underlying the simulations shown in Fig. 5.5. (b) distribution of long-time asymptotes $a_z(t)$ for $t \gg 2\pi\omega_c$, based on 100 simulations. Parameters values as in Fig. 5.5. . . 52

5.7 Amplitude $|C_{k\pm}|^2$ of the coefficients in the D2-ansatz, with multiplicity $M = 10$, for one simulation approaching the eigenstate $|+_z\rangle$, at the beginning (red) and at the end (black) of the simulation. In (a), the simulation was performed with constant modulations and in (b) with time-dependent modulations. Parameter values as in Fig. 5.3 and Fig. 5.5, respectively. . . . 53

5.8 Energy dynamics for one simulation with (a) constant and (b) time-dependent modulations. The interaction between the object and the environment leaves a register in the energy of the environment. While stabilization of the energy of each term is observed in the case of constant modulations, the end of the interaction in the time-dependent protocol leaves the environment with a higher energy. Because of the vanishing of the energy of the spin and the interaction, total energy is equal to the energy of the environment at the end of the process. Parameter values as in Fig. 5.3 and Fig. 5.5, respectively. 54

5.9 Energy density of the environment, Eq. (5.9), for constant (a) and time-dependent modulations (c), as function of the frequencies and time. The corresponding energy densities of the interaction, according to Eq. (5.10) are shown in panels (b) and (d), respectively. Time is scaled as $\omega_c t$ and frequencies as ω/ω_c. Color code ranges from positive (blue) to zero (white) to negative (red) values. Parameter values as in Fig. 5.3 for constant and as in Fig. 5.5 for time-dependent modulations. 55

5.10 Simulation of two subsequent measurements of the same observable $\hat{\sigma}_z$ of the spin, with unbiased initial state $|\psi_{\rm O}(0)\rangle = |+_x\rangle$ of the spin and random initial conditions of the environment, Eq. (5.5), for the first measurement. The protocol, see text, is implemented based on the Hamiltonian (3.6) with time-dependent modulations $f_{\rm O}(t)$ and $f_{\rm OE}(t)$. The state of the spin after the first measurement (full lines) is kept as entrances condition of the second measurement (dashed lines), the environment is initiated in a new random condition, see step 4 of the protocol. The figure shows the components of the Bloch vector (color code as in Fig. 5.3) vs. time for a first measurement resulting in the eigenstates $|+_z\rangle$ (panel a) and $|-_z\rangle$ (b). Light blue and grey lines indicate the modulation functions $f_{\rm O}(t)$ and $f_{\rm OE}(t)$, resp. Time is scaled as $\omega_c t$, parameter values are as in Fig. 5.5. 57

5.11 Simulations of measurements with the environment prepared in linear superpositions, (5.13), of pairs of initial states that converge to opposite outcomes, parameterized by a mixing angle ϕ. (a) Long-time averages $a_{z\infty}(\phi)$ of the polarization for discrete values $\phi_n = n\pi/12$, $n = 0, \ldots, 6$ (blue dots), compared to the fit (5.15) (red curve). (b) Probability density, Eq. (5.16) (red curve), corresponding to the fit (5.15), compared to the histogram (blue) of $a_{z\infty}$ show in Fig. (5.6) 59

6.1 Time evolution of the partial (blue) and the linear entropy (red) of the spin, with unbiased initial state $|\psi_{\rm O}(0)\rangle = |+_x\rangle$ of the spin and random initial conditions of the environment, Eq. (5.5), modeled by the Hamiltonian 3.6 with time-independent modulations. Time is scaled as $\omega_c t$, parameter values as in Fig. 5.3. 63

6.2 Time evolution of the partial (blue) and the linear entropy (red) of the spin, with unbiased initial state $|\psi_{\rm O}(0)\rangle = |+_x\rangle$ of the spin and random initial conditions of the environment, Eq. (5.5), modeled by the Hamiltonian 3.6 with time-dependent modulations. Time is scaled as $\omega_c t$, parameter values as in Fig. 5.5. 64

A.1 Structure of the square matrix M in Eq. (A.3). 67

Introduction

In 2022 the hundredth anniversary of the completion of the Stern-Gerlach experiment [1, 2] is commemorated. This is a paramount experiment for quantum theory leading to the discovery of a purely quantum property without classical analog, the spin, and revealing the quantum nature of microscopic phenomena. It also condenses the main features of the measurement process in quantum mechanics. By its simplicity, it has been used to illustrate the strangeness and counterintuitive traits of quantum phenomena and to introduce the main concepts of the theory in many textbooks [3].

The objective of measuring is to determine the state of a system of interest. The concept of state refers to the knowledge about a system the observer has or can access through measurements applied on the system. The observer defines a set of properties that can be attributed to the system and by means of a measuring apparatus a definite value for each property is found. A more precise determination of the state of system is reached by measuring with more precision the defined properties and by adding new properties to the system. If there exists a strong dependence between the quantities, they convey redundant information about the system. Therefore, the properties must be independent in order to contribute new knowledge about the system. With an ideal measurement, it is possible to determine the values of each property with certainty, resulting in a more complete knowledge of the system.

In the more abstract sense, the state of a classical system is specified by a set of N variables. The values of these variables can be arranged in N-dimensional vectors, thus the state can be represented with these vectors. In the presence of environmental factors, such as noise, it is not possible to determine with certainty the corresponding values of the variables. Therefore, classical states are represented in general by probability distributions on the variables space [4]. Maximum knowledge of the system can be achieved by performing ideal measurements in order to determine the values for all the defined variables. In this sense, the measurement process only exposes the values of preexisting properties of the system. Moreover, there exist measurements on classical systems that produce a change of the state of the system, meaning a change of the vector values, after is completion. However, there is nothing that makes us think that the measured property did not have a definite value prior to measurement.

This scenario changes radically in quantum mechanics. The state of a quantum system is represented by a vector in Hilbert space which evolves in time according to the Scrhödinger equation. A more general representation involves the density operator evolving in time according to the von Neumann equation. Physical observables are represented in terms of Hermitian operators acting on these states. In its standard interpretation, the state of the quantum system provides maximum knowledge of it. Even with maximum

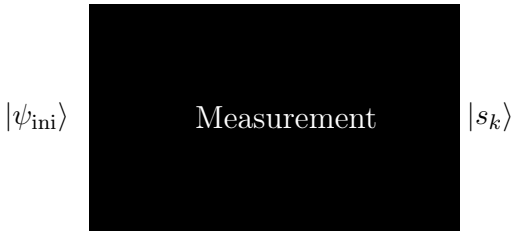

FIGURE 1. Measurement as a black box. The initial state $|\psi_{\text{ini}}\rangle$ is transformed into the eigenstate $|s_k\rangle$ of the measured observable $\hat{S}$. The outcome is the corresponding eigenvalue s_k. Quantum mechanics tells us the possible outcomes of future measurements and the probability of obtaining them. It also indicates the final state after measurement. Nevertheless, how this occurs is not contemplated by the postulate.

knowledge, the prediction of the result of a given measurement with certainty is in general unachievable. The theory can only provide the possible outcomes of the measurements and their corresponding probabilities, as is established by the essential interpretative concept in quantum mechanics: the Born's rule. Knowledge of a quantum system is equivalent to the knowledge about possible outcomes of future measurements [4].

In general, the measurement of an observable of a quantum system in each experimental setup changes the state of the system. This change, however, is of a different nature compared with classical systems. In a quantum system, the state obtained after measuring corresponds to a complete actualization of the available information of the system. Consequently, information on physical observables present in the initial state prior to measurement is irreversibly lost after it. This relates to the existence of noncommuting observables in quantum mechanics. The measurement of one physical observable with precision inevitably implies the increase of the uncertainty in another observable that does not commute with the former. For instance, the determination of the position with high precision entails a high uncertainty of momentum. In the limiting case, the complete knowledge of one quantity forbids the determination of the other. Clearly, an exhaustive measurement of all the physical quantities attributed to one quantum system is not possible, in stark contrast with classical systems.

In quantum mechanics an operational approach is assumed to account for the measurement process. This process is included within the theory as a postulate, indicating which are the possible outcomes and the probability of obtaining them. It also gives the state the system is left in after measurement. In a projective measurement, the initial state is projected onto one of the eigenstates of the operator representing the measured observable and the outcome is the corresponding eigenvalue. It is worth mentioning that this postulate assumes that randomness is a characteristic trait of quantum measurement. On the other hand, how the observed system suffers this change on its state is not addressed by the measurement postulate (Fig. 1).

The agreement between predictions of quantum mechanics and observations in real experiments evidences the success of the theory. Despite of this fact, the interpretation of the theory and how it shapes our view of the world is still a matter of intense debate. Different and somehow competing interpretations coincide in their predictions, yet they give a completely different sense of the world. The measurement process is the cornerstone of this debate.

In the standard interpretation of quantum mechanics, the collapse of the state vector is invoked in order to understand the observation of a definite outcome after measuring. This process is conceived as a discontinuous transition incompatible with unitary time evolution. Although the importance of the interaction between the observed system and the apparatus in the measurement process was identified since the beginning of the theory, the question about what kind of interaction would produce the collapse is not addressed. The properties of the system are defined a priori by the experimenter, but any observable can be measured in principle. In order to bring quantum phenomena to the domain of classical facts we live in, the Copenhagen interpretation imposes the condition that the apparatus must be classical. To understand quantum measurement, classical and quantum phenomena are involved. In this sense, classical mechanics cannot emerge from quantum mechanics; both have a complementary character to provide a complete view of the measurement process.

The effect of the interaction of the object of measurement with the apparatus was clarified by the von Neumann measurement scheme. In this account, the observed system as well as the measurement apparatus are considered quantum systems. Correlations between the possible outcome states of the observed system with states of the apparatus are created through their interaction. The collapse of the state vector is introduced in this scheme as a discontinuous transition to a mixed state in terms of the eigenstates of the measured observable. The probability of random outcomes in each run of the measurement is then given by this mixed state. Thus, quantum measurement is understood as a two-step process. However, the collapse is still included as a process incompatible with unitary dynamics.

Models proposed by Zurek [5, 6], Joos and Zeh [7] reconcile the state vector collapse introduced in the von Neumann measurement scheme with unitary time evolution. In these models, an initial pure state evolves gradually in time to a mixed state because of the loss of coherence in the density operator induced by the interaction of the observed system with the measurement apparatus and the environment. What the observer can measure is limited by the ability to design a measurement apparatus such that its interaction with the environment ensures the conservation of its correlations with the observed system.

More general measurements recognize the fact that in many experimental setups the system is not left in an eigenstate after measurement. Measurements defined in terms of more general operators, not necessarily projectors, are called positive operator-valued measures (POVM). Some measurements are based on the idea that information about the observed system can be obtained by perturbing it the least. When the state of the system has small changes compared to projection onto eigenstates of the measured operator, the measurement is called weak. In some measurement setups a clear distinction of the measurement outcome is not always possible. When in a measurement there are regions where the experimenter cannot distinguish clearly the observed result, the measurement is called unsharp [8]. These examples show that the possibilities of quantum measurements have been pushed beyond the projection onto eigenstates of the measured observable.

The account of the measurement in this thesis follows the two-step von Neumann measurement scheme and explains the second step, the collapse of the state vector, as a continuous process within unitary dynamics. This process is a consequence of the interaction with the environment, leaving the system in a mixed state of the eigenstates of the measured operator. This thesis aims to go beyond this picture to understand the contribution of the environment in the last step of the process, where a definite outcome is obtained.

A reasonable description of the measurement process in agreement with experimental setups comprises different stages of it. In first place, the observed system is prepared in a definite state and the measurement apparatus is calibrated prior to the measurement. Then, the object interacts with the measurement apparatus leading to the establishment of correlations between both systems. The loss of coherence induced by the interaction leaves the system in a state described by a diagonal density operator, the first state vector collapse. Finally, a second state vector collapse occurs leading to a final pure state of the system corresponding to one of the possible eigenstates of the measured operator. An outcome is reached at the end of the process, guaranteeing the reproducibility of the measurement.

In the current account of the measurement process, the entire process is observed at the level of the system only by keeping track of its time evolution in the presence of the apparatus and the environment, usually in terms of master equations. These equations are deduced to obtain the dynamics of the observed system by tracing out the degrees of freedom of the external systems interacting with it. Their derivation and simplification to closed solvable forms account for the state of the system in a statistical fashion, preventing the access to individual runs of the measurement. They only include the effect of the apparatus and the environment in an indirect way without considering details of the internal structure of these systems. The success of this approach in incorporating the first state vector collapse within unitary dynamics does not guarantee a complete description of the entire process including the second state vector collapse.

The irreversible character of the loss of coherence in the state of the observed system relies on the infinite number of degrees of freedom assumed to model the environment. With all these requirements to reproduce the first state vector collapse, an entire account of the measurement process seems unfeasible. However, recent studies in chemical physics and quantum optics have shown that dissipation and decoherence can be effectively reproduced on the relevant time scales of the observed system by coupling it with a finite heat bath [9, 10].

In this thesis a model within the framework of unitary time evolution for a description of the entire measurement process in quantum mechanics, starting from an initial pure state of the observed system through all the steps leading to a final pure state corresponding to one of the possible eigenstates of the measured operator, is proposed. The model is expected to exploit the advantages of unitary time evolution while circumventing its main difficulty, the inability to reproduce the first state vector collapse, using finite heat baths. This hybrid approach allows to define in detail the initial states of the observed system and the environment allowing the simulation of individual runs of measurements for different sets of initial conditions. Arguments asserting the incompatibility of the second state vector collapse with the superposition principle can also be evaluated with this approach. Conservation of entropy in unitary time evolution enables to track the information exchange during the measurement process. One of the crucial parameters of the model is the number of degrees of freedom of the environment. A balance between convergence of the results and the required computation time with the available resources is of fundamental importance. Powerful exact numerical methods for the time evolution of open quantum systems are needed in order to facilitate this balance. With this model we can reproduce essential features of the second state vector collapse.

Spin measurements are a prototypical example of quantum measurement. For particular initial states it constitutes the quantum analog of tossing a coin, a paradigmatic

example of randomness. With the smallest quantum system with nontrivial dynamics, a two-state system, spin measurements simplify the description of the measurement process. Coupling the two-state system to a finite heat bath in the context of spin measurements results in a spin-boson model, a versatile and well-known model for a system interacting with a bosonic environment. The large amount of available research conducted on the spin-boson model facilitates the delimitation of the optimal parameters of the model, moving the focus to a paramount factor in it, the search of appropriate initial conditions capturing the main features of spin measurement setups.

The proposed model provides a detailed account of the entire measurement process, reproducing essential features of the first and second state vector collapse within unitary time evolution. It contributes with new elements to the measurement problem debate and explores possible explanations of the origin of randomness in quantum mechanics, drawing a closer connection with the classical counterpart.

The overall structure of the thesis takes the form of six chapters. Chapter 1 introduces the measurement postulate and the main elements of the current account of the measurement process starting from the von Neumann measurement scheme and finishing with the key ingredients of the decoherence program. A brief review of the Stern-Gerlach experiment and its theoretical account is also included. A discussion about randomness and its characteristics in classical and quantum systems ends the chapter.

Chapter 2 begins by laying out the general elements in the description of systems interacting with an environment and the two alternative routes to obtain their dynamics. The essentials of the Feynman-Vernon and Caldeira-Leggett model are discussed. Then, the generalities of the finite heat bath approach and the multi-Davydov ansatz, the time evolution method implemented in this thesis, are presented.

The third chapter develops the proposed model for spin measurements, resulting in a spin-boson model. The dynamics of the spin-boson model is reviewed for the limiting cases with one and infinitely many environmental degrees of freedom. The symmetry properties of the Hamiltonian and their consequences in the spin measurement context are discussed. General considerations regarding the initial states of the observed system and the environment in order to faithfully reproduce unbiased spin measurements are presented. The chapter ends with the discussion of the argument showing the inconsistency of the superposition principle and the second state vector collapse.

Chapter 4 studies the dynamics of the spin for a particular set of initial conditions of the environment considering the limit $T \to 0$ of its thermal equilibrium state with the excited state of the spin. Although these initial conditions do not meet the requirements for unbiased measurements, they are useful to delimit the appropriate parameter values for simulating spin measurements. The dynamics of the spin with slight variations of the previous environment initial conditions is also studied in this chapter.

The fifth chapter presents the main results of this research. The dynamics of a spin for initial conditions of the environment emulating as far as possible the main traits of spin measurements are discussed. Characteristics of the dynamics during spin measurement with this model are evaluated with the aid of physical observables such as the energy. Flexibility to model different measurement schemes is included with time-dependent modulating functions. Two measurement protocols are considered in this chapter. Repeatability of quantum measurements is also studied with the proposed model. Finally, the time-

evolution of the spin is obtained with superpositions of initial states of the environment resulting in opposite outcomes.

Chapter 6 analyzes the information dynamics in spin measurements simulated with our model. In first place, the quantities required to study information in quantum systems are introduced. Then, the expected dynamics of the information in the measurement process is presented. The results of the simulations are contrasted with the expected behavior in the last part of the chapter.

Finally, the conclusion gives a summary of the findings of this research. Different improvements to the model and possible extensions for further research are also discussed.

CHAPTER 1

Measurement and randomness in quantum mechanics

Although quantum mechanics provides the possible outcomes of experiments, randomness is embedded in the theory. By its characteristics, randomness in quantum systems is considered of a more fundamental nature compared with classical systems. How a definite outcome emerges from the measurement process is not explained by the operational account given by quantum theory. The problem of how an initial state of the observed system produces a particular output in a measurement on quantum systems is called the measurement problem.

It was clear since the inception of quantum theory the importance of the interaction between the apparatus and the observed system in the measurement process. The Copenhagen interpretation invokes complementarity of quantum and classical systems to understand the measurement process. The classical character of the outcomes observed in the apparatus is the result of the interaction between a classical system (the apparatus) and a quantum system. A deviation from this point of view is introduced by von Neumann in its description of the measurement process. For him both system and apparatus are quantum systems. Their interaction produces correlations between the states of both systems. From this correlated state it is possible to infer the state of the system by looking at the state of the apparatus. However, if the initial state of the system is a superposition state, the superposition principle ensures that the total state of system and apparatus is after the interaction an entangled state, clearly, without a classical character. This caveat made von Neumann introduce the state vector collapse (first) as a final process in his measurement scheme. After the build-up of correlations, the state collapses into a classical mixture of the possible outcomes of the measured observable.

The decoherence process is the result of the entanglement between system and environment as consequence of their interaction. This process has two main consequences, (i) the loss of coherences in the state of the system and (ii) the emergence of robust states treated differently by the interaction with the apparatus. The integration of the first state vector collapse within unitary time evolution was possible thanks to the decoherence program. The measurement problem, as was stated above, is still not addressed by this account of the process.

In the following, the measurement postulate is introduced and the current description of the measurement process within the decoherence program is discussed in more detail.

1.1 The measurement postulate

Pure states of quantum systems are represented by vectors belonging to the Hilbert space, $|\psi\rangle \in \mathcal{H}$. An ensemble of pure states $|\psi_k\rangle$ with corresponding weights p_k, such that $\sum_k p_k = 1$, constitutes a mixed state represented by the density operator

$$\hat{\rho} = \sum_k p_k \, |\psi_k\rangle\langle\psi_k| \, . \tag{1.1}$$

Time evolution of the initial state $|\psi(0)\rangle$ is obtained by the action of the time evolution operator $\hat{U}$,

$$|\psi(t)\rangle = \hat{U}(t) \, |\psi(0)\rangle \, , \quad \hat{U}(t) = \exp\left(-\frac{i}{\hbar}\hat{H}(t)\right). \tag{1.2}$$

This operator is unitary and linear. The former property ensures that the norm of the state is preserved during time evolution leading to the conservation of the probability. The latter says that if the initial state is a superposition state of the form

$$|\psi(0)\rangle = C_1 \, |\psi_1\rangle + C_1 \, |\psi_2\rangle \, , \tag{1.3}$$

where $C_1, C_2 \in \mathbb{C}$, the time-evolved state is

$$|\psi(t)\rangle = C_1\hat{U}(t) \, |\psi_1\rangle + C_1\hat{U}(t) \, |\psi_2\rangle \, . \tag{1.4}$$

If the initial state of the system is mixed, $\hat{\rho(0)}$, the state at time t is given by

$$\hat{\rho}(t) = \hat{U}(t)\hat{\rho}(0)\hat{U}^{\dagger}(t). \tag{1.5}$$

It is worth stressing that unitary time evolution, Eqs. (1.2) and (1.5), maps pure states into pure states and mixed states into mixed states, respectively.

The action of the measurement process on the initial state of the system is included within quantum mechanics as a postulate. The measurement of a physical quantity is described by the action of a set of measurement operators $\hat{M}_m$ that satisfy the completeness relation [11]

$$\sum_m \hat{M}_m M_m^{\dagger} = \hat{I}. \tag{1.6}$$

Each operator is characterized by its outcome m. If the initial state of the system is $|\psi\rangle$, the measurement gives the outcome m with a probability

$$p_{\mathrm{G}}(m) = \langle\psi|\hat{M}_m^{\dagger}\hat{M}_m|\psi\rangle \tag{1.7}$$

and collapses the system onto the state

$$|\psi_m\rangle = \frac{\hat{M}_m \, |\psi\rangle}{\sqrt{p_{\mathrm{G}}(m)}}. \tag{1.8}$$

This formulation of the measurement postulate includes the more general measurement schemes defined by the positive operator-valued measure (POVM) [8]. This kind of measurement is based on the idea of obtaining information of the system of interest by observing a second system interacting with it.

If the measurement operators are orthogonal projectors $\hat{M}_m = \hat{P}_m$, then the measurement of the physical quantity, represented by the Hermitian operator

$$\hat{M} = \sum_m m\hat{P}_m, \tag{1.9}$$

gives the outcome m with probability

$$p_{\mathrm{P}}(m) = \langle\psi|\hat{P}_m|\psi\rangle \tag{1.10}$$

and leaves the system in the state

$$|\psi_m\rangle = \frac{\hat{P}_m|\psi\rangle}{\sqrt{p_{\mathrm{P}}(m)}}. \tag{1.11}$$

The last kind of measurement is called projective. According to the measurement postulate, it implies the projection of the initial state onto one of the eigenvectors of the measurement operator $\hat{M}$. Additionally, if the system is already in an eigenstate prior to the measurement, the state of the system after measurement remains the same ensuring the repeatability of quantum measurements.

As an example of the application of this postulate, consider a measurement of vertical component of the spin. This quantity is represented by the operator $\hat{\sigma}_z|\pm_z\rangle = \pm|\pm_z\rangle$. If the initial state of the system is

$$|\psi(0)\rangle = C_+|+_z\rangle + C_-|-_z\rangle, \tag{1.12}$$

the measurement postulate says that we can obtain either ± 1 as the outcome with probabilities $|C_+|^2$ and $|C_-|^2$, respectively. Correspondingly, the state of the system collapses either onto $|+_z\rangle$ or $|-_z\rangle$.

The transformation of the state dictated by the postulate is assumed to be irreversible and instantaneous. In the previous example, information about the non-commuting observable $\hat{\sigma}_x$ contained in the initial state (1.12) is completely lost after measurement of $\hat{\sigma}_z$. On the other hand, the application of this postulate does not involve the time, thus the outcome is obtained instantaneously.

Although the measurement postulate is rooted in observation of different experiments on quantum systems, the measurement process is not described itself as a physical process. It was clear since the birth of quantum mechanics that experiments on quantum systems involve the interaction between the observed system, the object (O), and the measurement apparatus, the meter (M). However, this characteristic is not included in the measurement postulate. Moreover, the transformation implied by quantum measuring violates the superposition principle and therefore it seems incompatible with unitary time evolution.

These observations have not prevented researchers from tackling the description of quantum measuring as a physical process within unitary time evolution. By considering both object and meter, emerges the question about the duration of this process [12], the possibility of its reversibility [13] and its total integration within unitary dynamics [14].

The roots of these attempts could be traced back to the pioneering description due to von Neumann [15]. Together with the decoherence program, it is established as the most complete description of the measurement process within the standard theory of quantum mechanics.

1.2 Measurement as a process in time

Any experimental setup aimed to measure a physical property on a quantum system involves the interaction between the quantum object and, typically, a macroscopic meter. This is the starting point on a physical description of the measurement process. While the measurement postulate takes an input state of the object and transforms it into another state without a specific process behind it, the physical description of the process aims to devise a mechanism where, because of the interaction between both systems, it suffers a smooth transition until the reach of a definite outcome of the measurement. In the following, the discussion will be centered on projective measurements.

The characteristics of the measurement process allows to divide further the general measurement problem mentioned above. An account of the measurement process should address the questions [16]

- why a superposition state is not observed as an outcome of the measurement in the apparatus.
- why the interaction between the system and the apparatus shows a preference for some states (i. e. the eigenstates of the measured operator) and no others.
- why at the end of each run of the measurement a definite outcome is observed.

The decoherence program [17] is successful in explaining the first two questions. The progress in the understanding of the measurement process it provides is undeniable. However, the third question, is out of the reach of this approach [18].

1.2.1 Interaction between object and meter

A meter is designed to give information about the state of the object by looking at its state. Prepared in an initial state before the measurement, it should have another state after the measurement from which the state of the object can be inferred. Different states of the object should give different and distinguishable states of the meter. Therefore, the first step of the measurement process is the creation of correlations between both systems.

Considered as quantum systems in the von Neumann measurement scheme, the object and the meter constitute a bipartite system with total Hilbert space $\mathcal{H}_{\mathrm{O}} \otimes \mathcal{H}_{\mathrm{M}}$. States of the total system can be written in terms of basis vectors of the Hilbert space of the object $|s_j\rangle \in \mathcal{H}_{\mathrm{O}}$ and the meter $|a_k\rangle \in \mathcal{H}_{\mathrm{M}}$, $|s_j\rangle \otimes |a_k\rangle = |s_j\rangle\,|a_k\rangle$.

For simplicity, consider again a two-state system whose Hilbert space is spanned by the vectors $\{|+_z\rangle, |-_z\rangle\}$. Let the apparatus be in an initial pure state $|\psi_{\mathrm{M}0}\rangle$. It is reasonable to assume that before the measurement object and meter do not interact. Therefore, the initial state of the total system can be written as a product state. Suppose now a unitary

evolution of the total system such that

$$\begin{aligned} |\Psi_0\rangle = |\psi_{\mathrm{O}0}\rangle\,|\psi_{\mathrm{M}0}\rangle = |+_z\rangle\,|\psi_{\mathrm{M}0}\rangle \xrightarrow{\hat{U}_{\mathrm{OM}}} |+_z\rangle\,|\psi_{\mathrm{M}+}\rangle\,, \\ |\Psi_0\rangle = |\psi_{\mathrm{O}0}\rangle\,|\psi_{\mathrm{M}0}\rangle = |-_z\rangle\,|\psi_{\mathrm{M}0}\rangle \xrightarrow{\hat{U}_{\mathrm{OM}}} |+_z\rangle\,|\psi_{\mathrm{M}-}\rangle\,. \end{aligned} \tag{1.13}$$

The state of the object does not change after the interaction; thus, it is said that the interaction leads to a nondemolition measurement [19, 20].

If now the initial state of the object is a superposition state of the form (1.12), the linearity of the time evolution produces the final state

$$(C_+\,|+_z\rangle + C_-\,|-_z\rangle)\,|\psi_{\mathrm{M}0}\rangle \xrightarrow{\hat{U}_{\mathrm{OM}}} C_+\,|+_z\rangle\,|\psi_{\mathrm{M}+}\rangle + C_-\,|-_z\rangle\,|\psi_{\mathrm{M}-}\rangle\,. \tag{1.14}$$

The superposition only observed in the object state at the beginning is transferred to the environment due to the interaction of both systems, leaving the total system in an entangled state. By observing the state of the meter $|\psi_{\mathrm{M}\pm}\rangle$, the state of the object $|\pm_z\rangle$ can be inferred. It is possible to describe POVM measurements [21] and projective measurements of observables with continuous spectrum [22] as result of interactions, in the same spirit as showed above, with the appropriate unitary operators.

The interaction between object and meter results in the creation of correlation between states. However, it is not possible to claim that a measurement was made. In first place, the right-hand side of (1.14) is a superposition state which cannot be observed as a result of a measurement. Second, it is not possible to identify which states of the object are correlated with the states of the environment by this interaction. To see this, suppose for simplicity that $|C_+| = |C_-| = 1/\sqrt{2}$. Making a change of basis

$$|\pm_z\rangle = \frac{1}{\sqrt{2}}(|+_x\rangle \pm |-_x\rangle) \tag{1.15}$$

the state on the right-hand side of (1.14) can be written as

$$\frac{1}{\sqrt{2}}(|+_z\rangle\,|\psi_{\mathrm{M}+}\rangle + |-_z\rangle\,|\psi_{\mathrm{M}-}\rangle) = \frac{1}{\sqrt{2}}(|+_x\rangle\,|\psi'_{\mathrm{M}+}\rangle + |-_x\rangle\,|\psi'_{\mathrm{M}-}\rangle) \tag{1.16}$$

where

$$|\psi'_{\mathrm{M}\pm}\rangle) = \frac{1}{\sqrt{2}}(|\psi_{\mathrm{M}+}\rangle) \pm |\psi_{\mathrm{M}-}\rangle)). \tag{1.17}$$

Hence, it is not clear whether the interaction creates correlations between $|\pm_z\rangle$ and $|\psi_{\mathrm{M}\pm}\rangle)$ or between $|\pm_x\rangle$ and $|\psi'_{\mathrm{M}\pm}\rangle)$. This is known as the basis ambiguity problem.

For these reasons, the step (1.14) is called a premeasurement. It does not provide a complete account of the measurement. To reach such account, von Neumann introduced the collapse of the state vector as a process that transforms an initial pure state into a mixed state of the eigenstates of the measured operator

$$|\psi_{\mathrm{O}0}\rangle = C_+\,|+_z\rangle + C_-\,|-_z\rangle \xrightarrow{\mathcal{R}} |C_+|^2\,|+_z\rangle\langle+_z| + |C_-|^2\,|-_z\rangle\langle-_z|\,. \tag{1.18}$$

The density matrix (1.18) obtained after the $\mathcal{R}$ process can be interpreted depending on the experiment setup. If the experiment deals with an ensemble of systems prepared in the same state, the density matrix represents the expected statistics of the final outcomes

of the measurements on the ensemble. On the other hand, if the density matrix describes the state of a single system, it represents the ignorance the experimenter has about the state of the system. The system is in either $|+_z\rangle$ or $|-_z\rangle$, it is just that the experimenter does not know in which one.

The two-step von Neumann measurement scheme gives a more complete description of the measurement process. Despite that fact, it introduces a new process on the state of the object that is incompatible with unitary time evolution. Decoherence conciliates both processes. To discuss how this is achieved, a tool for obtaining the state of one of the composing systems in a bipartite system must be introduced.

1.2.2 Partial trace

It is possible to obtain the state of one of the subsystems from the total state of a composite system by means of the operation called partial trace. Even if the total state of the composite system is pure, it does not guarantee that the state of the subsystem is pure. In fact, in a bipartite system, a mixed state for one of the subsystems after the application of the partial trace indicates entanglement. The partial trace produces a reduced density operator representing the state of the desired subsystem.

If the total state of the composite system of object and meter is $\hat{\rho}_{\mathrm{OM}}$, the state of the object can be obtained as

$$\hat{\rho}_{\mathrm{O}} = \mathrm{Tr}_{\mathrm{M}}(\hat{\rho}_{\mathrm{OM}}). \tag{1.19}$$

This trace is taken over the degrees of freedom of the meter. In the simplest case of a product state $\hat{\rho}_{\mathrm{OM}} = |\psi_{\mathrm{O}}\rangle\langle\psi_{\mathrm{O}}| \otimes |\psi_{\mathrm{M}}\rangle\langle\psi_{\mathrm{M}}|$, the partial trace is obtained as

$$\hat{\rho}_{\mathrm{O}} = \mathrm{Tr}_{\mathrm{M}}(|\psi_{\mathrm{O}}\rangle\langle\psi_{\mathrm{O}}| \otimes |\psi_{\mathrm{M}}\rangle\langle\psi_{\mathrm{M}}|) = |\psi_{\mathrm{O}}\rangle\langle\psi_{\mathrm{O}}| \,\mathrm{Tr}_{\mathrm{M}}(|\psi_{\mathrm{M}}\rangle\langle\psi_{\mathrm{M}}|)). \tag{1.20}$$

The motivation behind the definition of the partial trace operation is that it should give a state for the subsystem that is compatible, according to the measurement postulate, with the expected statistics of measurements applied locally on that subsystem. In fact, the trace operation is the only operation giving the correct state according with this criterion [11]. It is important to stress that including the partial trace in the description of the measurement process amounts to assume the collapse of the state vector indicated by the measurement postulate [23].

1.2.3 Environment-induced superselection

The partial trace applied on the state (1.14) produces the state of the object

$$\begin{aligned}\hat{\rho}_{\mathrm{O}} =& |C_+|^2 \,|+_z\rangle\langle+_z| + |C_-|^2 \,|-_z\rangle\langle-_z| \\ &+ C_+C_-^* \,|+_z\rangle\langle-_z| \,\langle\psi_{\mathrm{M}-}|\psi_{\mathrm{M}+}\rangle + C_-C_+^* \,|-_z\rangle\langle+_z| \,\langle\psi_{\mathrm{M}+}|\psi_{\mathrm{M}-}\rangle \,.\end{aligned} \tag{1.21}$$

The reduced density operator (1.21) becomes diagonal whenever the overlap between meter states vanishes $\langle\psi_{\mathrm{M}+}|\psi_{\mathrm{M}-}\rangle = 0$. This implies that the states of the meter pointing to different states of the object are completely distinguishable. The interaction leading to this process reduces the state of the observed system to a diagonal form in the basis $\{|+_z\rangle\,, |-_z\rangle\}$.

The continuous monitoring of the state of the object leads to an increasing distinction of the meter states and therefore a better resolution of the state of the object. The state of the meter should be read in the world of classical facts. For this reason, typical models of decoherence assume the meter as a macroscopic object composed by a huge number of degrees of freedom. The multiple interaction between these degrees of freedom with the object conduces to a gradual increase of the distinction of meter states in time [18]

$$\langle \psi_{\mathrm{M}+} | \psi_{\mathrm{M}-} \rangle \propto e^{-t/t_d} \tag{1.22}$$

where t_d is known as the decoherence time. Therefore, the first state vector collapse is assumed as a continuous process in time [24]. If the state of the meter describes a macroscopic system $|\psi_{\mathrm{M}\pm}\rangle = |\psi_{\mathrm{M}\pm 1}\rangle \, |\psi_{\mathrm{M}\pm 2}\rangle \cdots |\psi_{\mathrm{M}\pm N}\rangle$, the overlap between distinct meter states pointing different eigenstates of the measured operator is

$$\langle \psi_{\mathrm{M}+} | \psi_{\mathrm{M}-} \rangle = \langle \psi_{\mathrm{M}+1} | \psi_{\mathrm{M}-1} \rangle \, \langle \psi_{\mathrm{M}+2} | \psi_{\mathrm{M}-2} \rangle \cdots \langle \psi_{\mathrm{M}+N} | \psi_{\mathrm{M}-N} \rangle \, . \tag{1.23}$$

As soon as one of the components of the meter distinguishes the states of the object, the overall state does the same. With an increasing number of components, the time required for this to happen decreases. In the limit of an infinite number the time becomes smaller giving the impression of an instantaneous transition.

The interaction between the object and the apparatus does not treat the different states of the object in the same manner. As is shown in (1.14), the initial superposition state of the object entangles with the states of the meter. It is not the case for a superposition of the form

$$\left| \psi'_{\mathrm{O}}(0) \right\rangle = \frac{1}{\sqrt{2}} (|+_x\rangle \pm |-_x\rangle) = |\pm_z\rangle \tag{1.24}$$

because under the same interaction the final state is

$$\left| \psi'_{\mathrm{O}(0)} \right\rangle |\psi_{\mathrm{M}0}\rangle \xrightarrow{\hat{U}_{\mathrm{OM}}} = |\psi_{\mathrm{M}\pm}\rangle \, |\pm_z\rangle \, . \tag{1.25}$$

The interaction is defined in such a way that the eigenstates of the measured operator are more robust to the action of the meter. They are less prone to being entangled with the states of the meter hence they are less sensitive to the interaction. This distinction established by the interaction selects some preferred states of the object, or pointer states, as they are usually called. If the pointer states are a basis of the Hilbert space of the object $\mathcal{H}_{\mathrm{O}}$, they conform a preferred basis of this space. In the measurement of the vertical component of the spin used here so far, the pointer states are the eigenstates of the measured operator $\hat{\sigma}_z \, |\pm_z\rangle = \pm \, |\pm_z\rangle$. The spectral decomposition $\hat{\sigma}_z$ allows to verify that

$$\left[\hat{H}_{\mathrm{OM}}, \hat{\sigma}_z \right] = 0 \tag{1.26}$$

with the interaction Hamiltonian $\hat{H}_{\mathrm{OM}}$. This important property allows to identify the preferred states for a given interaction.

The measurement of a physical quantity requires the design of a specific measurement setup. The measurement apparatus should interact with the observed system so as to the eigenstates of the desired observable emerge as the pointer states.

It is not clear, however, which pointer states are selected by the interaction of object and meter due to the basis ambiguity problem mentioned before. In order to clarify this

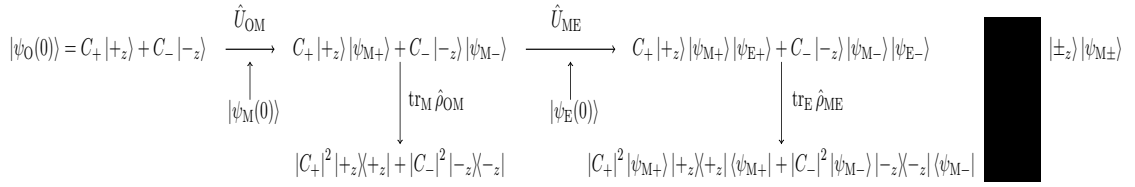

FIGURE 1.1. Spin measurement according to the decoherence program. The entire system composed of the object, the meter and the environment evolve unitarily. At the level of the object, its initial pure state becomes a mixed state due to the interaction with the meter. The environment preserves the correlations between both subsystems and defines clearly the pointer states in the measurement. How the object collapses onto one of the possible eigenstates of the measured observable (second state vector collapse), recovering a pure state, is not considered in this approach.

ambiguity a third system is introduced in the picture: the environment. If the environment is prepared in an initial state $|\psi_E(0)\rangle$, its interaction with the meter is defined as

$$\begin{aligned}&\left(C_+\,|+_z\rangle\,|\psi_{M+}\rangle + C_-\,|-_z\rangle\,|\psi_{M-}\rangle\right)|\psi_E(0)\rangle \xrightarrow{\hat{U}_{ME}}\\ &C_+\,|+_z\rangle\,|\psi_{M+}\rangle\,|\psi_E+\rangle + C_-\,|-_z\rangle\,|\psi_{M-}\rangle\,|\psi_E-\rangle\,.\end{aligned} \tag{1.27}$$

Due to Schmidt decomposition, the state of a bipartite system can be always written as a superposition of product states of the object and the meter. It is not the case for a tripartite system and just a special kind of interaction would give the state (1.27). After calculating the partial trace of this state, the joint state of the object and meter, if the states $|\psi_E\pm\rangle$ are distinguishable, reads

$$\hat{\rho}_{OM} = |C_+|\,|+_z\rangle\langle+_z|\,|\psi_{M+}\rangle\langle\psi_{M+}| + |C_-|\,|-_z\rangle\langle-_z|\,|\psi_{M+}\rangle\langle\psi_{M-}|\,. \tag{1.28}$$

In an experiment the setup is designed to measure one specific observable on the system. According to the decoherence program this is so because the chain of interactions between the three subsystems involved fixes the observable it can measure and the information it can obtain from the system. Its interaction with the object correlates the states and selects the least sensitive states of the object to decoherence. Its interaction with the environment is such that it preserves the correlations between object and meter states, clearly distinguishing the pointer states.

The question about why only one of the outcomes is observed at random is not included in this description (Fig. 1.1). Once the mixed state is reached, the object is in a definite state, but the experimenter does not know which one. The last step, where the state of the object is projected onto one of the eigenstates of the measured operator is assumed as an effect of the random nature of the quantum measurement. Decoherence describes the first state vector collapse, but it is unable to explain the second. This view is summarized by Pessoa [23] as: an explanation of the second collapse implies an explanation of the first, but an explanation of the first does not imply an explanation for the second.

1.3 The EPR experiment

Entanglement is a key ingredient in the description of the measurement process in quantum mechanics. It is a property of compound systems where the state of the entire system cannot be written as a product state of individual states of each subsystem. Therefore, from an entangled state it cannot be claimed that each subsystem is in a definite state.

Entanglement is an example of the deviation of quantum phenomena from the common experience of the classical world. It is a resource that opens applications beyond the possibilities of classical systems [25]. It is also a source of the striking character of quantum phenomena, challenging fundamental ideas rooted in physics that shape our view of the world. The Einstein-Podolsky-Rosen experiment (EPR) [26] is a prominent thought experiment showing these features.

The EPR argument was conceived to point out the incompleteness of quantum mechanics. It is rooted in two principles: locality and realism [27]. The former states that actions made in a measurement setup cannot disturb the results of another measurement spatially separated from the first one. The latter states that if a property of a system can be predicted with certainty, without disturbance of the system, the property has a definite value independent of the observation.

To present the argument, consider two spins prepared in the entangled state

$$|\Psi\rangle = \frac{1}{\sqrt{2}}(|-\rangle_1 |+\rangle_2 - |+\rangle_1 |-\rangle_2). \tag{1.29}$$

where the subindices $1, 2$ indicate the spin the state belongs to. Each spin is obtained by two experimenters Alice and Bob, far away from each other. If Alice performs a spin measurement in a selected direction in her laboratory, due to the entanglement, she can predict with certainty the outcome of the same measurement performed by Bob only knowing the outcome of her own measurement. Consequently, according to local realism, spin has a definite value in the selected direction, and the experimental setup guarantees that the measurement made by Alice does not affect the measurement of Bob. This led the authors to the conclusion that standard quantum mechanics does not provide a complete description of quantum phenomena.

If local realism is necessary for a reliable description of quantum phenomena, the standard view of quantum mechanics is not complete. However, there exists another option. If quantum mechanics gives in fact the most complete description of these phenomena, at least one of the principles of local realism is not valid. It is important to emphasize that EPR does not question the correctness of quantum mechanics and its predictions.

An experimental evaluation would conduce to a solution of this paradox. Bell inequalities [28] established a condition that any theory assuming local realism must satisfy. Surprisingly, standard quantum mechanics, which provides the correct predictions according to experiments, violates this condition. Hence, at least one of the assumptions of local realism is incorrect. For instance, hidden variables theories assume realism, but then non-locality must be accepted as a feature of quantum phenomena.

The discussion proposed by EPR has important implications for the interpretation of essential concepts in the theory. It shows the existence of stronger correlations in quantum systems, with consequences for randomness observed in measurement outcomes.

For the purposes of this thesis, it is not necessary to consider the entire system discussed in EPR. By focusing on measurements performed only by either Alice or Bob without reference to the other experimenter, we refrain from discussions about non-locality, Bell inequalities and hidden variable theories. Alternative systems can be considered for the study of quantum measurements. Photons with opposite polarizations and singlet spin states (Eq.(1.29)) are good candidates. Single spin measurements can be performed using the well-known Stern–Gerlach experiment.

1.4 Stern–Gerlach experiment

The Stern–Gerlach experiment is one of the most known experiments revealing the quantum nature of atoms. The discovery of electron spin came from this experiment, originally conceived to test the predictions of two competing theories about the behavior of atoms crossing a magnetic field [29]. In its original setup, a collimated beam of silver atoms prepared in an oven with their magnetic moments oriented randomly, goes through an inhomogeneous magnetic field oriented in the z direction. The incoming beam splits into two components, showing the quantization of the magnetic moment μ_z of the atoms. The splitting was identified by the deposition pattern observed in a glass treated chemically. Deposition of a considerable number of atoms is needed to identify clearly the pattern. More recent setups of the experiment use cesium atoms, an inhomogeneous magnetic field in a vacuum chamber and a galvanometer designed to measure small currents [30].

Although quantization of the magnetic moment is observed through distinct positions of the beam arriving to the glass or measured by the galvanometer, the Stern-Gerlach measures the momentum not the position. By measuring the momentum, the magnetic moment of the atoms can be inferred [31]. This, however, establishes correlations between an internal degree of freedom (spin) with an external degree of freedom (position). According to (1.14), the interaction of the atom with the magnet gives

$$|\Psi_0\rangle = \frac{1}{\sqrt{2}}(|+_z\rangle + |-_z\rangle)\left|\psi_{\mathrm{M}0,\vec{r}}\right\rangle \rightarrow \frac{1}{\sqrt{2}}(|+_z\rangle\left|\psi_{\mathrm{M}+,\vec{r}}\right\rangle + |-_z\rangle\left|\psi_{\mathrm{M}-,\vec{r}}\right\rangle), \tag{1.30}$$

where $\left\langle\vec{r}\middle|\psi_{\mathrm{M}0,\vec{r}}\right\rangle = \psi_0(\vec{r})$ and $\left\langle\vec{r}\middle|\psi_{\mathrm{M}\pm,\vec{r}}\right\rangle = \psi_\pm(\vec{r}\pm d\vec{z})$ are the spatial wavefunctions before and after the passing through the magnet, respectively. The deflection of the beam is represented by a displacement d in the z direction. A projective measurement is obtained when the two wavepackets $\psi_\pm(\vec{r}\pm d\vec{z})$ are completely distinguished [32]. In is important to note that (1.30) shows that the magnet does a premeasurement, and one cannot claim that a complete measurement is achieved. Only when the beam arrives to the screen (glass or galvanometer), indicating a definite outcome, is the measurement process complete.

Different theoretical approaches have been proposed to study this experiment. Semiclassical approaches describes Stern-Gerlach experiment in terms of classical trajectories followed by the beams. The equations of motion of each trajectory have been deduced using spinors [33]. Within this approach, it is assumed that the deflection of the beams is produced by the force

$$\vec{F} = \nabla(\vec{\mu}\cdot\vec{\mathbf{B}}) = \mu_z\frac{\partial B_z}{\partial z}. \tag{1.31}$$

By modeling the beam as a Gaussian wavepacket, in [34] the dynamics of the beams for a spin-1 particle is studied. It is shown that even for the idealized experiment, there exists

the probability of not having a deflection of the beams and of incorrect readouts in the detection.

Explicit accounts of the measurement apparatus and the environment are also considered. The Stern–Gerlach experiment is used as an example of the interaction between an observed quantum system and a classical meter in an approach following the Copenhagen interpretation of measurements [35]. Fully quantum mechanical accounts [36, 37] consider the effect of other components of the magnetic field. An asymmetry in the resulting pattern is expected [36]. According to this study, the probability distribution concentrates in the direction where the magnetic field decreases and spreads in the other direction. It is also argued that even in the ideal case when the spin is in one eigenstate of the measured observable, the measurement could change its state (spin-flip) and it is possible to have deflections that are not related with the spin state. In these studies, the initial state of the spin is a superposition of the eigenstates of the measured observable. To consider the random orientation produced by the oven, in [29] an initial mixed state is considered.

By modeling the environment as a set of harmonic oscillators, the evolution of the complete system leaves the spin in a mixed state composed of both outcomes in the experiment [38, 39] following the complete decoherence approach. In the experiment, the environment can be assumed to be the air particles around the setup. However, this can be questioned in the experiment setups including vacuum chambers. Following this approach, complementary studies using the Wigner function formalism has been used to study the loss of coherence that leads to a final mixed state [40].

Interesting phenomena are predicted when variations of the setup in the original Stern–Gerlach experiment are considered. Loss of coherence is expected when the experimental setup tries to recombine the two beams to recover the initial state of the beam. This process can be avoided with a detailed manipulation of the gradient of the magnetic field [41]. On the other hand, correlations between successive measurements of different components of the spin using different orientations of the magnets and the possibility of steering one measurement with a previous one, are predicted [42].

Although the Stern–Gerlach experiment is one of the most well-known experiments studied in quantum mechanics, there are still questions about it that need to be answered. Different theoretical approaches predict a variety of phenomena beyond the splitting of the beam. The entire process leading to a definite outcome in this experiment remains unclear in the available theoretical description.

1.5 Quantum randomness

In contrast with unitary time evolution, establishing a deterministic relationship between the initial state and the time-evolved state, the different outcomes emerging from the measurement process in quantum mechanics are considered a manifestation of true randomness in nature. Commonly interpreted as uncertainty about the possible result in an experiment, randomness can be observed in simple experiments, for example, tossing a coin. The possible outcome of this experiment in one trial, heads or tails, can be modeled as a random variable $X = \{0, 1\}$. Several trials would result in a sequence of the form $\{1, 0, 1, 0, 0, 0, 0, 1, \dots\}$. Depending on the characteristics of the sequence, it is considered the result of a random process.

There is no consensus about the definition of randomness. Alternative formalizations of this concept consider distinct characteristics of sequences to consider them random. Some assumed meanings of randomness in these formalizations are [43]:

- Randomness as unpredictability: even if one knows the possible results in an experiment, it is not possible to predict the outcome in each trial with certainty. Therefore, the observation of a regular pattern in the sequence is not expected if it is random.
- Randomness as typicality: a regular sequence, for instance full of 1, is less likely than a random one. Therefore, random sequences are the most typical.
- Randomness as complexity: using the concept of algorithmic complexity, a random sequence is such if the length of the algorithm to produce the sequence has the same length of the sequence.

The generation of random sequences is of paramount importance in many applications of several fields ranging from pure research to data protection and financial applications. In practice, there are two main sources of random numbers [44]. In one hand, there are some algorithms designed to produce sequence of numbers emulating the expected properties of random numbers. These algorithms are called pseudorandom generators. On the other hand, different signals of complex classical systems with chaotic dynamics are used to generate random numbers. Both methods have their limitations to produce sequences of random numbers. The former produces these numbers using an algorithm, so the method is in fact deterministic. In the latter, although a complex physical process is involved, they are deterministic in principle due to the characteristics of the equations of motion.

A detailed study of the toss of a coin showed that the probability of obtaining heads or tails differs in 1% due to the tendency of the coin to arrive as it started [45]. Moreover, the probability of one of the outcomes can be 100% with the appropriate adjustment of the initial conditions.

Randomness as unpredictability is more appropriate to characterize the observed outcomes in real experiments. From this perspective, there are two sources of randomness in classical systems, (i) when the initial conditions of the system cannot be fully determined and (ii) when only a small part of the total system or some degrees of freedom are of interest [46]. Examples in the former include chaotic systems and the use of average quantities to describe systems and the use of ensembles. In the latter, an example is Brownian motion and its description using the Langevin equation.

Randomness observed in quantum measurements seems to be different to its classical counterpart. If $|\psi_O\rangle$ specifies the state of a single system, then the outcomes of measurements are in general random and cannot be attributed to other degrees of freedom. For this reason, von Neumann considered quantum randomness as irreducible [15, 43]. Due to this characteristic, it is believed that quantum randomness is an improved kind of randomness. While randomness in classical systems can be attributed to a lack of information (apparent), in quantum systems it is an intrinsic property without a causal mechanism underlying it [47].

Following this reasoning, quantum phenomena can be exploited to obtain improved random number generators. For instance, spin measurements can be used to generate random sequences depending on the outcome of the measurement (Fig. 1.2). However, according to the different criteria of randomness defined above, if only the sequence is

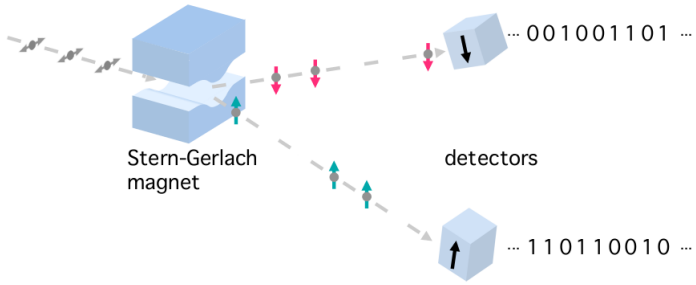

FIGURE 1.2. Random number sequences generated using spin measurements. It is believed that quantum phenomena constitute an improved source of random numbers since randomness in quantum mechanics seems to be an intrinsic property.

known it cannot be distinguished from other sequences generated with a classical source. The difference relies on how the sequence is generated and the impossibility of having a model to explain the emergence of this randomness in the quantum case [43].

Experimental realizations of random number generators exploding quantum measurements are variate. Using photons with entangled polarization states, in [48] outcomes of measurements on each photon made in separate locations are used as a random number generator. Randomness was verified by means of the violation of Bell inequalities. Another implementation using photons, considers in its implementation a beam splitter [44]. Autocorrelation function was used as a test of the efficiency of the generator. Another implementation considers the vacuum fluctuations in a laser cavity as a source of random numbers [49].

The discussion about quantum randomness is far from ending. The relationship between quantization and randomness in quantum systems is discussed in [50]. Using contextual objectivity, it is concluded that quantum randomness is a consequence of discrete contextual states. On the other hand, the correspondence apparent randomness-classical systems and intrinsic randomness-quantum systems is challenged. The existence of intrinsic randomness in classical systems is discussed in [51]. In addition, the relationship between imprecision of determining the initial conditions and quantum randomness is not completely discarded [43, 47].

The interpretation of the measurement process in quantum mechanics shapes the view of randomness in the observed outcomes. In the decoherence program, the process starts with an initial pure state and reaches at the end a mixed state involving the possible outcomes of the measurement. The transition from this state to one of the possible outcomes, a pure state again, is viewed as a consequence of the lack of knowledge about the state of the object, as is interpreted from the mixed state. The object is already in a definite state, but we do not know which one. In the measurement postulate the initial pure state, implying complete knowledge of the state, becomes one of the eigenstates of the measured observable in each measurement with certain probability. Both interpretations explain the projection onto one of the eigenstates of the measured operator because of the intrinsic randomness in quantum mechanics. A radical deviation from this point of view emerges when considering the unitary description of the entire measurement process including the first and second state vector collapse, putting quantum and classical randomness in the same footing. A discussion of the measurement process in terms of information should not be missing. It would end in the conclusion that the final state is a pure state again,

zero entropy of the object after the second collapse. Still, the impression remains that measurement of two-state systems with unbiased initial state generate entropy (as random numbers) equivalent to one bit per measurement (see, e. g., [52]). This randomness is not covered by von Neumann entropy.

CHAPTER 2

Dynamics of a system coupled to an environment

Closed quantum systems evolve according to unitary time evolution. In real setups, it is impossible to perfectly isolate a quantum system from its environment. However, the ideal closed system evolving unitarily in time is a good approximation when the interaction with the environment is negligible compared with the energy scale of the observed system. When this condition is broken, the time evolution of the real system deviates from the predicted by unitary time evolution. The system of interest is then called an open quantum system. In such cases a description of the entire system, including the environment, is required.

The total system is divided into two subsystems: a central system, comprising a subset of the total degrees of freedom of the total system, and the environment. The latter is usually modeled with a large amount or even an infinite number of degrees of freedom. Both subsystems are quantum and interact only between them. Therefore, without any external system interacting with the central system and what was called environment, the total system can be considered closed. Consequently, states of the entire system $|\Psi\rangle \in \mathcal{H}_{\mathrm{O}} \otimes \mathcal{H}_{\mathrm{E}}$ evolve in time according to a unitary time evolution operator $\hat{U}$.

The Hamiltonian of the system has three elements, the Hamiltonian of each subsystem and the interaction term

$$\hat{H} = \hat{H}_{\mathrm{O}} + \hat{H}_{\mathrm{E}} + \hat{H}_{\mathrm{OE}}. \tag{2.1}$$

The interaction Hamiltonian can be written in terms of operators acting on each subsystem only

$$\hat{H}_{\mathrm{OE}} = \sum_{l} \hat{A}_l \otimes \hat{B}_l, \tag{2.2}$$

where $\hat{A}_l$ acts on states of the central system and $\hat{B}_l$ acts on states of the environment. At the level of the system of interest, effects such as dissipation are observed in clear contrast with unitary time evolution. Focusing only on the state of the system of interest, its time evolution is nonunitary.

In classical systems dissipation is included phenomenologically. For instance, the dynamics of a particle immersed in a potential $V(q)$ subject to dissipation and the action of a stochastic force $\xi(t)$ due to the environment is described by the Langevin equation [53]

$$M\ddot{q}(t) + M\eta\dot{q}(t) + V'(q) = \xi(t). \tag{2.3}$$

Dissipation is included by the second term proportional to $\dot{q}(t)$, where η is the damping rate. Brownian motion is a prominent example described by equation (2.3).

More complex behavior results when the environment possesses memory. In such case, friction depends on the past values of $\dot{q}(t)$. The Langevin equation must be modified to account for these more complex dissipation effects

$$M\ddot{q}(t) + M\int_{-\infty}^{t} dt'\eta(t-t')\dot{q}(t') + V'(q) = \xi(t), \tag{2.4}$$

where the damping rate is time dependent. It can be written in terms of the frequency as

$$\tilde{\eta}(\omega) = \tilde{\eta}'(\omega) + i\tilde{\eta}''(\omega) = \int_{-\infty}^{\infty} dt\, \eta(t)e^{i\omega t}. \tag{2.5}$$

The aim of describing a central system interacting with its environment is to account for dissipation effects in quantum systems. A richer behavior emerges from such description of quantum systems. As was discussed in chapter 1, decoherence is another effect resulting from the interaction of both subsystems. The different existing methods for obtaining the time evolution of systems subject to the action of its environment can be organized in two groups. Such methods must capture the dissipation and decoherence effects. They are discussed in this chapter. Then, the essentials of the finite-bath approach are presented. Later, the Feynman-Vernon and Caldeira-Leggett models are briefly reviewed and finally the propagation method used in this work is presented.

2.1 Two different routes

The state of the central system is the primary concern in the description of an open quantum system. What one wants to determine is the influence of the environment in the time evolution of this state. What happens with the environment is commonly ignored or, due to its size and the intensity of the interaction, assumed to be negligible. In fact, the pioneering work of Feynman and Vernon [54] showed that it is possible to describe the time evolution of an open quantum system considering only the variables of the system. The action of the environment is encapsulated in what it is called the influence functional.

The state of the central system at time t can be obtained following two general strategies, as is shown in Figure 2.1. The first one consists in deducing a dynamical map $V : \mathcal{H}_O \to \mathcal{H}_O$ connecting the state $\hat{\rho}_O(0)$ with the state at time t, $\hat{\rho}_O(t)$. In the second one the state of the entire system is evolved unitarily until time t and from this state the reduced density operator of the central system is extracted. Both routes must produce the same final state.

The first group of methods has the advantage of working only with the variables of the central system, in a similar fashion of the influence functional. This can be done in several ways including path integral methods, stochastic processes in Hilbert space and common system-plus-environment models [53]. The effect of the environment is included indirectly in extra terms added to the equation of motion of $\hat{\rho}_O(t)$. The disadvantages are that finding an adequate dynamical map is not always possible and, in general, solving the equation of motion requires some assumptions to simplify it.

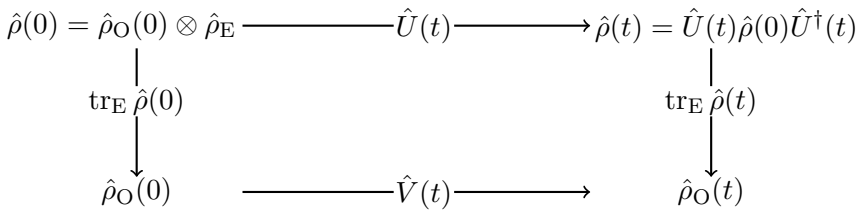

FIGURE 2.1. The time evolution of the central system can be obtained following two different routes. In the first route, the initial state of the central system is evolved to its final state at time t by means of a dynamical map. In the second route, the time evolution of the entire system is obtained first, then the state of the central system is extracted from this state via the partial trace. Adapted from [55].

As a closed system, the system-plus-environment state can be evolved with the appropriate unitary time evolution operator. Therefore, in principle, it is always possible to obtain its time evolution. Nevertheless, practical implementations of the methods in the second group requires a finite number of degrees of freedom of the environment. This demands clever ways of writing the equations of motion and efficient numerical methods to solve them.

2.1.1 Statistical approach

Focusing on the state of the central system, an equation of motion comprising the action of the environment on the system must be deduced. There are alternative methods to deduce such an equation. Within the standard framework of quantum mechanics, this can be achieved in terms of dynamical maps.

A dynamical map is an operation on the state of the central system such that it takes the initial state $\hat{\rho}_{\mathrm{O}}(0)$ and transforms it in the state at time t

$$\hat{\rho}_{\mathrm{O}}(t) = V(t)\hat{\rho}_{\mathrm{O}}(0) = \mathrm{tr}_{\mathrm{E}}\{\hat{U}(t)[\hat{\rho}_{\mathrm{O}}(0) \otimes \hat{\rho}_{\mathrm{M}}(0)]\hat{U}^{\dagger}(t)\}. \tag{2.6}$$

Nonunitary evolution of the reduced density operator produced by the interaction with the environment is accomplished by this map. Methods implementing this strategy include in general all master equations. Depending on the studied system and the approximations considered a large variety of master equations can be deduced.

In order to map states into states, the map must be a completely positive, trace-preserving linear map. In some cases, the map is not completely positive, yet the loss of positivity can be used to indicate the breakdown of some approximations assumed [56]. Another desired property for the dynamical map is the semigroup property

$$V(t_1)V(t_2) = V(t_1 + t_2), \quad t_1, t_2 \geq 0. \tag{2.7}$$

If some mathematical conditions are meet, one can find a linear map such that

$$V(t) = \exp(\mathcal{L}t), \tag{2.8}$$

where $\mathcal{L}$ is called the generator of the semigroup V. With this relationship, time derivative of (2.6) leads to

$$\dot{\hat{\rho}}_{\mathrm{O}}(t) = \mathcal{L}\hat{\rho}_{\mathrm{O}}(t). \tag{2.9}$$

A master equation has in general the form (2.9). Its solution gives the state of the central system at time t.

To illustrate the general procedure to obtain these kind of equations, consider first the unitary evolution of the state of the entire system. Its evolution is given by the von Neumann equation

$$\dot{\hat{\rho}}_{\mathrm{OE}}(t) = -\frac{i}{\hbar}\Big[\hat{H}, \hat{\rho}_{\mathrm{OE}}(t)\Big] = \mathcal{L}\hat{\rho}_{\mathrm{OE}}(t). \tag{2.10}$$

where $\mathcal{L}$ is the Liouvillian superoperator. Considering the general form of the Hamiltonian (2.1), the Liouvillian can be written as $\mathcal{L} = \mathcal{L}_{\mathcal{O}} + \mathcal{L}_{\mathcal{E}} + \mathcal{L}_{\mathcal{OE}}$. If a projector operator is defined such that $\hat{\rho}_{\mathrm{O}} = \hat{P}\hat{\rho}_{\mathrm{OE}}$, then

$$\hat{\rho}_{\mathrm{OE}} = \hat{P}\hat{\rho}_{\mathrm{OE}} + (\hat{I} - \hat{P})\hat{\rho}_{\mathrm{OE}}. \tag{2.11}$$

With these elements, the state of the central system at a given time t can be written as

$$\begin{aligned}\dot{\hat{\rho}}_{\mathrm{O}}(t) =& \hat{P}\mathcal{L}\hat{\rho}_{\mathrm{O}}(t) + \int_0^t dt' \hat{P}\mathcal{L}\exp\Big[(\hat{I} - \hat{P})\mathcal{L}t'\Big](\hat{I} - \hat{P})\mathcal{L}\hat{\rho}_{\mathrm{O}}(t - t') \\ &+ \hat{P}\mathcal{L}\exp\Big[(\hat{I} - \hat{P})\mathcal{L}t\Big](\hat{I} - \hat{P})\hat{\rho}_{\mathrm{OE}}(0).\end{aligned} \tag{2.12}$$

This expression is known as the Nakajima-Zwanzig equation. It formally gives the equation of motion for the state of the central system. However, its evaluation is quite involved, hence some assumptions are required to simplify it.

A first approximation is to consider that the coupling between system and the environment is weak. This implies that interaction with the central system does not modify the state of the environment. A second approximation is to consider that the evolution of $\hat{\rho}_{\mathrm{O}}$ depends only on its value at time t and not on its complete history. Both assumptions are known as the Born-Markov approximation. Additionally, the projector operator $\hat{P}$ can be chosen so that it commutes with $\mathcal{L}_{\mathrm{O}}$ and the projection on the initial state of the environment $(\hat{I} - \hat{P})\hat{\rho}_{\mathrm{OE}}(0) = \hat{\rho}_{\mathrm{E}}(0)$ can be ignored. With these considerations, the equation of motion can be written as

$$\dot{\hat{\rho}}_{\mathrm{O}}(t) = \hat{P}(\mathcal{L}_{\mathrm{O}} + \mathcal{L}_{\mathrm{OE}})\hat{\rho}_{\mathrm{O}}(t) + \int_0^t dt' \hat{P}\mathcal{L}_{\mathrm{OE}}\exp\Big[(\hat{I} - \hat{P})\mathcal{L}t'\Big](\hat{I} - \hat{P})\mathcal{L}_{\mathrm{OE}}\hat{\rho}_{\mathrm{O}}(t). \tag{2.13}$$

The first term on the right-hand side of (2.13) accounts for the unitary time evolution while the second comprises all nonunitary effects.

The most general completely positive, trace-preserving linear map has the form

$$\hat{\rho}'_{\mathrm{O}} = \sum_l \hat{A}_l \hat{\rho}_{\mathrm{O}} \hat{A}_l^\dagger, \tag{2.14}$$

where the operators $\hat{A}_l$ satisfy the condition

$$\sum_l \hat{A}_l \hat{A}_l^\dagger = \hat{I}. \tag{2.15}$$

For these dynamical maps, the master equation can be written in the Lindblad form

$$\dot{\hat{\rho}}_{\mathrm{O}}(t) = -\frac{i}{\hbar}\left[\hat{H}_{\mathrm{O}}, \hat{\rho}_{\mathrm{O}}(t)\right] + \frac{1}{2}\sum_{l}\left\{\left[\hat{L}_l\hat{\rho}_{\mathrm{O}}(t), \hat{L}_l^{\dagger}\right] + \left[\hat{L}_l, \hat{\rho}_{\mathrm{O}}(t)\hat{L}_l^{\dagger}\right]\right\}. \tag{2.16}$$

The operators $\hat{L}_l$ are called Lindblad operators and they must be deducted depending on the concrete application. The use of master equations in the Lindblad form is common in many fields of quantum physics.

Information of the environment is included typically in the master equation in terms of bath correlation functions

$$\left\langle \hat{B}_k^{\dagger}(t)\hat{B}_l(t-t')\right\rangle = \mathrm{tr}_{\mathrm{E}}\left[\hat{B}_k^{\dagger}(t)\hat{B}_l(t-t')\hat{\rho}_{\mathrm{E}}\right] \tag{2.17}$$

where $\hat{B}_{l,k}$ are operators in the interaction Hamiltonian (2.2) acting on the environment only. It is worth stressing the time-invariant nature of the state of the environment pointed out in (2.17). Bath correlation functions can be simplified significantly if a continuous spectrum of frequencies is considered. This is not only mathematically convenient, but it is a physically sensible assumption due to the vast number of degrees of freedom composing the environment.

Relaxation of quantum systems interacting with an environment has been largely studied using this approach. General models to study decoherence have also followed mainly this route. There is however an alternative route to study open quantum systems, offering the possibility of studying these systems in regimes where assumptions made to deduce quantum master equations are not valid.

2.1.2 Unitary approach

The challenge of obtaining the time evolution of the entire system requires methods to solve the time-dependent Schrödinger equation for a system with many degrees of freedom. In this respect, different strategies have been proposed and applied successfully to open quantum systems. First proposals in this direction includes semiclassical approximations as the frozen Gaussian method [57] and the Herman-Kluk propagator [58]. More elaborate methods include the multi-configuration time-dependent Hartree method (MCTDH) and its different variations [59, 60]. The relationship between the variational coherent states, the coupled coherent states and Herman-Kluk methods has been pointed out in [61]. These methods have been studied and applied in quantum chemistry to understand different phenomena involving the dynamics of molecular aggregates.

The main assumption in this route for the time evolution of open quantum systems is that dynamics of the central system converges with a moderate number of degrees of freedom modeling the environment. This is a challenging task to achieve because the number of orthogonal basis states required to solve the time-dependent Schrödinger equation increases exponentially with the number of degrees of freedom. Therefore, even for a small number of degrees of freedom, the solution of the equations of motion seems unfeasible.

To circumvent this difficulty, states of the system must be written in terms of convenient basis states that allow to overcome the exponential scaling. Due to their properties, coherent states are suited for this task. Once the state is written in terms of such states, the application of variational principles leads to equations of motion of the parameters

specifying the state. Solution of these equations amounts to solve the time-dependent Schrödinger equation.

For a one-dimensional harmonic oscillator with ground state $|0\rangle$, a general coherent state is defined as

$$|\gamma\rangle = \hat{D}(\gamma)\,|0\rangle\,, \tag{2.18}$$

where

$$\hat{D}(\gamma) = \exp\Big(\gamma\hat{a}^\dagger - \gamma^*\hat{a}\Big) \tag{2.19}$$

is a displacement operator. The complex number

$$\gamma = \sqrt{\frac{m\omega}{2\hbar}}\left(q + i\frac{p}{m\omega}\right) = \mathrm{Re}(\gamma) + i\mathrm{Im}(\gamma) \tag{2.20}$$

defines the phase-space coordinates $\mathbf{r} = (p, q)$ of the centroid of the coherent state.

Coherent states form an overcomplete basis set of the Hilbert space

$$\int d^2\gamma \frac{1}{\pi}\,|\gamma\rangle\langle\gamma| = \hat{I}, \tag{2.21}$$

but it is not orthogonal because the overlap between two coherent states $|\gamma\rangle$, $|\gamma'\rangle$

$$\left|\langle\gamma|\gamma'\rangle\right| = \exp\Big(-\left|\gamma - \gamma'\right|^2\Big) \tag{2.22}$$

is always positive. An advantage of overcompleteness is that subsets of coherent states arranged in a grid $\gamma_{n,m} = \lambda(n+im)$, where $n, m \in \mathbb{Z}$, constitute an approximate complete set if $0 < \lambda < \sqrt{\pi}$ [62]. A complete basis set is obtained when $\lambda = \sqrt{\pi}$, called a von Neumann lattice, where each coherent state occupies exactly one Planck cell in phase space.

The time evolution of coherent states under the action of the harmonic oscillator Hamiltonian conserves its shape and the centroid follows a classical trajectory in phase space [63]. In this sense, coherent states are the closest analog of classical states in quantum mechanics. However, under the action of more general Hamiltonians a coherent state does not remain as a coherent state.

The properties of coherent states are exploited by various methods to solve the time-dependent Schrödigner equation. This is particularly convenient for systems comprising a large but finite number of degrees of freedom. In the context of open quantum systems, these methods can be extended to account for the dynamics of the entire system composed by the central system and its environment. The state of the central system can be obtained easily by tracing out the degrees of freedom of the environment.

The main concern of this route is the convergence of the results, but it constitutes a numerical exact method for the dynamics of open quantum systems. Notice that no further assumptions are included in this strategy, allowing to explore regions where master equations do not work once convergence is guaranteed. For the model proposed in this work the second route for the time evolution of open quantum systems is more appropriate.

2.2 Feynmann-Vernon and Caldeira-Leggett models

As was mentioned before, the Langevin equation allows a phenomenological description of dissipation in classical systems. However, it is desirable to have a microscopic model justifying this description. The Caldeira-Leggett model provides this microscopic account of dissipation. It constitutes the most general Hamiltonian leading to the Langevin equation in its classical limit [53]. This model follows the general framework of a quantum system interacting with a linear dissipative environment defined by Feynmann and Vernon [54].

Assume that the Hamiltonian of the entire system have the form (2.1) with

$$\hat{H}_{\mathrm{O}} = \frac{\hat{p}^2}{2M} + V(\hat{q}). \tag{2.23}$$

where $V(\hat{q})$ is the potential and $\hat{p}$, $\hat{q}$ are the momentum and position operators of the central system, respectively. The main assumption of the Caldeira-Leggett model is that the dynamics of the central system does not perturb the state of the environment significantly. It means that if the environment is composed of a number N of modes, each of them couples weakly with the central system. Under this condition, in the dynamics of the environment double excitation between energy levels is negligible and its response can be assumed to be linear [64].

In this scenario, the dynamics of the system is correctly obtained if the Hamiltonian of the environment and the coupling have the form

$$\hat{H}_{\mathrm{E}} = \sum_{n=1}^{N} \left(\frac{\hat{p}_n^2}{2m_j} + \frac{1}{2} m_n \omega_j^2 \hat{x}_n^2 \right) \tag{2.24}$$

$$\hat{H}_{\mathrm{OE}} = \sum_{n=1}^{N} F_n(\hat{q}) \hat{x}_n + \delta V(\hat{q}). \tag{2.25}$$

The linear coupling term causes a renormalization of the potential $V(\hat{q})$. To compensate for this effect, the second term in the right-hand side of (2.25) is added. A separable interaction term is obtained by choosing the same function of the central system coordinates in (2.25) weighted by some coefficients for each n

$$F_n(\hat{q}) = C_n F(\hat{q}). \tag{2.26}$$

In the classical limit, the damping rate can be expressed in terms of the parameters of the Caldeira-Leggett model. The connection is made by means of the spectral density function

$$J(\omega) = \frac{\pi}{2} \sum_n g_n^2 \delta(\omega - \omega_n) \tag{2.27}$$

where $g_n = c_n^2 / m_n \omega_n$. Instead of considering this discrete spectral density, one can draw a connection with a suitable continuous function $J(\omega)$ if the environment contains many modes so that frequencies form a continuum.

The form of the spectral density should consider the characteristics of dissipation as well as the particularities of the system studied. When dissipation depends only on the state of the velocity $\dot{q}(t)$ at time t, the frequency damping rate is constant $\tilde{\eta}(\omega) = \alpha$. This

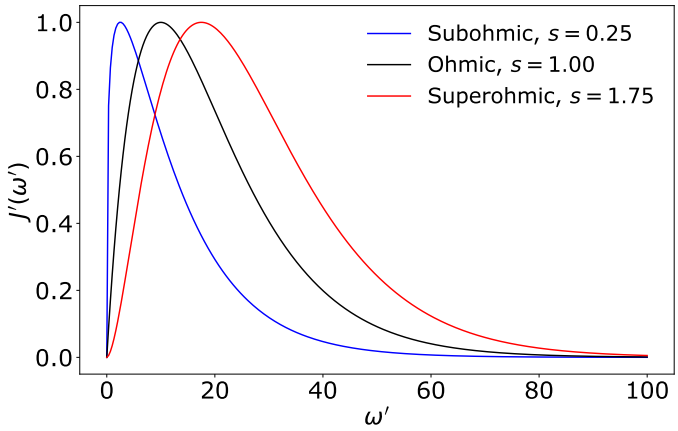

FIGURE 2.2. Spectral density function $J'(\omega') = J(\omega)/\omega_c$ with $\omega' = \omega/\omega_c$ and an exponential cut-off function. Depending on the value of the exponent s, the spectral density function emphasizes the low-frequency modes (subohmic) or the high-frequency modes (superohmic) with respect to the ohmic case.

case is described by a spectral density of the form $J(\omega) = \alpha\omega$. Dissipation in this limit is called ohmic.

More general dissipative effects could be frequency dependent. To model this situation, it is convenient to consider a power law dependence of the spectral density function $J(\omega) \propto \omega^s$, where s is any positive number. Dissipation for $0 < s < 1$ is called subohmic, $s = 1$ ohmic and $s > 1$ superohmic. On the other hand, to avoid divergences of physical quantities in the limit $\omega \to \infty$ an appropriate cutoff function $f_{\text{co}}(\omega/\omega_c)$ is included. The cutoff frequency ω_c indicates that for values $\omega \gg \omega_c$ the spectral density function becomes negligible. With these considerations, a generic form of the spectral density function used in applications reads

$$J(\omega) = \frac{\pi}{2}\alpha\omega_c^{1-s}\omega^s f_{\text{co}}(\omega/\omega_c). \tag{2.28}$$

The parameter α is usually called the Kondo parameter and it indicates the overall coupling between the environment and the central system. Typical cutoff functions are [65]

$$\begin{aligned} f_{\text{co}}(\omega/\omega_c) &= \theta(1-\omega/\omega_c) && \text{Heaviside,} \\ f_{\text{co}}(\omega/\omega_c) &= e^{-\omega/\omega_c} && \text{Exponential,} \\ f_{\text{co}}(\omega/\omega_c) &= \tfrac{1}{1+(\omega/\omega_c)^2} && \text{Drude.} \end{aligned} \tag{2.29}$$

The Caldeira-Leggett model establishes a general method to model the environment as a set of harmonic oscillators coupled linearly to the central system in terms of their coordinates. The time evolution of an open quantum system is reduced to the time evolution of the central system and a finite number of harmonic modes. With a moderate number of these modes, dynamics of the system can be obtained using time propagation methods in terms of coherent states.

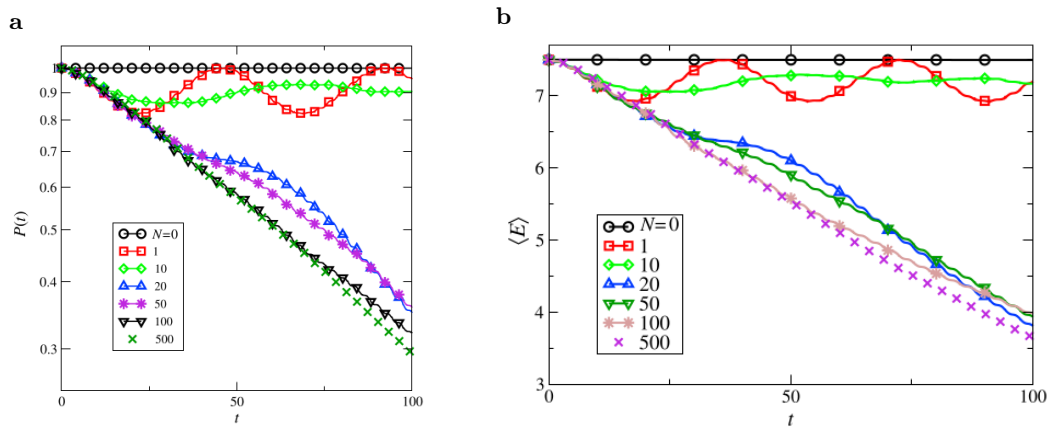

FIGURE 2.3. Approach to decoherence and dissipation in harmonic oscillator coupled linearly to a heat bath comprising a finite number of boson modes, for increasing mode number N. (a) Semilogarithmic plot of the purity of the reduced density operator for the central oscillator, as function of time. (b) Mean energy of the central oscillator vs. time. Color and symbol codes for $N = 0, 1, 10, 20, 50, 100, 500$ in the insets. Reproduced from [10].

2.3 Finite-bath models

The idea behind the use of a finite number of degrees of freedom to model the environment is to take advantage of the time evolution of closed systems while reproducing dissipative and damping effects in the relevant time scales of the observed system. This approach has been applied to study microscopic models for these phenomena in classical as well as quantum systems.

The description of dissipation in classical systems, based on usual methods in statistical mechanics, is justified for systems comprising an infinite number of particles, representing a continuous spectrum of frequencies. However, it has been shown that with a finite number of particles for the environment this effect can be effectively reproduced on the observed system. Thermalization of a central harmonic oscillator coupled with a finite bath was studied in [66]. In this study, thermalization is only observed for specific values of the mass and the frequency of the central harmonic oscillator and the particles composing the bath. The energy exchange with the environment has a strong dependence on the number of particles modeling the environment. For lower values, energy is recovered by the central system, but dissipative effects are stronger with an increasing number of particles. This dependence is related to the Poincaré recurrence time of the system [67]. The ergodic nature of the system coupled with a finite bath was pointed out in [68].

The ability of this approach to reproduce dissipation is compromised by the degrees of freedom of the central system. With a central system composed of a small number of harmonic oscillators, dissipation is not observed for a finite bath with a typical number of particles of the environment [69]. On the other hand, there exists an intricate relationship between the dynamics of the central system and the structure of the environment. The relationship between energy exchange and the non-linear, even chaotic, behavior of the central system and the environment is studied in [70, 71].

Recent findings have shown that not only dissipation but also decoherence effects have been successfully reproduced in quantum systems using this approach. The thermalization of molecules in solution can be reproduced satisfactorily by coupling to a small number of harmonic oscillators [9, 10]. No more than $N \sim 10$ modes are necessary to mimic decoherence and dissipation on chemically relevant time scales, despite the unitarity of the time evolution (Fig. 2.3).

Although the usual description of dissipation assumes an infinite number of degrees of freedom for the environment, these studies have shown that this phenomenon can be effectively reproduced with a finite heat bath. With this environment characterized by a discrete spectrum, revivals in the dynamics of the central system are expected. The time required for these revivals can be diminished by increasing the number of harmonic oscillators modeling the environment. Therefore, an environment with a discrete but dense spectrum coupled with a central system is adequate for studying dissipation and decoherence on relevant time scales.

2.4 Multi-Davydov ansatz

The Davydov ansatz was devised to study excitations in one-dimensional molecular chains [72, 73, 74]. It states a solution of the time-dependent Scrödinger equation as a superposition of number states with time-dependent coefficients. In the same spirit, one can consider coherent states instead

$$|\psi(t)\rangle = \sum_{l=1}^{M} C_l(t)\,|\gamma_l(t)\rangle\,, \tag{2.30}$$

where both the coefficients and the displacements of the coherent states are time dependent. The parameter M is the multiplicity and indicates the number of coherent states considered in the ansatz. The time-dependent displacement is characterized by the coordinates at time t of its centroid

$$\gamma_l(t) = \sqrt{\frac{m\omega}{2\hbar}}\left(q_l(t) + i\frac{p_l(t)}{m\omega}\right). \tag{2.31}$$

As was mentioned before, finite sets of coherent states constitute a good basis set of the Hilbert space. This property can be generalized for a number N of modes in terms of multi-mode coherent states

$$|\boldsymbol{\gamma}_l(t)\rangle = \bigotimes_{n=1}^{N} |\gamma_{ln}(t)\rangle\,, \tag{2.32}$$

where $|\gamma_{ln}(t)\rangle$ are one-mode coherent states. The overlap between two multi-mode coherent states reads

$$\left|\langle\boldsymbol{\gamma}|\boldsymbol{\gamma}'\rangle\right| = \exp\left(-\sum_{n=1}^{N}\left|\gamma_n - \gamma_n'\right|^2\right). \tag{2.33}$$

For an environment modeled as a set of harmonic oscillators, the ansatz (2.30) with multi-mode coherent states (2.32) works as a good basis set avoiding the exponential scaling when more modes are added to the environment. A grid of M multi-mode coherent states, with the appropriate distance between them, must be constructed in the $2N$-dimensional phase space.

The ansatz can be extended to include a central system coupled to an environment modeled by a number N of harmonic oscillators. If the central system has a discrete spectrum, its Hilbert space is spanned by an orthogonal basis set $\{|v_j\rangle\}_{j=1}^{N_\mathrm{O}}$, with N_O the dimension of the Hilbert space. A basis vector of the total Hilbert space $\mathcal{H}_\mathrm{O} \otimes \mathcal{H}_\mathrm{E}$ can be constructed in terms of the basis set for the central system and the coherent states serving as basis set of $\mathcal{H}_\mathrm{E}$. There are different alternatives for such construction. In the D1-ansatz, for each basis vector of the central system $|v_j\rangle$ there is a multi-mode coherent state associated to it. A given state of the entire system is then written as

$$\left|\Psi^M_{\mathrm{D1}}(t)\right\rangle = \sum_{l=1}^{M}\sum_{j=1}^{N_\mathrm{O}} C_{jl}(t)\,|v_j\rangle\left|\boldsymbol{\gamma}_{jl}(t)\right\rangle. \tag{2.34}$$

In contrast, in the D2-ansatz all the basis vectors $|v_j\rangle$ share the same coherent state

$$\left|\Psi^M_{\mathrm{D2}}(t)\right\rangle = \sum_{l=1}^{M}\left(\sum_{j=1}^{N_\mathrm{O}} C_{jl}(t)\,|v_j\rangle\right)|\boldsymbol{\gamma}_{l}(t)\rangle. \tag{2.35}$$

An intermediate option between (2.34) and (2.35), termed as D1.5-Davydov ansatz, is proposed in [75].

Equations of motion for the coefficients and displacements of the coherent states can be deduced by application of the Dirac-Frenkel variational principle [76]

$$\left\langle \Psi\delta\middle| i\hbar\frac{d}{dt} - \hat{H}\middle|\Psi\right\rangle = 0. \tag{2.36}$$

The equations of motion for the D1-ansatz are

$$\langle v_j|\left\langle\vec{\gamma}_{jk}\middle| i\hbar\frac{d}{dt} - \hat{H}\middle|\Psi^M_{\mathrm{D1}}(t)\right\rangle = 0, \tag{2.37a}$$

$$\sum_{j=1}^{N_\mathrm{O}} C^*_{jk}\,\langle v_j|\left\langle\vec{\gamma}_{jk}\middle|\hat{a}_r\left(i\hbar\frac{d}{dt} - \hat{H}\right)\middle|\Psi^M_{\mathrm{D1}}(t)\right\rangle = 0. \tag{2.37b}$$

with $\hat{a}_r$ the annihilation operator acting on states of the mode r. For the D2-ansatz the equations are

$$\langle v_j|\left\langle\vec{\gamma}_{k}\middle| i\hbar\frac{d}{dt} - \hat{H}\middle|\Psi^M_{\mathrm{D1}}(t)\right\rangle = 0, \tag{2.38a}$$

$$C^*_{jk}\,\langle v_j|\left\langle\vec{\gamma}_{k}\middle|\hat{a}_r\left(i\hbar\frac{d}{dt} - \hat{H}\right)\middle|\Psi^M_{\mathrm{D1}}(t)\right\rangle = 0. \tag{2.38b}$$

The number of parameters to be determined in the numerical implementation of these propagation methods are $MN_\mathrm{O}(N+1)$ for the D1-ansatz and $M(N_\mathrm{O}+N)$ for the D2-ansatz. The latter has proven to have better performance and stability in simulations for different systems, including the spin-boson model, a central piece for this work [77]. For this reason, simulations in this work were obtained with the D2-ansatz.

Using as basis set of the Hilbert space of the spin the eigenstates of the $\hat{\sigma}_z$ operator, the D2-ansatz for a spin coupled to an environment modeled as a set of harmonic oscillators

reads

$$\left|\Psi_{\mathrm{D2}}^{M}(t)\right\rangle = \sum_{l=1}^{M}(C_{l+}\left|+_z\right\rangle + C_{l-}\left|-_z\right\rangle)\left|\boldsymbol{\gamma}_l(t)\right\rangle . \tag{2.39}$$

The explicit derivation of the equations of motion of the ansatz (2.39) and further details of the implementation are found in the appendix.

CHAPTER 3

A model for spin measurements

In this chapter the proposed model to simulate the entire spin measurement process within the framework of unitary dynamics is introduced. For the purposes of this work, a simplified model comprising the object (O) and the environment (E) is considered. After some reasonable considerations within the spin measurement context, a spin-boson model is finally obtained. Then, dynamics of spin-boson model are reviewed for two limiting cases $N = 1$ (Rabi model) and $N \to \infty$, with N the number of modes of the environment.

Symmetries present in the Hamiltonian and the initial state of the object will lead to the requirement of an initial asymmetry of the initial state of the environment to observe the breaking of the symmetry in the final state of the object. This effect is demonstrated first with the Rabi model.

Finally, conditions needed for the initial state of the environment to simulate unbiased measurements are established. The important argument against the unitary description of the entire measurement process regarding superposition states is also discussed.

3.1 Constructing the model

As was shown in chapter 1, the most complete account of measurement process as a continuous process in unitary time evolution involves three subsystems: the object, the meter and the environment. The Hamiltonian describing the entire system contains the free Hamiltonian of each subsystem, the object-meter and the meter-environment interaction terms

$$\hat{H} = \hat{H}_{\mathrm{O}} + \hat{H}_{\mathrm{M}} + \hat{H}_{\mathrm{E}} + \hat{H}_{\mathrm{OM}} + \hat{H}_{\mathrm{ME}}. \tag{3.1}$$

If there were an interaction between the object and the environment, one would separate the degrees of freedom of the environment and consider an extended apparatus. Then, this new system can be described by the general Hamiltonian (3.1).

If one is interested in modeling a projective spin measurement, the desired direction for the measurement can be specified in the interaction term. In that case the distinction between meter and environment, and their internal structure is not of primary importance. In order to simplify as much as possible the model, meter and environment are merged in one subsystem, reducing the number of components to two and the Hamiltonian to three

terms, the self-energies of object and environment and their coupling

$$\hat{H} = \hat{H}_{\mathrm{O}} + \hat{H}_{\mathrm{E}} + \hat{H}_{\mathrm{OE}}. \tag{3.2}$$

Prior measurement the object should be prepared in a definite initial state. For a spin, an energy splitting between energy levels is required. It is typically accomplished by aligning the spin to a magnetic field $\mathbf{B} = B\mathbf{u}_B$ in the direction $\mathbf{u}_B$ of the intended initial polarization, here the x-direction, related to the energy splitting by $\hbar\omega_0 = \mu B$ (with $\mu = g_s\mu_B/2$, the magnetic moment of the spin, g_s denoting the spin g-factor and μ_B the Bohr magneton). This preparation step is represented by the self-energy term

$$\hat{H}_{\mathrm{O}} = \frac{1}{2}\hbar\omega_0\hat{\sigma}_x, \tag{3.3}$$

where the standard notation for the Pauli matrices is assumed.

The self-energy term of the environment can be modeled as a set of harmonic oscillators, following the Caldeira-Leggett model. Considering the form of the time-evolution algorithm to be implemented in the simulations, it is convenient to write this Hamiltonian in terms of annihilation and creation operators

$$\hat{H}_{\mathrm{E}} = \sum_{n=1}^{N} \hbar\omega_n \hat{a}_n^\dagger \hat{a}_n. \tag{3.4}$$

The zero-point energy term is dropped because it only contributes with an overall phase in the dynamics of the system [77].

The intended measurement operator is $\hat{\sigma}_z$, therefore, the model represents measurements of the z-component of the spin. Assuming a strictly linear coupling between this operator and the position operators of the bath modes [78], the interaction Hamiltonian reads

$$\hat{H}_{\mathrm{OE}} = \hat{\sigma}_z \sum_{n=1}^{N} \hbar g_n (\hat{a}_n^\dagger + \hat{a}_n). \tag{3.5}$$

For this interaction term, the dynamics of the system is not affected by the counter-term required to compensate the renormalization of the potential (2.25) because it is proportional to the identity operator [77]. Adding an extra term to the self-energy Hamiltonian (3.3) proportional to the measured operator $\hat{\sigma}_z$ amounts to include a bias on the measurement.

With these elements, the Hamiltonian takes the form of a spin-boson model

$$\hat{H} = \frac{1}{2}\hbar\omega_0\hat{\sigma}_x f_{\mathrm{O}}(t) + \sum_{n=1}^{N} \hbar\omega_n \hat{a}_n^\dagger \hat{a}_n + \hat{\sigma}_z \sum_{n=1}^{N} \hbar g_n (\hat{a}_n^\dagger + \hat{a}_n) f_{\mathrm{OE}}(t). \tag{3.6}$$

The time-dependent modulating functions $f_{\mathrm{O}}(t)$ and $f_{\mathrm{O}}(t)$ are included to have the flexibility to model different measurement protocols. Sigmoid or box-shaped profiles can be used to turn on or off the self-energy and coupling terms. As a spin-boson model, there are multiple possible options of experimental realizations, for instance, a two-level atom in a high-Q cavity. It is worth mentioning that a similar model to measure the position of an electron, in which the meter is modeled as two-level atom in a metastable state together with the electromagnetic field, is suggested in [14].

3.2 Dynamics of the spin-boson model: from $N = 1$ to $N \to \infty$

In the spin-boson model, the smallest quantum system with nontrivial dynamics interacts linearly with an environment of harmonic oscillators. Under the appropriate conditions, a system described by a continuous coordinate in a potential with two minima, can be described as a two-level system [79]. Despite its simplicity, the spin-boson model has demonstrated its versatility in variate applications such as electron transfer theory [46, 80], different systems involving the interaction with radiation in quantum optics [81], donor and acceptor dynamics in conductivity [82], among others. Even some aspects involved in complex processes such as photosynthesis can be understood with this model [83]. Two limiting cases largely studied in literature serve as reference for this work. When the number of modes is infinite and when there is only one.

With only one mode, $N = 1$, the spin-boson model is a standard model for light-matter interaction known as the Rabi model

$$\hat{H}_{\mathrm{R}} = \frac{1}{2}\hbar\omega_0\hat{\sigma}_x + \hbar\omega_1\hat{a}^\dagger\hat{a} + \hbar g_1\hat{\sigma}_z(\hat{a}^\dagger + \hat{a}). \tag{3.7}$$

In applications in quantum optics, it is common to find the operators $\hat{\sigma}_x$ and $\hat{\sigma}_z$ interchanged, while the form (3.7) is more common in solid state physics. Both are related by a rotation around the y-axis. Under the rotating wave approximation, the Rabi Hamiltonian (3.7) reduces to the Jaynes-Cummings model [84]

$$\hat{H}_{\mathrm{JC}} = \frac{1}{2}\hbar\omega_0\hat{\sigma}_x + \hbar\omega_1\hat{a}^\dagger\hat{a} + \hbar g_1(\hat{\sigma}_-\hat{a}^\dagger + \hat{\sigma}_+\hat{a}), \tag{3.8}$$

With $\hat{\sigma}_\pm = (\hat{\sigma}_x \pm i\hat{\sigma}_y)/2$. This approximation is valid when $|\omega_0 - \omega_1| \ll \omega_0 + \omega_1$ and $g_1 < \omega_0$ [85]. Conservation of the number of excitations in the Jaynes-Cummings model makes it exactly solvable. However, even without such approximation, the spectrum of the Rabi model can be obtained analytically [86].

The quantity of interest in the dynamics of the spin-boson, Rabi and Jaynes-Cummings models is usually the polarization $P(t) = \langle\hat{\sigma}_z\rangle$. Therefore, initial states of the spin are the eigenvalues of $\hat{\sigma}_z\,|\pm_z\rangle = \pm\,|\pm_z\rangle$. In studies where the environment is in its ground state, the spin is prepared in the excited state $|+_z\rangle$. Agreement between the standard form of the Hamiltonian in quantum optics and the rotated Rabi model (3.7) is found if for the latter the initial states are the eigenvalues $\hat{\sigma}_x\,|\pm_x\rangle = \pm\,|\pm_x\rangle$ and the quantity considered is $\langle\hat{\sigma}_x\rangle$.

Generalizations of the rotating wave approximation, working in domains where the original does not hold, has been proposed [87]. The dynamics of the Rabi model in the adiabatic limit $\omega_0 < \omega_1$ is studied in [88] with initial thermal and coherent states for the harmonic oscillator. A clear distinction between collapses and revivals in the polarization is observed in these circumstances. Decoherence observed in the atom is related with photon production and this process is inhibited by damping [89]. In this last study, it is also claimed that antirotating terms present in the Rabi model are responsible for the observation of quantum reversibility and the emergence of chaos. It contrasts with the findings in [90], where it has been shown that chaos observed in the semiclassical analog of the Rabi model is not related with the dynamics of the quantum model with the same parameter values.

The evolution into factorized final states in the Jaynes-Cummings model, with the harmonic oscillator prepared in a coherent state with large average photon number, were interpreted as the build-up of correlations between the state of the spin and distinguishable states of the field, in the sense of the von Neumann measurement scheme [91]. A dynamical driven spin, where the effect of the central system on the environment is not neglected, shows transitions between mixed and pure states in its time evolution [92]. The frontier between the quantum regime and its classical counterpart is examined in [93]. It is argued that in this model the classical limit, interpreted as the transition from a pure state into a mixture, is reached without a related decoherence process.

In the opposite limit $N \to \infty$, an analytical solution of the spin-boson model was proposed in [94]. Using the block matrix representation, the time evolution operator of this system can be written in a closed form. The detailed study of this system by means of an integral functional approach [79] showed a rich dynamical behavior depending mainly on the nature of the dissipation modeled by the environment and its initial state. On the other hand, it is recognized the primary role of the low-frequency modes ($\omega \lesssim \omega_0$) in the behavior of the polarization $P(t)$. The non-interacting blip approximation (NIBA) is developed in this work as a powerful approximation to simplify calculations giving accurate results for the dynamics of the spin-boson model for a wide range of parameters.

In the subohmic regime, the dynamics ranges from localization at $T = 0$ to incoherent relaxation for $T \neq 0$. In the ohmic regime, the dynamics depends on the strength of the coupling showing localization, exponential decay, incoherent relaxation, and damped oscillations depending on this parameter. In the superohmic case, the dynamics shows mainly damped oscillations with a crossover to exponential relaxation at a particular temperature value.

This behavior was confirmed and complemented by other studies implementing different time-evolution approaches. The spin-boson with Drude cutoff function and ohmic dissipation was studied using the MCTDH method in [82, 95]. Different regimes depending on the cutoff frequency were explored; from adiabatic, where the environment time scale is slow compared to the spin time scale $\omega_0/\omega_c > 1$, to the nonadiabatic limit $\omega_0/\omega_c < 1$. The strong coupling regime with a moderately adiabatic environment ($0.2 < \omega_0/\omega_c < 1$) is identified as the breakdown of the NIBA approximation.

The effect of different parameters of the spin-boson model on the dynamics is studied with the multi-layer multi-configuration time-dependent Hartree (ML-MCTDH) method in the subohmic [65] and ohmic [96] regimes. In these studies, the environment is prepared initially in its ground state. A transition between coherent damped motion to localization is identified in the subohmic case. The boundary between both behaviors depends on the coupling strength and the exponent s. This is in clear contrast with the ohmic case where the dynamics comprehends damped coherent motion, incoherent decay, and localization, with a well-defined boundary between each behavior. The existence of this phase transition in the subohmic regime is also confirmed in the study of the dynamics using the numerical renormalization group [97]. The possibility of coherent damped motion is predicted also in the latter study, and it is proved even in the case of strong dissipation in [98].

As was shown, the spin-boson model exhibits a rich dynamical behavior. In the context of simulating spin measurements with the proposed model, regions where localization is observed are of primary interest. Using this same language, the possible outcomes of the measured operator $\hat{\sigma}_z$ are clearly localized states with $P(t) = \pm 1$.

3.3 Parameters of the model

The spin boson-model is completely defined by the values of the frequencies ω_n and the coupling constants g_n. For a discrete spectrum with many frequencies, it is appropriate to draw connection with continuous spectral distributions and then discretize it in a suitable manner. The couplings can be obtained from the spectral density function in the same fashion as the frequency spectrum.

The spectral distribution is defined with the aid of the frequency density function $\rho_f(\omega)$. For a discrete spectrum, it takes the form [99]

$$\rho_f(\omega) = \sum_{\substack{n \\ \omega \leq \omega_n \leq \omega + d\omega}} \delta(\omega - \omega_n). \tag{3.9}$$

To obtain the discrete frequencies ω_n it is convenient to consider a continuous and normalized frequency density. With this function, the frequency axis can be divided in N equally weighted subintervals $[x_{n-1}, x_n]$ [100]. One can select one frequency of each subinterval as the desired ω_n, for instance, the lower limit, the median or the upper limit. If the number of modes is large enough the difference between the limits or the median is small and there is no reason to expect disagreement in the dynamics with the selection of the particular value of ω_n. If the lower limit is chosen, the condition that defines the frequencies ω_n reads

$$\int_0^{\omega_n} d\omega \rho_f(\omega) = \frac{n}{N+1}, \quad n = 1, \ldots N. \tag{3.10}$$

In the same spirit, considering the discrete version of $J(\omega)$ (2.27), the condition defining the couplings is

$$g_n^2 = \frac{2}{\pi} \int_{x_{n-1}}^{x_n} d\omega J(\omega). \tag{3.11}$$

Condition (3.10) and (3.11) can be written as $(x_n - x_{n-1})\rho_f(\omega) = 1/N + 1$ and $(x_n - x_{n-1})J(\omega)/\pi = g_n^2$, respectively. With these expressions, the couplings are given by

$$g_n^2 = \frac{2J(\omega_n)}{(N+1)\pi\rho_f(\omega_n)}. \tag{3.12}$$

An exponential frequency density

$$\rho_f(\omega) = \frac{N+1}{\omega_c} e^{-\omega/\omega_c}, \tag{3.13}$$

allows to write the frequencies ω_n explicitly using the condition (3.10)

$$\omega_n = \omega_c \ln\left(\frac{N+1}{N+1-n}\right). \tag{3.14}$$

Once the frequencies are determined, the coupling constants can be easily determined using the continuous spectral density (2.28) and the expression (3.12). Using an exponential cutoff in the spectral density, the coupling constants are given by

$$g_n^2 = \frac{\alpha \omega_c^{2-s} \omega_n^2}{2(N+1)}. \tag{3.15}$$

3.4 Symmetry properties

Symmetry is an important argument to justify the hypothesis that the environment must play a role in quantum measurement. If the Hamiltonian and the initial state of the object are symmetric under parity $z \to -z$, but the final state of the object breaks this symmetry, the only possible explanation is that the initial state of the environment must break the symmetry. This argument is mathematically more solid than information balances.

The spin-boson Hamiltonian possesses an important symmetry property: it is invariant under the parity transformation $P_z : z \to -z$. This inversion is achieved with the corresponding parity operator for the spin and for the harmonic modes composing the environment. The combined parity operator is

$$\hat{\Pi}_z = \hat{\Pi}_{z,\mathrm{O}}\hat{\Pi}_{z,\mathrm{E}} = \hat{\sigma}_x \exp\left(i\pi \sum_{n=1}^{N} \hat{a}_n^\dagger \hat{a}_n\right). \tag{3.16}$$

With this parity operator, the condition $\left[\hat{\Pi}_z, \hat{H}\right] = 0$ can be verified [101]. This symmetry implies that parity of states is a conserved quantity. Consequently, the total Hilbert space decomposes in two eigensubspaces of $\hat{\Pi}_z$

$$\mathcal{H} = \mathcal{H}_+ \oplus \mathcal{H}_-. \tag{3.17}$$

The states of the total system belonging to each subspace are composed of the eigenstates of the parity operators of the object and the harmonic oscillators. For the object, the eigenstates of the parity operator are $\hat{\sigma}_x |\pm_x\rangle = \pm |\pm_x\rangle$. For each harmonic oscillator, the parity operator is function of the number operator $\hat{n} = \hat{a}^\dagger \hat{a}$, therefore the eigenstates of this operator are $\hat{\Pi}_{z,\mathrm{E}} |n\rangle = (-1)^n |n\rangle$. Both eigensubspaces can be decomposed further in terms of the even (symmetric) and odd (antisymmetric) sectors of the Hilbert spaces of the object and the environment

$$\mathcal{H}_+ = \mathcal{H}_{+,\mathrm{O}} \otimes \mathcal{H}_{+,\mathrm{E}} \oplus \mathcal{H}_{-,\mathrm{O}} \otimes \mathcal{H}_{-,\mathrm{E}} \quad \text{and} \quad \mathcal{H}_- = \mathcal{H}_{-,\mathrm{O}} \otimes \mathcal{H}_{+,\mathrm{E}} \oplus \mathcal{H}_{+,\mathrm{O}} \otimes \mathcal{H}_{-,\mathrm{E}}. \tag{3.18}$$

The decomposition of the Hilbert space due to the parity symmetry has important consequences for spin measurements. If the initial state of the object and the environment belong to one of the subspaces (symmetric or antisymmetric), the dynamics induced by the spin-boson Hamiltonian keeps the total state in its corresponding eigensubspace. In addition, if the initial state of the object before the measurement satisfies $\langle \hat{\sigma}_z \rangle = 0$, the state is already invariant to P_z and it belongs to either $\mathcal{H}_{+,\mathrm{O}}$ or $\mathcal{H}_{-,\mathrm{O}}$.

The final state of the object after measurement, either $|+_z\rangle$ or $|-_z\rangle$, is clearly not invariant under P_z. The only possibility that the dynamics under the spin-boson Hamiltonian could leave the state of the object in such states is that the total initial state does not belong to $\mathcal{H}_+ \oplus \mathcal{H}_-$. The initial state of the environment must break the symmetry under P_z, whenever the initial state of the object satisfies it. In this sense, in the spin measurement context the dynamics of the total system should transfer the initial asymmetry present in the initial state of the environment to the state of the object. Since both invariant subspaces $\mathcal{H}_{+,\mathrm{O}}$ and $\mathcal{H}_{-,\mathrm{O}}$ have only one element in them, an initial state of the environment chosen at random will break the symmetry with probability 1.

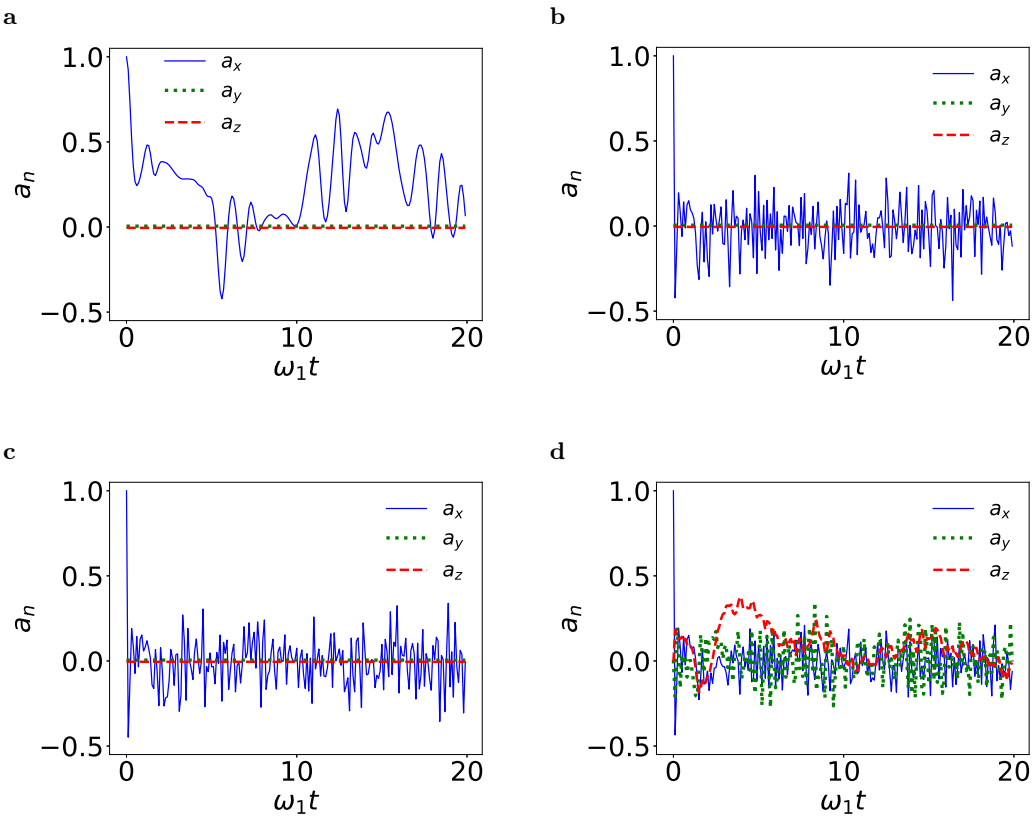

FIGURE 3.1. Simulation of spin measurements under well-defined symmetry conditions concerning parity $P_z : z \to -z$, Eq. (3.16). Panels show the time evolution of the components a_x (blue), a_y (green) and a_z (red), of the Bloch vector representing the state of the measured spin, prepared initially in the symmetric state $|\psi_{\mathrm{O}}(0)\rangle = |+_x\rangle \in \mathcal{H}_{+,\mathrm{O}}$, as function of scaled time $\omega_1 t$ under Hamiltonian (3.7) with a single boson mode, with particular initial states of the harmonic oscillator as follows: (a) ground state $|0_1\rangle$, (b) superposition of even Fock states $|2n_1\rangle$, $n_1 \in \mathbb{N}$ (element of the symmetric subspace $\mathcal{H}_{+,\mathrm{E}}$), (c) superposition of odd Fock states $|2n_1 + 1\rangle$ (element of the antisymmetric subspace $\mathcal{H}_{-,\mathrm{E}}$), (d) superposition of even and odd Fock states (no specific parity). Parameter values are $\omega_0/\omega_1 = 4$ and $g_1/\omega_0 = 2$.

The breaking of the symmetry in the spin state can be observed in Figure 3.1. The initial state of the object is the symmetric state $|+_x\rangle$. A deviation from the condition $\langle\hat{\sigma}_z\rangle = 0$ is observed only when the initial state of the environmental mode is neither symmetric nor antisymmetric.

3.5 Initial states of the object and the environment

The proposed model aims to reproduce the conventional measurement scheme resulting in a projection of the initial state of the object into the eigenspaces of the measured observable. Specifically, it is focused on measurements where each of the possible outcomes can be observed with the same probability. The initial states of the object and the environment should be selected to represent faithfully this setup.

It is reasonable to assume that object and environment have not interacted before the measurement. They are independent systems in a definite state. Therefore, the initial state of the entire system is

$$\hat{\rho}(0) = |\Psi(0)\rangle\langle\Psi(0)|\,, \quad |\Psi(0)\rangle = |\psi_{\mathrm{O}}(0)\rangle\,|\psi_{\mathrm{E}}(0)\rangle\,. \tag{3.19}$$

To reproduce a measurement with equal probabilities for each possible outcome, equivalent to tossing a fair coin, the initial state of the object must be invariant under $P_z : z \to -z$. Any superposition of the possible outcomes of the measurement, $|\pm_z\rangle$, giving a vector located at the equator of the Bloch sphere are valid states under this criterion. However, to properly interpret the self-energy Hamiltonian as a preparation phase, the appropriate choice for the initial state of the object is

$$|\psi_{\mathrm{O}}(0)\rangle = |\pm_x\rangle\,. \tag{3.20}$$

There are general properties that the initial state of the environment must fulfill. In first place, the state must not have a specific symmetry. Secondly, the state should reflect the uncontrollable nature of the degrees of freedom of the environment, thus it should not include a deliberate bias on the measurement. Finally, it should be compatible with the time-evolution algorithm. In this case, multi-Davydov ansatz requires the initial state of the environment to be written as a product of coherent states

$$\hat{\rho}_{\mathrm{E}}(0) = |\psi_{\mathrm{E}}(0)\rangle\langle\psi_{\mathrm{E}}(0)|\,, \quad \psi_{\mathrm{E}}(0) = \bigotimes_{n=1}^{N} |\gamma_n(0)\rangle\,. \tag{3.21}$$

The initial displacements of the modes should be selected to satisfy the conditions described above. A systematic bias is avoided if the multi-mode coherent state (3.21) fulfills

$$\begin{aligned} \left\langle \vec{Q}(0) \right\rangle &= 0, \quad \vec{Q}(0) = (q_1(0), q_1(0), \ldots, q_{\mathrm{N}}(0)), \\ \left\langle \vec{P}(0) \right\rangle &= 0, \quad \vec{P}(0) = (p_1(0), p_1(0), \ldots, p_{\mathrm{N}}(0)), \end{aligned} \tag{3.22}$$

where $\mathbf{r}_n = (q_n, p_n)$ are the phase-space coordinates of displacement of the n-th mode. The simplest option, all the modes prepared in the ground state $|\gamma_n(0)\rangle = |0_n\rangle$, $n = 1, \ldots, N$, will not result in $\langle\hat{\sigma}_z\rangle \neq 0$ because in that case the total state is invariant under $P_z : z \to -z$.

A convenient alternative is to sample the displacements from a probability distribution $p(\gamma_n, \gamma_n^*)$ with zero mean. For a sample of N displacements the condition of zero mean is not met perfectly, therefore, small random deviations are expected in each sample. These deviations reflect the fluctuations in the continuous limit.

Some considerations are needed to propagate the initial conditions (3.19) with the D2-ansatz. This method needs the construction of a grid of coherent states around the desired initial condition. For instance, in the Rabi model if the initial state of environmental harmonic oscillator is the ground state, the displacements of the M coherent states should be selected to form a grid with the ground state in the center. If the initial state is now γ_1, the grid should be constructed around this new center. In addition, the coefficients need to be adjusted in the D2-ansatz to be sure that the desired initial state is represented

properly in this ansatz. This can be done by choosing the initial coefficients as

$$C_{k\pm}(0) = \begin{cases} C_{k\pm}(0) \neq 0 & k = 1, \\ 0 & k \neq 1. \end{cases} \tag{3.23}$$

With all these elements, different measurement protocols can be implemented by different selections of the time-dependent modulating functions $f_{\mathrm{O}}(t)$ and $f_{\mathrm{OE}}(t)$. A crucial tool to follow the dynamics of the spin state $\hat{\rho}_{\mathrm{O}} = \mathrm{tr}_{\mathrm{E}}(\hat{\rho})$ is the Bloch vector

$$\begin{gathered} \hat{\rho}_{\mathrm{O}} = a_0(t)\hat{I}_{\mathrm{O}} + \mathbf{a}(t) \cdot \hat{\boldsymbol{\sigma}}, \\ \mathbf{a}(t) = (a_x(t), a_y(t), a_z(t)), \quad \hat{\boldsymbol{\sigma}} = (\hat{\sigma}_x, \hat{\sigma}_y, \hat{\sigma}_z). \end{gathered} \tag{3.24}$$

The initial condition (3.20) is defined by the coordinates $a_x(0) = \pm 1$, $a_y(0) = 0$, $a_z(0) = 0$ of the Bloch vector. In an ideal projective measurement, this initial state is projected to $a_x(0) = 0$, $a_y(0) = 0$, $a_z(0) = \pm 1$, corresponding to the poles of the Bloch sphere. The closeness of the simulations to a projective measurement will be assessed by the tendency of the Bloch vector to be localized around either of the poles of the Bloch sphere.

3.6 Initial superposition of states

One of the key features of unitary time evolution is the superposition principle. In the context of a unitary description of the measurement process, this principle imposes restrictions on the possible initial states leading to a definite outcome in a projective measurement [102]. The original argument refers to the initial states of the object. In this work, the focus is put on the initial state of the environment. Hence, this important argument is reviewed focusing on the initial state of the environment in a spin measurement.

Consider two initial states of the entire system of the form (3.20 and 3.21), which in the long term converge to opposite eigenstates of the measured operator $\hat{\sigma}_z$

$$\begin{aligned} |\Psi_{0-}\rangle &= |-_x\rangle\,|\psi_{\mathrm{E}0-}\rangle \xrightarrow[t\to\infty]{\hat{U}_{\mathrm{M}}} |-_z\rangle\,|\psi_{\mathrm{E}\infty-}\rangle\,, \\ |\Psi_{0+}\rangle &= |-_x\rangle\,|\psi_{\mathrm{E}0+}\rangle \xrightarrow[t\to\infty]{\hat{U}_{\mathrm{M}}} |+_z\rangle\,|\psi_{\mathrm{E}\infty+}\rangle\,. \end{aligned} \tag{3.25}$$

According to the superposition principle, a state of the form $C_1\,|\Psi_{0-}\rangle + C_2\,|\Psi_{0+}\rangle$, with $C_1, C_2 \in \mathbb{C}$, is also a valid state for the environment. The time evolution with this superposition state is

$$|-_x\rangle\,(C_1\,|\Psi_{0-}\rangle + C_2\,|\Psi_{0+}\rangle) \xrightarrow[t\to\infty]{\hat{U}_{\mathrm{M}}} C_1\,|-_z\rangle\,|\psi_{\mathrm{E}\infty-}\rangle + C_2\,|+_z\rangle\,|\psi_{\mathrm{E}\infty+}\rangle\,. \tag{3.26}$$

Suppose that there exist states of the object $\left|\psi'_{\mathrm{O},\infty}\right\rangle$ and the environment $\left|\psi'_{\mathrm{E},\infty}\right\rangle$ such that

$$C_1\,|-_z\rangle\,|\psi_{\mathrm{E}\infty-}\rangle + C_2\,|+_z\rangle\,|\psi_{\mathrm{E}\infty+}\rangle = \left|\psi'_{\mathrm{O},\infty}\right\rangle\left|\psi'_{\mathrm{E},\infty}\right\rangle. \tag{3.27}$$

Due to the orthogonality of the measured operator eigenstates $\langle +_z|-_z\rangle = 0$, the total state after time evolution can only be written as a product state if $|\psi_{\mathrm{E}\infty+}\rangle = k\,|\psi_{\mathrm{E}\infty-}\rangle$ for some

$k \in \mathbb{C}$. However, in that case

$$(C_1 |-_z\rangle + C_2 k |+_z\rangle) |\psi_{\mathrm{E}\infty-}\rangle = \left|\psi'_{\mathrm{O},\infty}\right\rangle \left|\psi'_{\mathrm{E},\infty}\right\rangle . \tag{3.28}$$

This shows that for the superposition state of the environment, the object evolves to a state which is not an eigenstate of the measured operator. The result does not forbid an unitary account of the measurement process. It says that within such a description there exist states of the environment with indefinite outcomes.

The time evolution of the spin with initial superposition states for the environment as are depicted in this argument will be evaluated later in this work. This will allow us to investigate in detail the dependence of the state of the spin in the long time for different initial superposition states.

CHAPTER 4

Polarized initial conditions

In the previous chapter some requirements on the initial conditions of the environment to reproduce faithfully a typical spin measurement were discussed. Particularly, compatibility with the D2-ansatz restricts the possible states to be written as a product of coherent states. Before considering initial conditions more appropriate for spin measurements, it would be illustrative to have at hand known initial conditions that can be written in this form, even if they do not fulfill the other requirements.

Polarized initial conditions are found when thermal equilibrium between the environmental harmonic oscillators and the spin prepared in the excited state [77, 98] is reached. In the limit of zero temperature, the equilibrium state of the environment can be written as a pure state compatible with the D2-ansatz. In this initial state, each mode is displaced in the real axis depending on its frequency and coupling constant. All the displacements have the same sign giving a mean value different from zero. In this sense, it is an intermediate step between the symmetric ground state and the desired initial conditions for spin measurements. The appropriate range for the parameters of the spin-boson model, where it is more likely to reproduce the spin measurement scenario, will be delimited by studying the dynamics of the Bloch vector with these particular initial conditions. Features of these conditions will suggest some properties of the possible distributions to sample the displacements satisfying all the requirements.

In the first part of this chapter, the polarized initial conditions are defined in general and the closed form for zero temperature is presented. The dynamics with these conditions for ohmic and subohmic regimes are explored, showing that the latter is more adequate for the aims of this work. For the moment, it is sufficient to consider constant modulating functions. Next, the effect of varying the parameters of the model in the asymptotic state of the spin is shown. A simple transformation of the polarized initial conditions will have the effect of driving the spin to the opposite pole. Finally, the results with an extra parameter included in the polarized initial conditions are discussed.

4.1 Thermal equilibrium and polarized initial conditions

If the spin is prepared initially in the ground state $|-_z\rangle$, it is reasonable to think that the initial state of the environment in equilibrium with this state of the spin, at zero

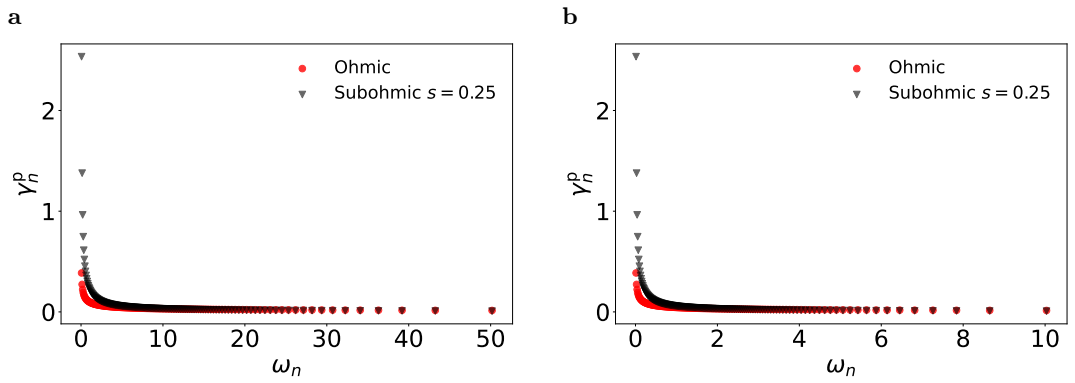

FIGURE 4.1. Magnitude of the initial displacements (4.4) defined by the initial state (4.5) for ohmic and subohmic environments with 150 modes. Different values of the cutoff frequency, in (a) $\omega_c/\omega_0 = 10$ and in (b) $\omega_c/\omega_0 = 2$, do not change the magnitude of the displacements.

temperature, is the ground state $|\mathbf{0}\rangle$. Contrary to one might think, if the initial state of the spin is $|+_z\rangle$ the equilibrium state of the environment deviates from the ground state.

The state of the environment in equilibrium with the excited state of the spin is defined by the thermal density operator

$$\hat{\rho}(0) = \hat{\rho}_{\mathrm{O}}(0) \otimes \hat{\rho}_{\mathrm{E}}^{\mathrm{T}}(0) = |+_z\rangle\langle+_z| \otimes \frac{\exp\left[-\beta(\hat{H}_{\mathrm{E}} + \hat{O}_{\mathrm{E}})\right]}{Z_{\mathrm{E}}}, \tag{4.1}$$

where $\beta = 1/kT$, $\hat{O}_{\mathrm{E}}$ is the operator in the interaction Hamiltonian $\hat{H}_{\mathrm{OE}}$ acting on the environment and $Z_{\mathrm{E}} = \mathrm{tr}_{\mathrm{E}}\left\{\exp\left[-\beta(\hat{H}_{\mathrm{E}} - \hat{O}_{\mathrm{E}})\right]\right\}$ is the partition function. In the case of the spin-boson model, the thermal density operator reads

$$\hat{\rho}_{\mathrm{E}}^{\mathrm{T}}(0) = \frac{\exp\left\{\sum_{n=1}^{N} \hbar\omega_n \hat{a}_n^\dagger \hat{a}_n + \hbar g_n(\hat{a}_n^\dagger + \hat{a}_n)\right\}}{Z_{\mathrm{E}}}. \tag{4.2}$$

In the simplest case $N = 1$, it can be shown that (4.2) reduces to [77]

$$\hat{\rho}_{\mathrm{E}}^{\mathrm{T}}(0) = (1 - \exp[-\beta\hbar\omega_1])\hat{D}_{\gamma_{n_1}^{\mathrm{p}}}^\dagger \sum_{n_1=0}^{\infty} \exp(-\beta\hbar\omega_1)\,|n_1\rangle\langle n_1|\,\hat{D}_{\gamma_{n_1}^{\mathrm{p}}}, \tag{4.3}$$

written in terms of the eigenstates of the harmonic oscillator $|n_1\rangle$ and the displacement operator

$$\hat{D}_{\gamma_{n_1}^{\mathrm{p}}}\,|0_1\rangle = \left|\gamma_{n_1}^{\mathrm{p}}\right\rangle, \quad \gamma_{n_1}^{\mathrm{p}} = \frac{g_1}{\omega_1}. \tag{4.4}$$

At zero temperature the state is $\hat{\rho}_{\mathrm{E}}^{\mathrm{T}}(0) = \hat{D}_{\gamma_{n_1}^{\mathrm{p}}}^\dagger\,|0_1\rangle\langle 0_1|\,\hat{D}_{\gamma_{n_1}^{\mathrm{p}}}$. In the case of N modes, each of them is displaced accordingly, therefore, the initial state of the environment can be written as

$$|\psi_{\mathrm{E}}(0)\rangle = \hat{D}_{\boldsymbol{\gamma}^{\mathrm{p}}}^\dagger\,|\mathbf{0}\rangle = |-\boldsymbol{\gamma}^{\mathrm{p}}\rangle, \quad |\boldsymbol{\gamma}^{\mathrm{p}}\rangle = \left|\gamma_{n_1}^{\mathrm{p}}\right\rangle\left|\gamma_{n_2}^{\mathrm{p}}\right\rangle\cdots\left|\gamma_{N}^{\mathrm{p}}\right\rangle. \tag{4.5}$$

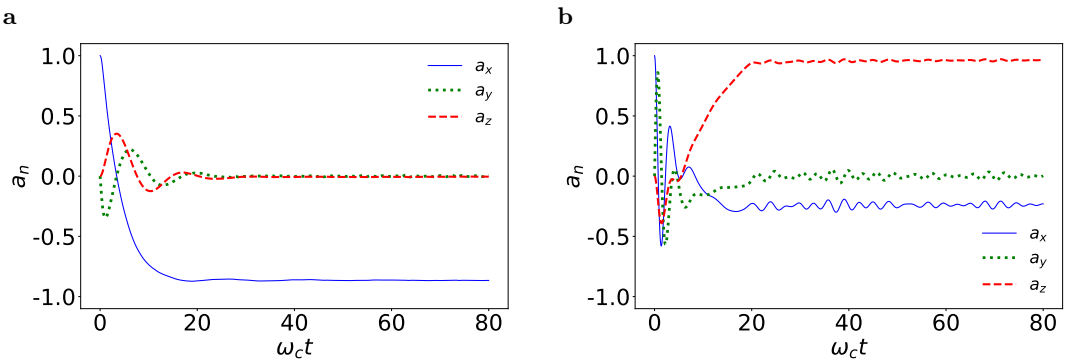

FIGURE 4.2. Time evolution of the Bloch vector with polarized initial conditions for the environment and a spin prepared initially in the state $|\psi_O(0)\rangle = |+_x\rangle$ for (a) ohmic and (b) subohmic regimes. Time is scaled in terms of the cutoff frequency $\omega_c = 2\omega_0$. Localization of the a_z component is enhanced in the latter case. The number of modes was $N = 150$ and the multiplicity of the method was $M = 10$. Further parameters are $\alpha = 0.3$ and $s = 0.25$ for the subohmic environment.

The magnitude of the displacements are shown in Figure 4.1 for ohmic as well as subohmic environments. The displacements are larger for small frequencies and decay rapidly with increasing values of the frequencies. This decay is more pronounced in the subohmic regime, where the displacements are larger compared to the ohmic case. The change of the cutoff frequency does not change the displacements, it only changes the frequency interval where they are assigned.

4.2 Localization of the spin state

Once the polarized initial conditions are defined, the time evolution of the system can be obtained with the D2-ansatz. There is, however, some difficulties with the convergence of the dynamics with a moderate number of modes in the time evolution with polarized initial conditions in the subohmic regime. The magnitude of the displacements diverges when $\omega_n \to 0$. To obtain the correct dynamics of the system the small modes must be vastly oversampled. With an exponential frequency density, a vast number of modes are needed for convergence of the dynamics. This difficulty can be overcome with the displaced Hamiltonian strategy described in [77]. It consists in translating the displacements to the Hamiltonian by means of a unitary transformation. In this setting, the dynamics of the spin state with polarized initial conditions is equivalent to the propagation with the environment in the ground state under the action of the displaced Hamiltonian.

The comparison of the dynamics with polarized initial conditions with different dissipation models, using the same parameter values, reveals that in the subohmic regime the Bloch vector tend to localize in the vertical axis of the Bloch sphere pointing to its north pole. In contrast, for ohmic dissipation the initial state exhibits small deviations from zero of the components a_x and a_y that rapidly decay. The behavior of a_z signals the evolution towards the state of minimum energy $|-_x\rangle$. This indicates that dissipation dominates in the ohmic regime.

The behavior of the Bloch vector in the subohmic regime is closer to a spin measurement scenario. The initial state located at the equator moves toward one of the eigenvectors of the measured operator and stabilizes there. This suggests that time evolution with subohmic environments is the most promising regime to reproduce faithfully a spin measurement setting.

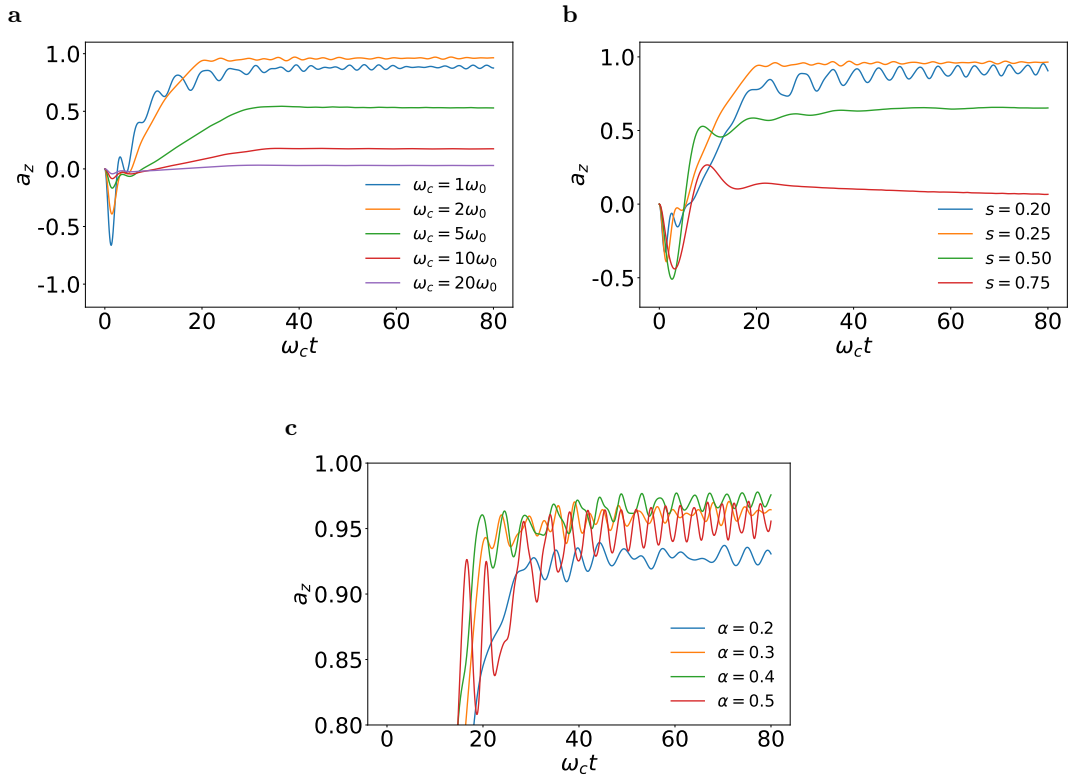

FIGURE 4.3. Behavior of the a_z component for different values of (a) the cutoff frequency ω_c, (b) the exponent s and (c) the Kondo parameter α for a subohmic environment with polarized initial conditions. Further parameters as in Fig. 4.2.

Localization is affected by different values of the parameters in the spin-boson model. Larger values of the cutoff frequency give states localized farther from the north pole of the Bloch sphere. However, for a cutoff frequency equal to the frequency of the spin $\omega_c = \omega_0$ the state localizes below the closest result with $\omega_c = 2\omega_0$.

Subohmic regime comprehends values of the exponent between $0 < s < 1$. Localization diminishes with environments closer to the ohmic case $s = 1$. This also happens for values below $s = 0.25$, where the stability of the localization is compromised due to the emergence of small oscillations around $a_z \neq 0$, compared with the dynamics observed with other values of s.

Increasing the overall strength of the coupling between the environment and the spin results in a smaller distance between the localized state and the value $a_z = 1$. This tendency is broken for values beyond $\alpha = 0.4$, where it starts to decrease.

Gathering these results, an environment characterized by a moderate adiabaticity ($\omega_0/\omega_c = 0.5$), in the deep subohmic regime ($s = 0.25$) and strongly coupled to the

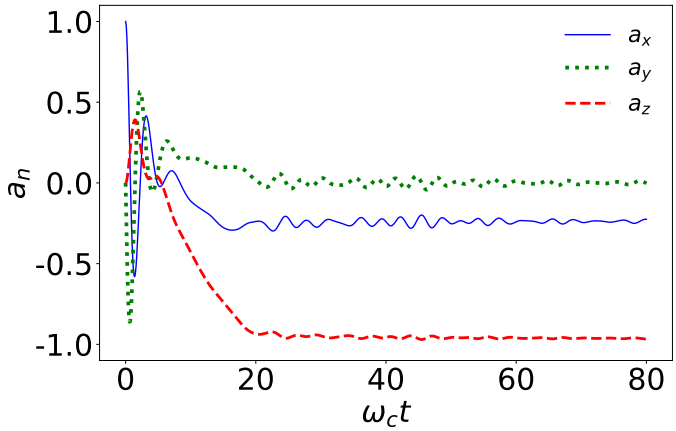

FIGURE 4.4. Dynamics of the Bloch vector with reflected initial conditions 4.6. The parameter values are the same as used in Figure 4.2b.

spin, enhances localization close to the north pole. Therefore, an environment with these characteristics seems to be the best candidate to simulate spin measurements.

4.3 Reflected polarized initial conditions

Localization of the a_z component is restricted to positive values with polarized initial conditions. Changes in the parameters of the spin-boson model only make its value closer to $a_z = 1$ or $a_z = 0$. Is it possible to obtain localization towards the other pole of the Bloch sphere?

Localization of the Bloch vector pointing to the south pole can be achieved by a change of the sign of the displacements. This is equivalent to considering the initial state of the environment

$$|\psi_{\mathrm{E}}(0)\rangle = \hat{D}_{\boldsymbol{\gamma}^{\mathrm{P}}} |\mathbf{0}\rangle = |\boldsymbol{\gamma}^{\mathrm{P}}\rangle \,, \tag{4.6}$$

derived in an analogous way from the thermal density operator

$$\hat{\rho}^{\mathrm{T}}_{\mathrm{E}}(0) = \frac{\exp\left\{\sum_{n=1}^{N} \hbar\omega_n \hat{a}_n^\dagger \hat{a}_n - \hbar g_n (\hat{a}_n^\dagger + \hat{a}_n)\right\}}{Z_{\mathrm{E}}}. \tag{4.7}$$

Reflected polarized initial conditions produces the desired change of sign of the values where a_z localizes. The behavior of a_x and a_z is similar as in Figure 4.2b. The dependence of this localization with respect to the parameters of the model is the same as with the normal polarized initial conditions.

There exists a dependence of the asymptotic value of a_z with respect to the particular initial conditions chosen for the environment. The average displacement of the modes is negative for polarized initial conditions and is positive for the reflected version of the displacements. In the former the dynamics tends to localize pointing to the eigenstate $|+_z\rangle$ while in the latter points to $|-_z\rangle$.

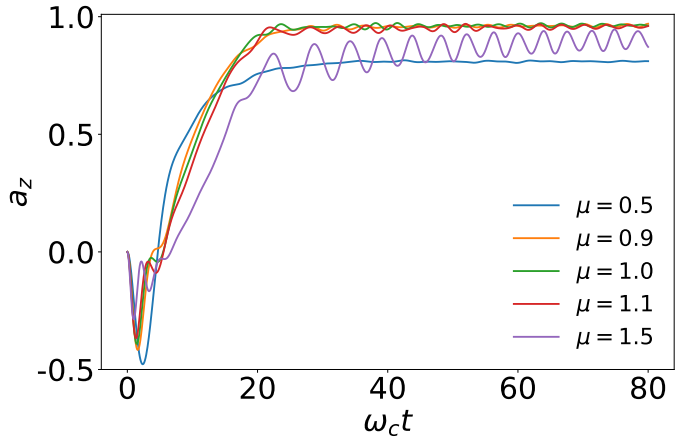

FIGURE 4.5. Dynamics of the Bloch vector component a_z with out-of-equilibrium initial conditions for different values of μ. Localization is observed for all the values shown but the closest asymptotic corresponds to $\mu = 1$. Parameters of the simulation are $\alpha = 0.3$, $s = 0.25$, $\omega_c = 2\omega_0$, $N = 150$ and $M = 10$.

4.4 Out-of-equilibrium initial conditions

Small deviations from the equilibrium state can be produced by introducing a general scaling of the coupling constants $g_n \to \mu g_n$ [98]. Depending on the value of this parameter, the relative distance between displacements can be increased or decreased. The displacements can be shifted from original ($\mu = -1$) to reversed ($\mu = 1$) initial conditions by adjusting the new parameter. This out-of-equilibrium states are defined, for zero temperature, by the displacements

$$\hat{D}_{\gamma_n^{\mathrm{p},\mu}} |0\rangle = |\gamma_n^{\mathrm{p},\mu}\rangle \,, \quad \gamma_n^{\mathrm{p},\mu} = \mu \frac{g_n}{\omega_n}. \tag{4.8}$$

Localization close to $a_z = 1$ is enhanced with increasing values of the parameter μ, for a moderate adiabatic environment ($\omega_0/\omega_c = 0.1$) and a spin prepared initially in the state $|+_z\rangle$ [98]. However, it is argued that this behavior is equivalent to including a time-dependent bias term $\hbar\varepsilon(t)\hat{\sigma}_z/2$ in the Hamiltonian of the object.

The behavior of the a_z component with an initial state of the spin $|+_x\rangle$ is depicted in Figure 4.5. Larger values of μ produce an asymptotic state closer to $a_z = 1$, but the maximum value is reached when $\mu = 1$. Beyond this value, localization is observed in lower values and its stability is compromised due to the presence of oscillations.

The dynamics of the Bloch vector with polarized initial conditions shows a transition of an initial state of the spin located at the equator to a long-term state that stabilizes pointing to the north pole of the Bloch sphere. By changing the sign of the initial displacements, localization tends toward the opposite pole. Out-of-equilibrium states, as defined above, do not produce asymptotic states closer to the poles.

Although polarized initial conditions do not fulfill the requirements for the initial state of the environment to model unbiased measurement protocols, they have been useful to identify susceptibility of the asymptotic state on the initial state of the environment. Moreover, the behavior of the dynamics of the spin with these initial conditions for different parameter values allowed to delimitate regions in the parameter space more appropriate

to reproduce the spin measurement process. An important feature to bear in mind, when considering the environment initial conditions, is that larger values of the displacements corresponding to low-frequency modes seems to favor localization close to the poles. This agrees with previous results found in the literature pointing out the importance of these modes in the long-term behavior of the spin state [79].

CHAPTER 5

Simulation of spin measurements

In the previous chapter the dynamics of the spin-boson model with particular initial conditions of the environment written as product of coherent states was obtained. From the observed dynamical behavior, a subohmic environment with moderate adiabaticity, strongly coupled with the spin, seems to be the most appropriate environment to simulate the spin measurement process. However, the initial conditions considered contain a clear bias in the sense described in chapter 3.

To meet the conditions for unbiased measurements, the displacements of the initial coherent states of each mode composing the environment should be drawn from a probability distribution in phase space. In this way, the centroids of the coherent states sample the selected probability distribution. It is of primary importance for unbiased measurements that the two-dimensional probability distribution has zero mean. A Gaussian distribution seems to be the best candidate for sampling the displacements. However, simulations done with such initial conditions have shown that it is not the case. More general distributions must be considered.

Once an appropriate distribution of the centroids is identified, the dynamics of the spin is studied for constant modulating functions as well as for more elaborated measurement protocol implemented by the time-dependent modulating functions. A finite duration of the interaction between the spin and the environment, together with a soft transition from the preparation step and the turning on of the interaction with the environment leads to simulations reproducing approximately all the phases of the spin measurement.

Different physical quantities are considered in order to characterize the process. In particular, the energy dynamics of each term in the Hamiltonian were followed during the whole process. A detailed account of the energy interchange between the spin and each mode conforming the environment highlights the prominent role of the low-frequency modes in the dynamics of the spin and its asymptotic state. Contrasts between constant and time-dependent modulating functions are pointed out.

Several runs of the simulations are gathered in histograms to show the expected measurement statistics. The results for constant modulating functions are compared with the time-dependent case. In the former, due to the variety of dynamics observed, only converged simulations are considered. In the latter, all the simulations converge, therefore, all of them were included in the statistics.

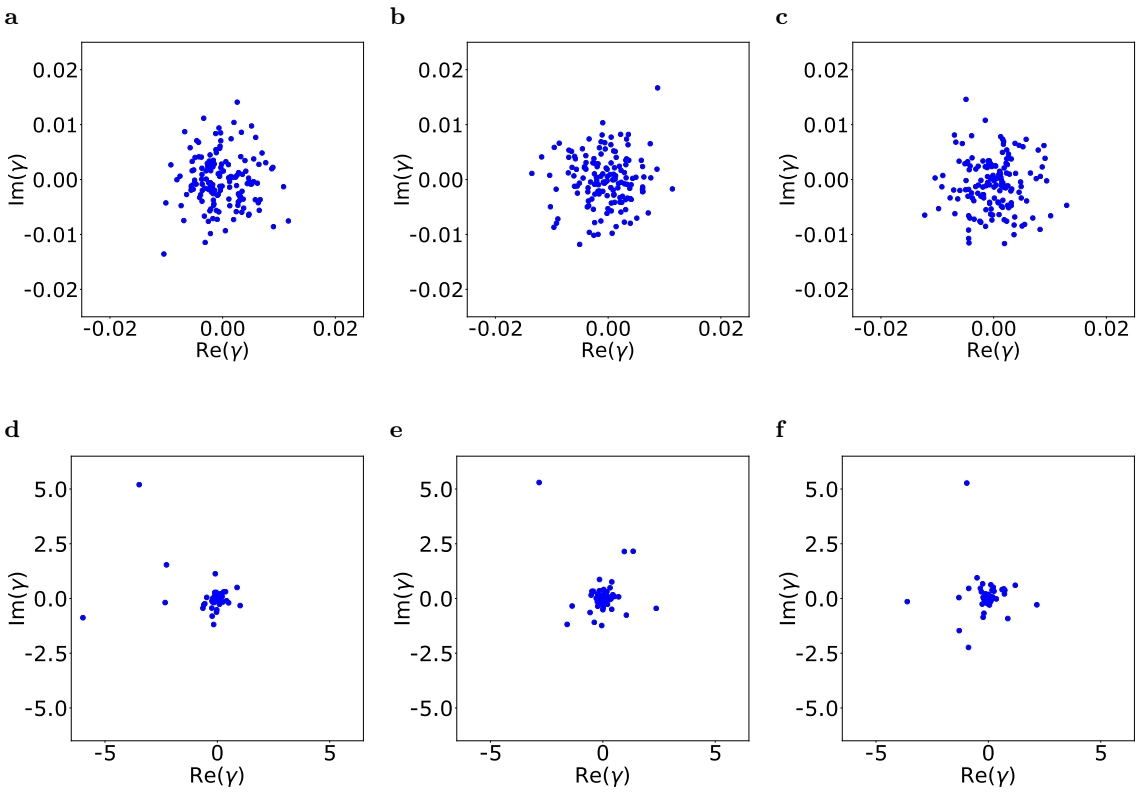

FIGURE 5.1. Examples of random ensembles of initial coherent states of the heath bath modes, distributed according to Eqs. (5.1) (panels a, b, c) and (5.5) (panels d, e, f). Blue dots mark the centroids of 150 coherent states in dimensionless phase space coordinates $\mathrm{Re}(\gamma) = \sqrt{m\omega/2\hbar}q$, $\mathrm{Im}(\gamma) = p/\sqrt{2\hbar m\omega}$. Parameter values are $k_BT = 0.2\hbar\omega_0$ and $\omega_c = 2\omega_0$.

An important feature of the measurement process is that once a measurement of an operator produces a given outcome, a successive measurement of the same operator on the output state of the first one must give the same outcome. A protocol to reproduce this feature with the model proposed is presented. Finally, the time evolution of linear superpositions of initial states of the environment leading to opposite outcomes is considered within the model.

5.1 Selecting unbiased initial states

The crucial step of selecting the initial state of the environment has not a unique answer due to the fact that any probability distribution with zero mean serve to meet this requirement. Common distributions used in quantum physics are the primary source at hand. However, at this exploratory state it is a matter of trial and error largely guided by physical intuition. A first step in this direction was the exploration of the dynamics with polarized initial conditions. Although they do not fulfill the conditions assumed for unbiased measurements, there was a reward of considering these initial conditions.

A Gaussian distribution centered at the origin of phase space is perhaps the simplest distribution fulfilling the conditions for unbiased measurements

$$p(\gamma_n, \gamma_n^*) = \frac{1}{\sqrt{2\pi}s} \exp\left(-\frac{|\gamma_n|^2}{2s^2}\right). \tag{5.1}$$

It can be interpreted as a thermal distribution of bosons if the standard deviation is written in terms of dimensionless temperature with respect to the photon energy $\hbar\omega$, $s^2 = k_{\mathrm{B}}T/2\hbar\omega$, where k_{B} is the Boltzmann constant. For a given temperature and a common frequency (for instance, the cutoff frequency), selecting the centroids of each mode amounts to sampling a Gaussian distribution in phase space.

Simulations of the spin dynamics using initial coherent states with centroids sampled from the Gaussian distribution (5.1) showed that the long-time asymptotic state of the spin is very fragile, and oscillations rapidly replace this state. Taking the results of the previous chapter as reference, a plausible explanation is that a "democratic" distribution, treating all the modes on the same footing, ignores the dominating role of the low-frequency modes in the long-term behavior of the spin. A simple experiment showed that a deliberate assignation of the farther displacements, sampled from the Gaussian distribution, to the low-frequency modes recovers a converged asymptotic state for the spin. This assignation is arbitrary and cannot be considered as an appropriate method to select the initial state of the environment.

It is necessary to consider another probability distribution such that its sampling discriminates the modes according to their frequencies. The Glauber-Sudarshan or P-function [103, 63] condenses different possibilities for such distributions. By means of this function, the density operator can be written in terms of coherent states. In general, if the density operator represents the state of an environment composed of N modes, this state can be written as

$$\hat{\rho} = \int d^2\boldsymbol{\gamma}\, P(\boldsymbol{\gamma}, \boldsymbol{\gamma}^*)\, |\boldsymbol{\gamma}\rangle\langle\boldsymbol{\gamma}|\,, \quad |\boldsymbol{\gamma}\rangle = \bigotimes_{n=1}^{N} |\gamma_n\rangle\,. \tag{5.2}$$

For one mode, the P-function of a thermal equilibrium state reads

$$P(\gamma_n, \gamma_n^*) = \frac{1}{\pi\,\langle n\rangle} \exp\left(-\frac{|\gamma|^2}{\langle n\rangle}\right). \tag{5.3}$$

This is a Gaussian distribution whose standard deviation is related with the average photon number $\langle n\rangle = 1/(e^{\hbar\omega_n/k_{\mathrm{B}}T} - 1)$. The shape of the thermal P-function depends on the temperature. In the limit $T \to 0$ it becomes sharp. Its broadening is related to the existence of thermal fluctuations. In the high-temperature limit $\langle n\rangle = 1/(e^{\hbar\omega_n/k_{\mathrm{B}}T} - 1) \to k_{\mathrm{B}}T/\hbar\omega$ and the function takes the form resembling Eq. (5.1)

$$P(\gamma_n, \gamma_n^*) = \frac{\hbar\omega}{\pi k_{\mathrm{B}}T} \exp\left(-\frac{\hbar\omega|\gamma_n|^2}{k_{\mathrm{B}}T}\right). \tag{5.4}$$

This function has been useful in the propagation of open quantum systems with environments prepared initially in thermal equilibrium states using the multi-Davydov ansatz [104]. Physical observables are obtained as the stochastic average of the dynamics obtained

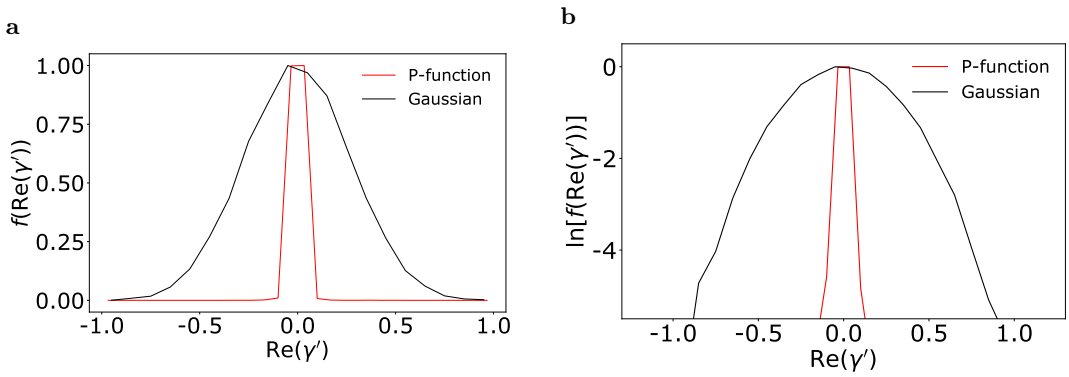

FIGURE 5.2. Continuous probability functions for $\mathrm{Re}(\gamma_n)$ obtained by binning the phase-space region where the displacements, generated using Eqs. (5.1) and (5.5), are found. Displacements and probability density function values are normalized to facilitate the comparison. The number of samples used to produce the probability density in (a) was $N = 10000$. The logarithmic scale in the vertical axis of plot (b) demonstrates the quadratic dependence of the argument of the exponential function in the Gaussian distribution and the deviation of the probability density function corresponding to the displacements of the P-function from this behavior.

with many samples of the multi-mode thermal P-function

$$P(\boldsymbol{\gamma}, \boldsymbol{\gamma}^*) = \prod_{n=1}^{N} P(\gamma_n, \gamma_n^*) = \prod_{n=1}^{N} \frac{e^{\hbar\omega_n/k_\mathrm{B}T} - 1}{\pi} \exp\Big(-(e^{\hbar\omega_n/k_\mathrm{B}T} - 1)|\gamma_n|^2\Big). \tag{5.5}$$

The P-function (5.5) belongs to the $2N$-dimensional phase-space. Sampling this function is equivalent to sample N Gaussian distributions, with different standard deviations, in the 2-dimensional phase-space. Each Gaussian can be sampled using well-known methods such as the Box-Müller method.

In Figure 5.1 examples of initial displacements of ensembles of $N = 150$ coherent states as scatter plots of their centroids in dimensionless phase space ($\mathrm{Re}\gamma_n$, $\mathrm{Im}\gamma_n$), generated according to the Gaussian distribution, Eq. (5.1) (panels (a) to (c)), and to the multi-mode thermal P-function Eq. (5.5), are compared. The Gaussian distribution produces more compact ensembles, while there exists extreme outliers in the ensembles produced by the multi-mode thermal P-function. The probability that these outliers correspond to the low-frequency modes is high because for these modes the standard deviation of the Gaussian distribution is large. Therefore, the probability of obtaining a large displacement in one sample of the Gaussian distribution corresponding to low-frequency modes is larger than for the corresponding distribution for high-frequency modes. For this reason, it is also expected that high-frequency modes concentrate around the origin. As was pointed out by the simulations with polarized initial conditions, these outliers are responsible for the increasing tendency of the spin to converge towards the eigenstates of $\hat{\sigma}_z$.

It could be confusing that such distributions of the displacements can be obtained with (5.5). After all, the product of Gaussian distributions is also a Gaussian distribution, so the final distribution of the displacements should be Gaussian. This is true if sufficient samples are obtained for each of the N Gaussian distributions. On the other hand, one

should remember that the total Gaussian distribution lives in the $2N$-dimensional phase-space and is there where all the samples converge to a Gaussian distribution. However, if only one sample is taken from each Gaussian distribution corresponding to each mode and if those N displacements are gathered in the 2-dimensional phase-space, as is shown in Fig. 5.1, they do not follow a Gaussian distribution.

The non-Gaussian distribution of the displacements can be checked by binning the region of the phase space where they are located. Counting the number of points in each bin and associating this frequency to the coordinates of the midpoint of the bin, produces a continuous density function. Figure 5.2 shows the result of this process for samples of $N = 10000$ following Eqs. (5.1) and (5.5). Only the distribution of the real part $\mathrm{Re}(\gamma_n)$ is shown, but the result is similar for the imaginary part $\mathrm{Im}(\gamma_n)$. It is clear that the displacements obtained from the P-function do not follow a Gaussian distribution. To further confirm this behavior, the logarithm of the probability density function is plotted against $\mathrm{Re}(\gamma_n)$ in Figure 5.2b. While the Gaussian distribution shows a quadratic behavior in this scaled plot, the density function associated with the displacements drawn from the P-function has a pronounced peak in the center.

Selecting the initial displacements from the P-function introduces the random character of the initial state of the environment in each sample taken from it. The overall distribution of the initial displacements tends to have zero mean. In addition, the low-frequency modes are more likely to have a larger initial displacement from the origin in phase space. Consequently, the sampling of the P-function fulfills the requirements for the selection of the initial state of the environment aimed to reproduce unbiased spin measurements.

5.2 Spin dynamics with unbiased initial states

With a proper method to obtain the initial state of the environment, all the elements of the model are ready to simulate measurements of $\hat{\sigma}_z$ under conditions where equally likely spin up or spin down outcomes are expected. It is necessary to select the parameters of the model in regions more probable to conduct the spin to asymptotic states closer to the poles of the Bloch sphere. On the other hand, the initial state of the spin should be prepared in invariant states under $P_z : z \to -z$ as in Eq. (3.20). The initial state of the environment should be prepared as random sample following Eq. (5.5). Some of the simulations shown in this section have been performed with $N = 150$ environmental modes, a number that allows an equilibrium between convergence of the results and computing time with the available resources. Complementary calculations with $N = 300$ enabled significant improvements in the simulations.

In the following, the results of simulations of the dynamics of the spin are presented for both constant and time-dependent modulating functions. In these simulations, the energy splitting of the spin is chosen to be negative $\hbar\omega_0 < 0$. With this selection, the ground state of the spin is $|+_x\rangle$, which is the initial state of the spin in the simulations.

First, the dynamics of the Bloch vector components $a_x(t)$, $a_y(t)$, $a_z(t)$ are presented for both measurement protocols. The statistics of the asymptotic states of $a_z(t)$ are then discussed. The dynamics of the energy with constant and time-dependent modulating functions is shown at the end of the section.

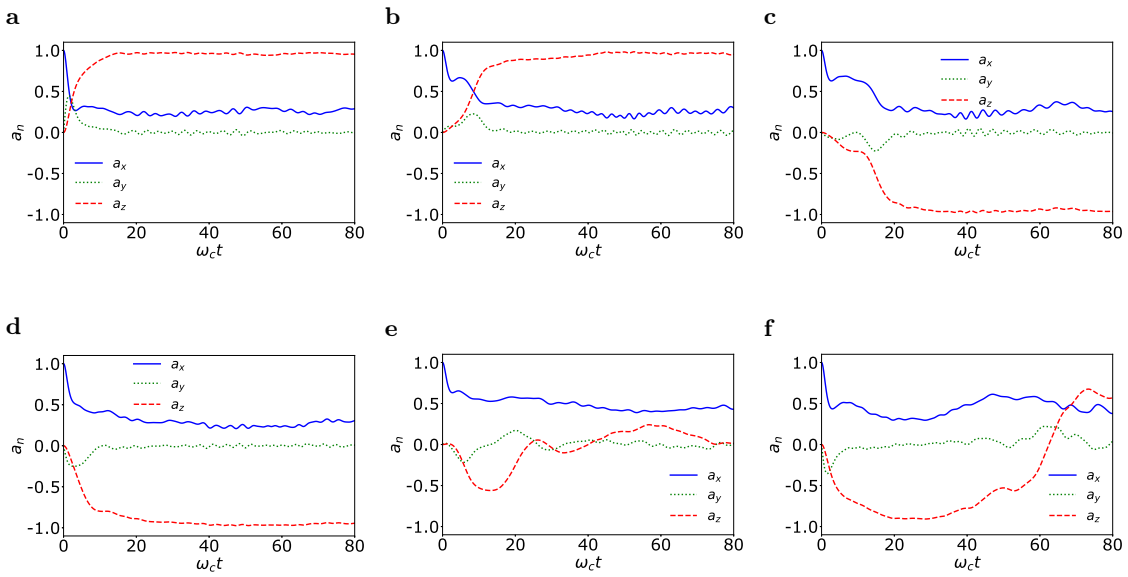

FIGURE 5.3. Simulations of measurements of the polarization of the spin, with unbiased initial state $|\psi_O(0)\rangle = |+_x\rangle$ of the spin and random initial conditions of meter and environment Eq. (5.5), modeled by the Hamiltonian (3.6) with time-independent modulations $f_O(t) = \text{const}$ and $f_{OE}(t) = \text{const}$. Panels (a) to (f) show the three components $a_x(t)$ (blue), $a_y(t)$ (green), and $a_z(t)$ (red) of the Bloch vector vs. time for different specific initial conditions of the environment. Time scaled as $\omega_c t$, with the cutoff frequency ω_c of the environment spectrum, see Eq. (2.28). Parameter values are $N = 150$, $M = 10$, $\alpha = 0.3$, $k_B T = 0.2\hbar\omega_0$, $\omega_c = 2\omega_0$.

5.2.1 Constant modulations

Several simulations were performed with constant modulating functions. The range of the parameters of the model were adjusted according to the most promising range of values obtained with polarized initial conditions. Some simulations with parameters out of this range confirm that localization of $a_z(t)$ is enhanced within this range.

Figure 5.3 shows some selected examples of the variate time evolution of the Bloch vector for constant modulating functions. In all simulations, the $a_x(t)$ component decays from its initial value $a_x = 1$ to a residual value in the interval $(0, 0.5)$. The $a_y(t)$ component deviates slightly from zero at the beginning of the time evolution, but it rapidly decays to zero and fluctuates around this value. The measured observable, $a_z(t)$, has essentially three types of behaviors: In some simulations, it increases to reach a value close to $a_z = 1$ and localizes there (panels a, b). In other simulations it decreases and reaches a value close to $a_z = -1$ (panels c, d). In many instances it continues fluctuating with slight or large amplitude around zero (panels e, f). Intermediate behavior between these categories, for instance, localization around values different from $a_z = -1$ or $a_z = 1$, are as well observed.

A complete statistic of the asymptotic values of $a_z(t)$ for $t \to \infty$ is not possible due to the different behavior exhibited by this component. Only a fraction of the total simulations has a long-time localized state. For 100 different runs, around 40% of the simulations show this behavior. The corresponding histogram is shown in Figure 5.4. A preference for the eigenvalues $a_z = -1$ and $a_z = 1$ of $\hat{\sigma}_z$ is clearly observed in this bimodal distribution. The

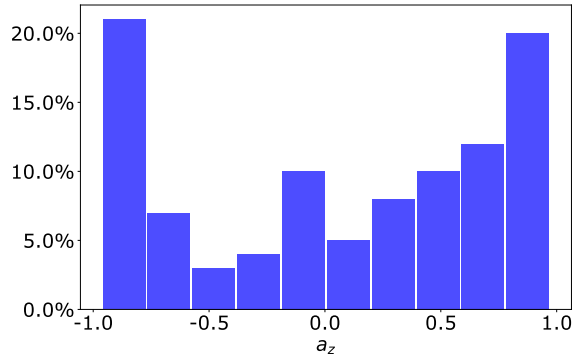

FIGURE 5.4. Distribution of long-time asymptotes $a_z(t)$ for $t \gg 2\pi/\omega_c$, counting only those 41 simulations among a sample of 100 runs that converge to a stable long-time localized states. Parameter values as in Fig. 5.3.

existence of a plateau between the two peaks reflects the fact that the component $a_z(t)$ can be localized around smaller values.

5.2.2 Time-dependent modulations

Dynamics of the Bloch vector is highly impacted by allowing the time dependence of the modulations $f_{\mathrm{O}}(t)$ and $f_{\mathrm{OE}}(t)$. The shape of these functions should be selected to capture the main futures of a typical measurement process. In particular, the finite duration in time of the interaction between object and meter, and the distinction between each phase in the measurement process (preparation and measurement) are captured by these functions. Consequently, the following protocol is assumed: The magnitude $f_{\mathrm{O}}(t)$ of the self-energy takes a positive value initially, representing the preparation of the spin in the ground state of $\hat{H}_{\mathrm{O}}$. It is then switched off, while the coupling strength rises by means of $f_{\mathrm{OE}}(t)$ from its initial value zero to a positive maximum and then decays.

Different shapes of the functions $f_{\mathrm{O}}(t)$ and $f_{\mathrm{OE}}(t)$ can be considered to apply this protocol. Several simulations obtained by changing the shape of both functions demonstrate that soft box-shaped profiles favor localization of $a_z(t)$ close to the eigenstates $a_z = \pm 1$ of $\hat{\sigma}_z$ (Fig. 5.6a). On the other hand, the relationship between the end of the preparation and the beginning of the interaction with the environment impacts this localization. A soft transition with a small overlap gives the best results in terms of localization of the component $a_z(t)$.

In stark contrast with constant modulations, all the simulations show localization of $a_z(t)$ around different values in the interval $(-1, 1)$. The time evolution of $a_x(t)$ and $a_y(t)$ allows to conclude that the Bloch vector localizes in the vertical axis, pointing to either pole of the Bloch sphere. Only a few initial conditions lead to stable values close to $a_z = 0$. There is a strong tendency of the long-time averages of the Bloch vector to converge against either one of the poles of the Bloch sphere (5.5a-e), approaching almost pure states close to of the measured operator $\hat{\sigma}_z$.

The behavior of the Bloch vector with time-dependent modulations is reflected in the statistics of the asymptotic values of $a_z(t)$. The 100% of the performed simulations were

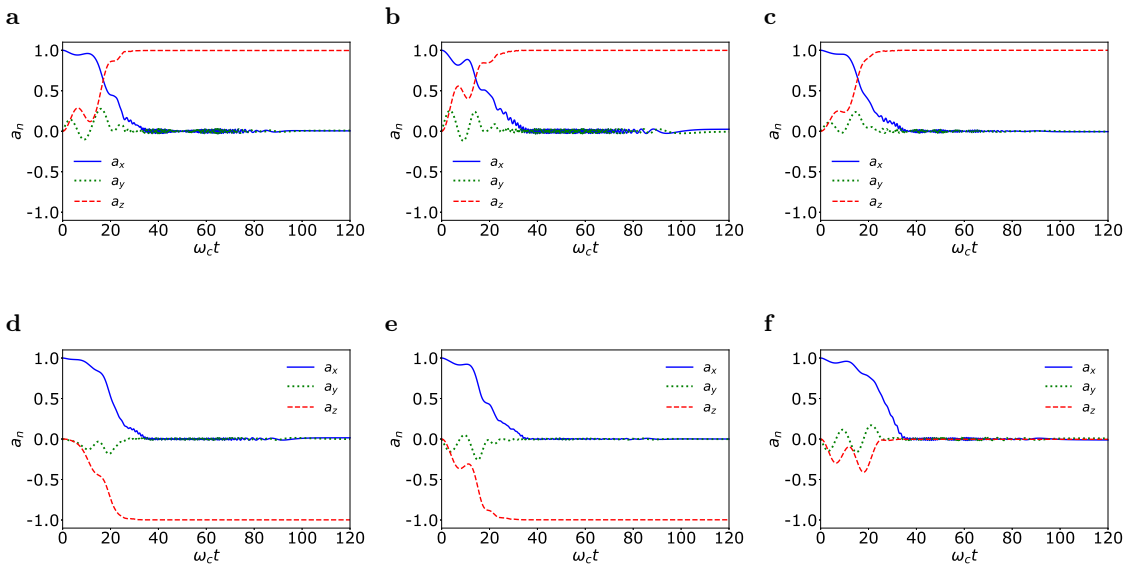

FIGURE 5.5. Simulation of measurements of the polarization of the spin, with unbiased initial state $|\psi_{\mathrm{O}}(0)\rangle = |+_x\rangle$ of the spin and random initial conditions of meter and environment, Eq. (5.5), modelled by the Hamiltonian (3.6) with time-dependent modulations $f_{\mathrm{O}}(t)$ and $f_{\mathrm{OE}}(t)$ as shown Fig. cite. Panels (a) to (f) show the three components $a_x(t)$ (blue), $a_y(t)$ (green) and $a_z(t)$ (red) of the Bloch vector vs. time for different specific initial conditions of the environment. Time is scaled as $\omega_c t$. The number of boson modes is $N = 300$, the Kondo parameter α varies with $f_{\mathrm{OE}}(t)$, reaching a maximum of $\alpha = 2$. Other parameter values are as in Fig. 5.3.

included in the histogram in Fig. 5.6b. The peaks around the values $a_z = \pm 1$ are now more pronounced and the intermediate plateau is lower than in Fig. 5.4.

5.2.3 Final state of the environment

The results of the previous sections show a tendency of the Bloch vector to localize around the eigenstates of the measured operator. For some simulations, the Bloch vector approaches the surface of the Bloch sphere, indicating an almost pure state. Considering that the total system is a bipartite system, a pure state of the object implies a pure state of the environment. This state can be a superposition state of the form

$$|\psi_{\mathrm{E,f}}\rangle = \sum_k C_k \, |\psi_{\mathrm{E},k}\rangle \tag{5.6}$$

or a definite state $|\psi_{\mathrm{E},k}\rangle$. Having these possibilities one might ask, what is the final state of the environment?

The state of the entire system at time t is written in terms of the D2-ansatz. For an asymptotic state approaching an almost pure state in the direction of either pole of the

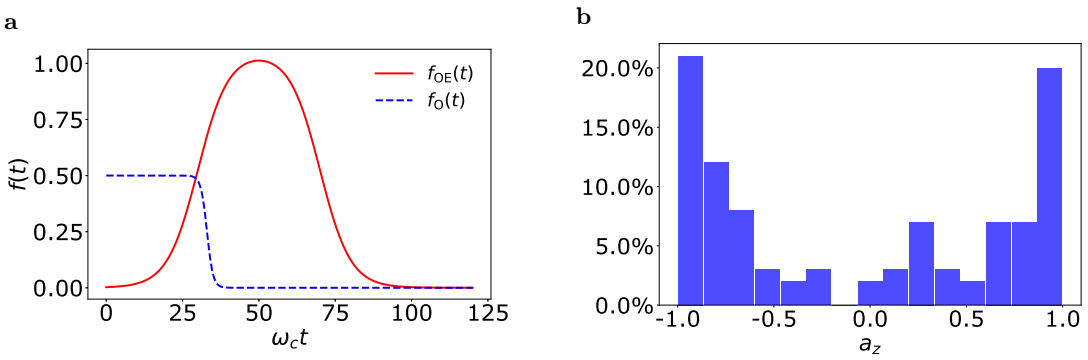

FIGURE 5.6. (**a**) Modulating functions $f_{\mathrm{O}}(t)$ (blue) and $f_{\mathrm{OE}}(t)$ (red) underlying the simulations shown in Fig. 5.5. (b) distribution of long-time asymptotes $a_z(t)$ for $t \gg 2\pi\omega_c$, based on 100 simulations. Parameters values as in Fig. 5.5.

Bloch sphere, one can write the total state as

$$|\Psi_\infty\rangle \approx |\pm_z\rangle \sum_{k=1}^{M} C_{k\pm} |\gamma_k\rangle \,. \tag{5.7}$$

Therefore, the environment will be in a definite state if only one of the coefficients is different from zero. In any other case, the environment will be in a superposition state of the corresponding multi-mode coherent states.

For constant modulations, the Bloch vector is far from the surface of the Bloch sphere, compared to the time-dependent counterpart. Therefore, it is expected contributions of the positive as well as negative coefficients in the ansatz expressing the final asymptotic state. However, the closeness of a_z to either of the eigenstates $a_z = 1$ or $a_z = -1$, implies a significant difference in the amplitudes of the coefficients C_{k-} or C_{k+} depending on which value a_z tends to (Fig. 5.7a). Ignoring the coefficients related with the opposite eigenstate, with constant modulations, the environment is left in a superposition state. This situation changes when time-dependent modulations are considered. As is shown in Fig. 5.7b, the dynamics leaves the total system in a pure state $|\Psi_\infty\rangle \approx |+_z\rangle |\gamma_k\rangle$, so the object and the environment are in definite states after the spin measurement.

5.2.4 Energy dynamics

Energy is the most important quantity to study the relaxation of an open quantum system. In this context, the interaction between object and environment in the spin measurement also involves an energy exchange between them. Due to the time dependence induced by the modulations in the Hamiltonian, the total energy of the system is not conserved. For constant modulations, conservation of the total energy can be used to assess the performance of the simulation.

Energy can be obtained for each term in the Hamiltonian of the entire system. For a Hamiltonian $\hat{H}$, energy is calculated from the D2-ansatz as

$$\langle E \rangle = \left\langle \Psi^M_{\mathrm{D2}}(t) \middle| \hat{H} \middle| \Psi^M_{\mathrm{D2}}(t) \right\rangle \tag{5.8}$$

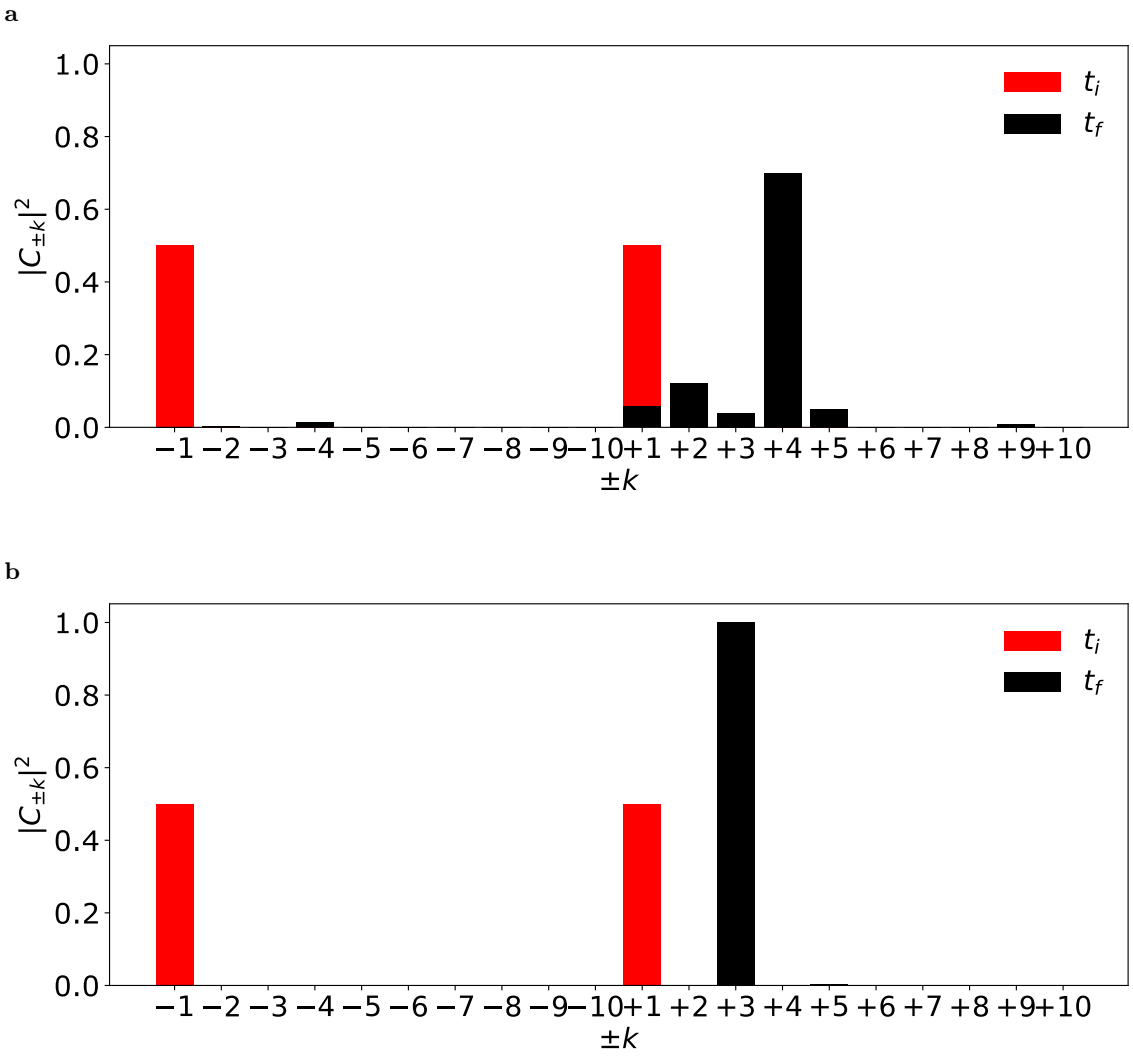

FIGURE 5.7. Amplitude $|C_{k\pm}|^2$ of the coefficients in the D2-ansatz, with multiplicity $M = 10$, for one simulation approaching the eigenstate $|+_z\rangle$, at the beginning (red) and at the end (black) of the simulation. In (a), the simulation was performed with constant modulations and in (b) with time-dependent modulations. Parameter values as in Fig. 5.3 and Fig. 5.5, respectively.

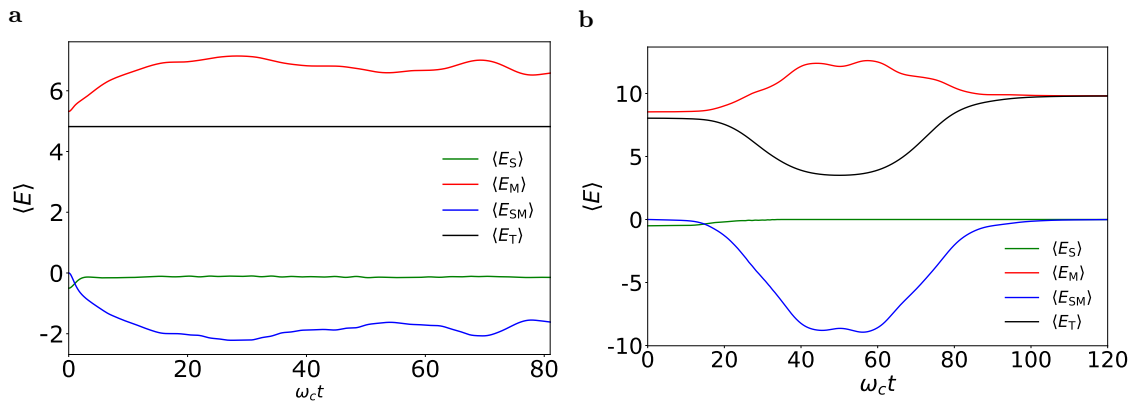

FIGURE 5.8. Energy dynamics for one simulation with (a) constant and (b) time-dependent modulations. The interaction between the object and the environment leaves a register in the energy of the environment. While stabilization of the energy of each term is observed in the case of constant modulations, the end of the interaction in the time-dependent protocol leaves the environment with a higher energy. Because of the vanishing of the energy of the spin and the interaction, total energy is equal to the energy of the environment at the end of the process. Parameter values as in Fig. 5.3 and Fig. 5.5, respectively.

Figure 5.8 shows the energy dynamics in the case of constant and time-dependent modulating functions. The behavior of the energy is similar for all the simulations performed in both cases. Conservation of energy is already verified in the former case. The energy of the spin increases rapidly as result of the interaction with the environment and stabilizes at zero. An increase of the energy of the environment is compensated for by the energy related to the coupling term. For constant modulations, they are specular images of each other.

The time dependence of the interaction leads to larger negative values for its energy, compared with the increase observed in the energy of the environment. The permanent interaction implied by constant modulations conduces to a stabilization of the energies of the environment and the interaction. In the time-dependent scenario, the energy of the environment increases to a definite value at the end of the process, when the coupling is turned off, compared to its initial value. The entire process leaves a register in the energy of the environment.

A detailed account of the energy exchange between the system and the modes composing the environment is given by the energy density of the environment

$$\rho_{\mathrm{E}}(\omega_n, t) = \rho_f(\omega_n) \left\langle \Psi^M_{\mathrm{D2}}(t) \middle| \hbar\omega_n \hat{a}^\dagger_n \hat{a}_n \middle| \Psi^M_{\mathrm{D2}}(t) \right\rangle \tag{5.9}$$

and the energy density of the coupling

$$\rho_{\mathrm{OE}}(\omega_n, t) = \rho_f(\omega_n) \left\langle \Psi^M_{\mathrm{D2}}(t) \middle| \hbar g_n \hat{\sigma}_z (\hat{a}^\dagger_n + \hat{a}_n) \middle| \Psi^M_{\mathrm{D2}}(t) \right\rangle . \tag{5.10}$$

These functions depend on the frequencies of the modes as well as the time. They can be plotted as density plots to identify the behavior of the energy depending on the frequency of the modes during the time evolution.

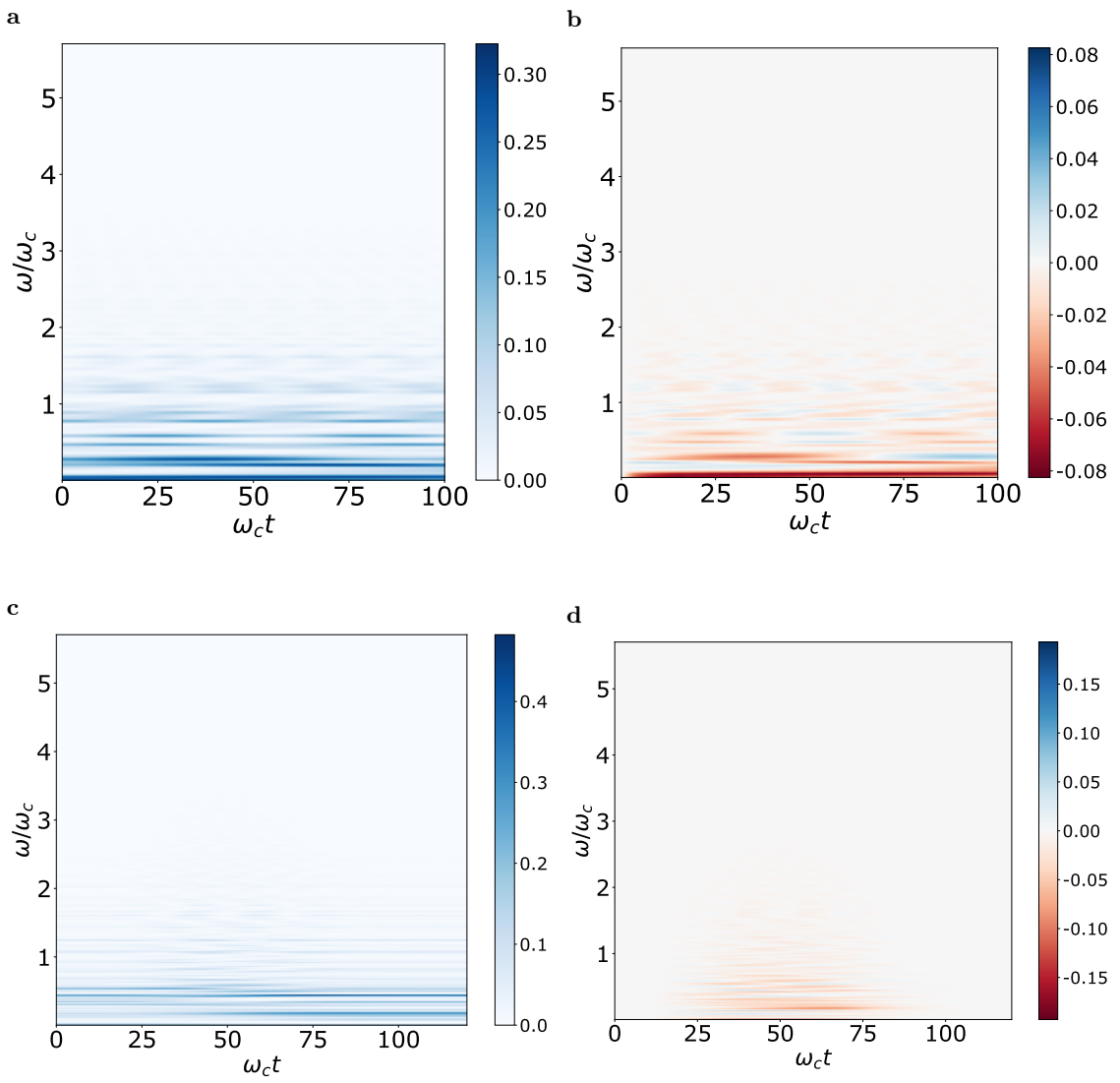

FIGURE 5.9. Energy density of the environment, Eq. (5.9), for constant (a) and time-dependent modulations (c), as function of the frequencies and time. The corresponding energy densities of the interaction, according to Eq. (5.10) are shown in panels (b) and (d), respectively. Time is scaled as $\omega_c t$ and frequencies as ω/ω_c. Color code ranges from positive (blue) to zero (white) to negative (red) values. Parameter values as in Fig. 5.3 for constant and as in Fig. 5.5 for time-dependent modulations.

The behavior of the energy density of the environment and coupling for constant modulations is shown in Figure 5.9, panels a and b. Energy is mainly distributed in the low-frequency modes of the environment. Stripes of more or less a steady value with respect to the frequency axis are observed, with slight variations in their intensity during the time evolution. This indicates that even in the low-frequency region energy is not distributed equally among the modes. In some of them, the increase of their energy values is more pronounced because of an effective coupling with the spin. This is confirmed by the energy density of the coupling, where regions with more intensity signal a higher energy

exchange with the spin. For frequencies beyond ω/ω_c the modes do not couple effectively with the spin and their dynamics is not affected by the interaction.

With time-dependent modulations (panels c and d), energy is even more concentrated in the low-frequency modes. During the time the coupling is turned on, the energy exchange with the environment involves a smaller portion of the low-frequency modes, therefore this interaction emphasizes the modes with energy values closer to the energy gap of the spin. This behavior of the energy distribution among the modes highlights the importance of the low-frequency modes in the asymptotic state of the spin.

5.3 Redundant measurements

An important characteristic of the quantum measurement process is that if the initial state of the object is already an eigenstate of the measured operator, the measurement does not change this state. In this sense, it is performed a nondemolition measurement on the initial state of the object, leading to a confirmation of the result of the measurement.

As a consistency check, redundant measurements on states eigenstates of the measured operator were performed. The simplest instance of such measurements is when the spin is prepared initially in an eigenstate of $\hat{\sigma}_z$. A measurement protocol including such preparation of the spin includes a self-energy Hamiltonian $\sim \hat{\sigma}_z$. The total Hamiltonian thus takes the form

$$\hat{H} = \frac{1}{2}\hbar\omega_0\hat{\sigma}_z f_{\mathrm{O}}(t) + \sum_{n=1}^{N}\hbar\omega_n\hat{a}_n^\dagger\hat{a}_n + \hat{\sigma}_z\sum_{n=1}^{N}\hbar g_n(\hat{a}_n^\dagger + \hat{a}_n)f_{\mathrm{OE}}(t). \tag{5.11}$$

The measured operator commutes with the Hamiltonian (5.11), therefore, this Hamiltonian preserves the eigenstates of the measured operator. Thus it is trivially guaranteed that the state will be in the same eigenstate that it had been prepared.

A more challenging scenario is when the first measurement serves as a preparation step for the second. The asymptotic state of the spin obtained in a first measurement becomes the initial state of a new measurement of the same operator. To simulate this setup with the proposed model, the following protocol is devised:

1. Prepare the spin in an unbiased initial state $|\psi_{\mathrm{O}}(0)\rangle = |+_x\rangle$ and the environment in a random initial condition, Eq. (5.5), as for a common unbiased measurement.

2. Simulate a measurement of $\hat{\sigma}_z$ according to the Hamiltonian (3.6), with time-dependent modulations $f_{\mathrm{O}}(t)$ and $f_{\mathrm{OE}}(t)$ as shown in Fig. 5.6a.

3. Assuming that after the measurement, the spin is already in a state close to $|-_z\rangle$ or $|+_z\rangle$, renormalize the Bloch vector $\mathbf{a} = (a_x, a_y, a_z)$ to $|\mathbf{a}|^2 = 1$, corresponding to a pure state.

4. Repeat the measurement of $\hat{\sigma}_z$ as above but keeping the self-energy term (3.3) switched off and initiating the environment in a new random initial condition, independent of its final state on exit of the first measurement.

Figure 5.10 shows the results of the application of the protocol for repeated measurements, where the output of the first measurement is the input of the second one.

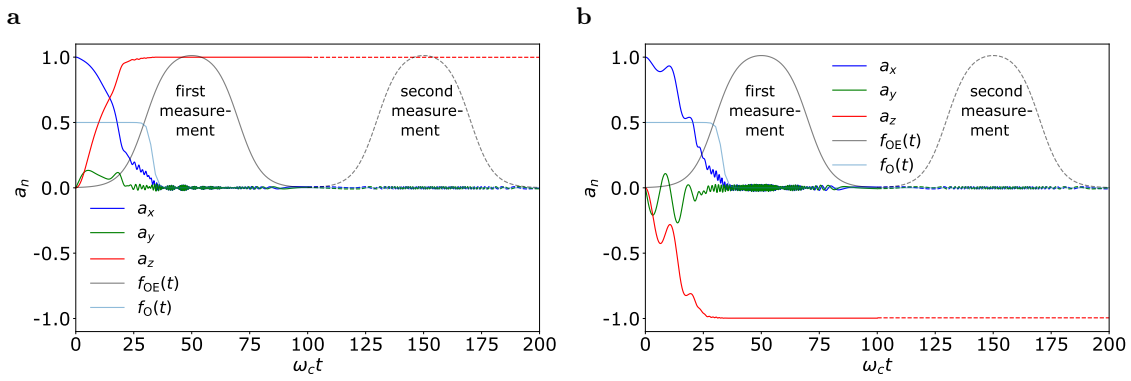

FIGURE 5.10. Simulation of two subsequent measurements of the same observable $\hat{\sigma}_z$ of the spin, with unbiased initial state $|\psi_O(0)\rangle = |+_x\rangle$ of the spin and random initial conditions of the environment, Eq. (5.5), for the first measurement. The protocol, see text, is implemented based on the Hamiltonian (3.6) with time-dependent modulations $f_O(t)$ and $f_{OE}(t)$. The state of the spin after the first measurement (full lines) is kept as entrances condition of the second measurement (dashed lines), the environment is initiated in a new random condition, see step 4 of the protocol. The figure shows the components of the Bloch vector (color code as in Fig. 5.3) vs. time for a first measurement resulting in the eigenstates $|+_z\rangle$ (panel a) and $|-_z\rangle$ (b). Light blue and grey lines indicate the modulation functions $f_O(t)$ and $f_{OE}(t)$, resp. Time is scaled as $\omega_c t$, parameter values are as in Fig. 5.5.

Simulations of the first measurement giving $|+_z\rangle$ (panel a) and $|-_z\rangle$ (panel b) were considered. In both instances, the second measurement confirms the state reached in the first measurement, independently of the new initial state of the environment when the second measurement begins.

5.4 Linear superpositions of initial states

In the last section of chapter 3 the argument considering the time evolution of superposition states of the environment leading to opposite eigenstates was discussed. The conclusion of this argument was that with such an initial condition, the final state reached by the object after the time evolution cannot be an eigenstate of the measured operator. However, one might ask about the dependence of the asymptotic state on the initial superposition state of the environment.

To evaluate this, consider two initial states of the total system such that in the long-time limit the object state converges to opposite eigenstates of the measured operator, $\hat{\sigma}_z$

$$\begin{aligned} |\Psi_{0-}\rangle &= |-_x\rangle\,|\psi_{E0-}\rangle \xrightarrow[t\to\infty]{} |-_z\rangle\,|\psi_{E\infty-}\rangle\,, \\ |\Psi_{0+}\rangle &= |-_x\rangle\,|\psi_{E0+}\rangle \xrightarrow[t\to\infty]{} |+_z\rangle\,|\psi_{E\infty+}\rangle\,. \end{aligned} \tag{5.12}$$

By including a mixing angle ϕ the superposition state between initial states of the total system can be written as

$$\begin{aligned} |\Psi_0(\phi)\rangle &= \cos(\phi)\,|\Psi_{0-}\rangle + \sin(\phi)\,|\Psi_{0-}\rangle \\ &= |-_x\rangle\,(\cos(\phi)\,|\psi_{\mathrm{E}0-}\rangle + \sin(\phi)\,|\psi_{\mathrm{E}0+}\rangle). \end{aligned} \tag{5.13}$$

where $\phi \in [0, \pi/2]$. This angle parametrizes the Hilbert space spanned by the states $|\psi_{\mathrm{E}0-}\rangle$ and $|\psi_{\mathrm{E}0+}\rangle$. The mixing angle scans continuously the range of initial conditions from $|\Psi_0(0)\rangle = |\Psi_{0-}\rangle$ through the symmetry superposition

$$|\Psi_0(\phi)\rangle = \frac{1}{\sqrt{2}}(|\Psi_{0-}\rangle + |\Psi_{0+}\rangle) \tag{5.14}$$

through $|\Psi_0(\pi/2)\rangle = |\Psi_{0+}\rangle$.

Time evolution with superposition states of the form (5.13) can be tested with the multi-Davydov ansatz method. It only requires selecting the multi-mode coherent states and the initial coefficients accordingly. Convergence of the dynamics is guaranteed if the initial multiplicity M is augmented to $2M$. However, simulations showed surprisingly that the dynamics converged with multiplicity M even with superposition states. This demonstrates the versatility of the multi-Davydov ansatz to propagate different initial states without major modifications.

The asymptotic state $a_{z\infty}$ reached by the object for six discrete values of the mixing angle ϕ (blue dots), between 0 and $\pi/2$, are shown in Figure 5.11a. For all superpositions with $\phi \neq \pi/4$ the state of the object tends to localize around values with $a_{z\infty} \neq 0$. Depending on the relative weight of the states $|\psi_{\mathrm{E}0-}\rangle$ and $|\psi_{\mathrm{E}0+}\rangle$ the Bloch vector points to the south or north pole of the Bloch sphere, respectively. The symmetric superposition (5.14) is the only instance where localization in $a_z = 0$ is observed. This behavior is expected because a definite outcome would break the symmetry of the total initial state. The distribution of the asymptotic values with respect to the mixing angle shows a nonlinear tendency, with the transition from $a_{z\infty}(0) \approx 1$ to $a_{z\infty}(\pi/2) \approx -1$ occurring predominantly around $\pi/4$. Consequently, the marginal values $a_{z\infty} \approx \pm 1$ have more weight compared to the transition region.

If an incoherent superposition of the long-time asymptotic states of the environment, with probabilities $p(|\Psi_{\infty+}\rangle) = (\cos(\phi))^2$ and $p(|\Psi_{\infty-}\rangle) = (\sin(\phi))^2$, is assumed, the expectation value of projective quantum measurements on this state results in a measured asymptotic value (red continuous curve in 5.11a)

$$\mathrm{E}[a_{z\infty}(\phi)] = (+1)(\cos(\phi))^2 + (-1)(\sin(\phi))^2 = \cos(2\phi). \tag{5.15}$$

It is the same outcome a projective measurement would predict for initial states $|\Psi_0(\phi)\rangle = (\cos(\phi)\,|+_z\rangle + \sin(\phi)\,|-_z\rangle)\,|\psi_{\mathrm{E}0}\rangle$ instead of Eq. (5.13), with unbiased random environment state $|\psi_{\mathrm{E}0}\rangle$. This fit allows to estimate the probability density distribution of $a_{z\infty}(\phi)$ as

$$p(a_{z\infty}) \sim \sqrt{1 + 1/(1 - a_{z\infty}^2)} \tag{5.16}$$

Comparing Eq. (5.16) in Fig. 5.11b with the histogram of long-time asymptotes shown in Fig. 5.6b, a remarkable agreement is found. In this sense, numerical results are consistent with the principle of linear superposition. This would suggest the uncomfortable conclusion that the nonzero probability of indefinite outcomes near $a_{z\infty} = 0$ is an unavoidable feature

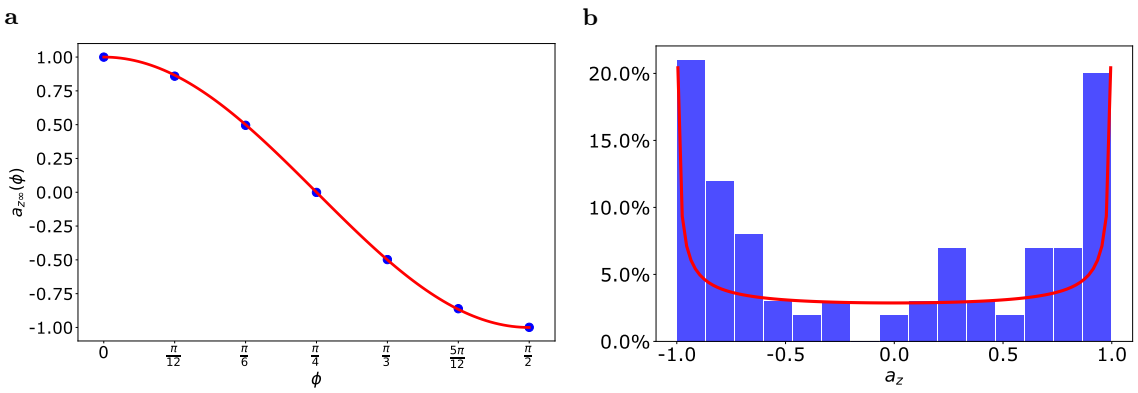

FIGURE 5.11. Simulations of measurements with the environment prepared in linear superpositions, (5.13), of pairs of initial states that converge to opposite outcomes, parameterized by a mixing angle ϕ. (a) Long-time averages $a_{z\infty}(\phi)$ of the polarization for discrete values $\phi_n = n\pi/12$, $n = 0, \ldots, 6$ (blue dots), compared to the fit (5.15) (red curve). (b) Probability density, Eq. (5.16) (red curve), corresponding to the fit (5.15), compared to the histogram (blue) of $a_{z\infty}$ show in Fig. (5.6)

for a unitary description of spin measurement including the object and a macroscopic environment.

CHAPTER 6

Information dynamics of spin measurements

The study of communication channels gave birth to the theory of information. Since then, this theory has shaped society and its development. Computer science is likely the first area to pop up when considering the information concept. The development of the computer carries the need for physical systems designed to store and process information. When quantum systems are used to achieve this task, we are talking about quantum information, an active and promising research field that is going to boost our ability to store and manipulate information in the years to come. The relationship between information and science does not rely only on the application of the latter to design better ways of processing the first. Information has been established as a fundamental concept with profound implications in physics, chemistry and biology.

The measurement process in quantum mechanics has benefited from this concept. The analysis provided from this perspective has shed light in the characteristics of the process [105]. The objective of the measurement process is to learn something about the state of the object through the interaction with the meter. Therefore, the dynamics of the information during the process is of primary importance. Studies in this direction [106, 107] explain the emergence of classical states as a consequence of information spreading to the environment. A complementary characterization of classical states is obtained by changing the focus to the environment. Different observers can obtain information independently of such states by looking at the environment due to the existence of different copies of this information [108, 109]. From this perspective, the environment is considered a communication channel between the measured system and the different observers.

Information has inspired novel interpretations of quantum mechanics with profound implications in its fundamentals. By defining as elementary systems those who can carry the minimum amount of information, 1 bit, a fundamental principle for quantum mechanics has been proposed in [52]. With this principle, the impossibility of obtaining information of noncommuting observables in spin measurements is explained as a consequence of the limitation of the spin to carry more than 1 bit of information. This appealing line of reasoning implies an intrinsic character of randomness in quantum mechanics because its fundamental principle is the assumption of a preexisting bit of information coming from nowhere.

A major step in the measurement process is the establishment of correlations between the subsystems involved. In quantum systems there exist stronger correlations in compar-

ison with classical systems. Entanglement is an example of such correlations without a classical analog, but it is not the only one. Quantum discord [110, 111] is an example of a more general quantum correlations: two quantum systems could not be entangled, yet there exist quantum correlations between them. In general, total correlations in bipartite quantum systems can be divided into classical and quantum correlations [112]. Classical correlations are also relevant in quantum processes. For instance, information gained in measurements where the meter is prepared initially in a mixed state are proportional to these correlations [113]. For initial pure states, correlations are divided equally between quantum and classical. For this reason, an entanglement measure suffices to characterize their correlations.

At the end of the measurement process the environment gains information of the spin state. In our model, the final state of the object depends on the initial state of the environment. This suggests a bilateral exchange of information between the two subsystems that can be captured by the appropriate information measures. In this chapter the dynamics of the information during the entire measurement process is analyzed in terms of purity and partial entropies.

6.1 Quantification of the knowledge about a system

Entropy is a familiar concept in thermodynamics while the term information is more common in computer science and communication, usually expressed in bits. Although having different origins, entropy and information are formally the same. They can be put in the same footing by means of the alogrithmic information content, the minimum number of bits required to efficiently store a record [114]. In this sense, we can interpret entropy and information as manifestations of the same concept.

Entropy is a measure of the uncertainty about the state of a given system before we obtain it. The more uncertainty we have the more information is required to specify the state of the system. Consequently, less likely states have a larger information content. This is so because the surprise of obtaining such state is bigger [115]. For a classical system, with N possible states $X = x_1, x_2, \ldots, x_N$ with corresponding probabilities p_i, the average entropy is given by

$$H(X) = -\sum_{i=1}^{N} p_i \log p_i \tag{6.1}$$

know as Shannon entropy. The equivalent measure for a quantum system, whose state is given by the density operator $\hat{\rho}$, is the von Neumann entropy

$$S(t) = -\operatorname{tr}[\hat{\rho}\log(\hat{\rho})]. \tag{6.2}$$

For a pure state, the von Neumann entropy is equal to zero, indicating a complete knowledge of the system. It increases when the system is in a mixed state. If the dimension of the Hilbert space of the system is N, the value of the von Neumann entropy for a completely mixed density operator is $\log N$.

Von Neumann entropy can be calculated on any density operator. For the entire system comprising the object and the environment, it is possible to obtain the entropy of each

subsystem, for instance the object, by means of the partial entropy

$$S_{\mathrm{O}}(t) = -\operatorname{tr}_{\mathrm{O}}[\hat{\rho}_{\mathrm{O}} \log(\hat{\rho}_{\mathrm{O}})]. \tag{6.3}$$

The partial entropy of the environment is obtained by an analogous expression. For a bipartite system, equation (6.3) quantifies entanglement between states of the subsystems [116]. Another useful quantity is the linear entropy

$$S_{\mathrm{O}}^{\mathrm{lin}}(t) = 1 - \operatorname{tr}_{\mathrm{O}}(\hat{\rho}_{\mathrm{O}}^2). \tag{6.4}$$

This measure shows the deviation of the object state from a pure state.

Total correlations between the object and the environment are measured by the mutual entropy

$$S_{\mathrm{O}\cap\mathrm{E}}(t) = S_{\mathrm{O}} + S_{\mathrm{E}} - S_{\mathrm{OE}}. \tag{6.5}$$

It includes classical as well as quantum correlations [113]. In our model the total state is always pure and evolves unitarily. Therefore, the entropy of the joint state is conserved, and it is equal to zero. On the other hand, in a bipartite system the Schmidt decomposition guarantees that partial entropies of object an environment are the same at any time

$$S_{\mathrm{O}}(t) = S_{\mathrm{E}}(t). \tag{6.6}$$

Consequently, correlations between subsystems are equal to

$$S_{\mathrm{O}\cap\mathrm{E}}(t) = 2S_{\mathrm{O}} = 2S_{\mathrm{E}}. \tag{6.7}$$

Taking into account the symmetric division of correlations, there is an amount of S_{O} of quantum correlations in the form of entanglement.

A relative entropy, with respect to the value corresponding to the completely mixed state, can be defined as

$$S^{\mathrm{R}}(t) = \log N - S(t). \tag{6.8}$$

When $S(t) = 0$ the relative entropy has its maximum value $\log N$ and diminishes its value as soon as $S(t)$ increases. Total knowledge of the state implies a maximum on the relative information (6.8). Therefore, it can be interpreted as a measure of the actual information of the system prior to a measurement to determine its state.

6.2 Information transfer in quantum measurement

Although the unitary time evolution ensures conservation of the total information, the interaction between the object and the environment during the measurement process implies its exchange in terms of the establishment of correlations. Following the discussion in [106], consider a spin measurement where the environment is composed by N subsystems with corresponding Hilbert spaces of dimension $\dim(\mathcal{H}_k) = n_k$, with $k = 1, \ldots, N$. Actual information of the initial product state $\hat{\rho}_{\mathrm{OE}}(0) = |\psi_{\mathrm{O}}(0)\rangle\langle\psi_{\mathrm{O}}(0)| \otimes |\psi_{\mathrm{E}}(0)\rangle\langle\psi_{\mathrm{E}}(0)|$ is given by Eq. (6.9). The actual information is totally composed of the knowledge of the individual

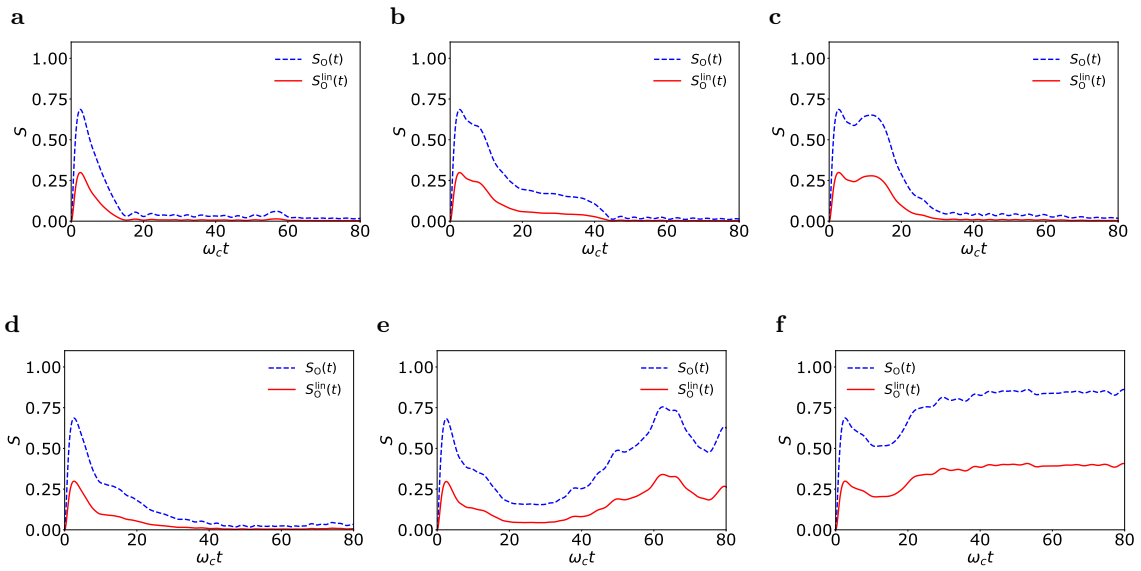

FIGURE 6.1. Time evolution of the partial (blue) and the linear entropy (red) of the spin, with unbiased initial state $|\psi_{\rm O}(0)\rangle = |+_x\rangle$ of the spin and random initial conditions of the environment, Eq. (5.5), modeled by the Hamiltonian 3.6 with time-independent modulations. Time is scaled as $\omega_c t$, parameter values as in Fig. 5.3.

states of each subsystem.

$$\begin{aligned} S^{\rm R}_{\rm OE}(0) &= \log\left(2\prod_{k=0}^{N} n_k\right) - {\rm tr}[\hat{\rho}_{\rm OE}\log(\hat{\rho}_{\rm OE})], \\ &= \log\left(2\prod_{k=0}^{N} n_k\right) = \log 2 + \log\left(\prod_{k=0}^{N} n_k\right) = S^{\rm R}_{\rm O}(0) + S^{\rm R}_{\rm E}(0). \end{aligned} \tag{6.9}$$

If the initial state of the spin has the form (1.12), interaction with the environment conduces to the state

$$|\Psi_{\rm OE}(0)\rangle = (C_+|+_z\rangle + C_-|-_z\rangle)\,|\psi_{\rm E}(0)\rangle \xrightarrow{\hat{U}_{\rm OE}} |\Psi_{\rm OE}(t')\rangle = C_+|+_z\rangle\,|\psi_{\rm E+}\rangle + C_-|-_z\rangle\,|\psi_{\rm E-}\rangle\,. \tag{6.10}$$

The state on the right-hand side of (6.10) has the same actual information as the initial state, Eq. (6.9). However, once decoherence has vanished the coherences on the reduced density operator of the object, the corresponding information for each subsystem is now

$$\begin{aligned} S^{\rm R}_{\rm O}(t') &= \log 2 - (|C_+|^2\log|C_+|^2 + |C_-|^2\log|C_-|^2), \\ S^{\rm R}_{\rm E}(t') &= \log\left(\textstyle\prod_{k=0}^{N} n_k\right) - (|C_+|^2\log|C_+|^2 + |C_-|^2\log|C_-|^2). \end{aligned} \tag{6.11}$$

Clearly, the actual information at t' is not equal to the actual information of the state of the entire system, $S^{\rm R}_{\rm O}(t') + S^{\rm R}_{\rm E}(t') < S^{\rm R}_{\rm OE}(t') = S^{\rm R}_{\rm OE}(0)$. Therefore, we can ask about the fate of the missing information $S_{\rm c} = S^{\rm R}_{\rm OE}(0) - (S^{\rm R}_{\rm O}(t') + S^{\rm R}_{\rm E}(t'))$.

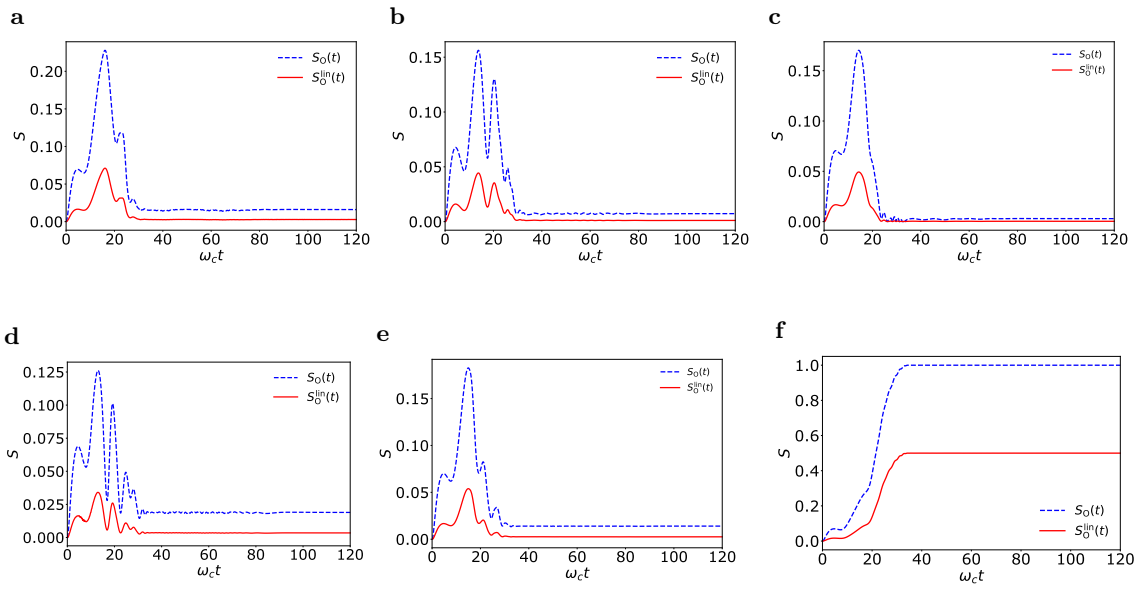

FIGURE 6.2. Time evolution of the partial (blue) and the linear entropy (red) of the spin, with unbiased initial state $|\psi_O(0)\rangle = |+_x\rangle$ of the spin and random initial conditions of the environment, Eq. (5.5), modeled by the Hamiltonian 3.6 with time-dependent modulations. Time is scaled as $\omega_c t$, parameter values as in Fig. 5.5.

The knowledge about the individual state of the object and the environment diminishes after the interaction. In particular, the information about the state of the spin is completely lost when $C_+ = C_- = 1/\sqrt{2}$. This effect is a consequence of the transfer of information into the environment degrees of freedom in terms of correlations between both subsystems. The information about the individual state is lost because it is not possible to talk about it as an individual system after the interaction. The spin is completely connected to the environment through correlations. To be precise, information is not destroyed. According to Zurek, before measurement, the complete knowledge of the initial state implies the existence of correlations between object and environment with the experimenter. These correlations are replaced by the correlations between subsystems after the interaction.

The above discussion does not include the second state vector collapse. Once the measurement projects the spin onto either of the possible eigenstates of the measured operator, its state is pure again, meaning a complete knowledge of the spin state as an individual system, is recovered again at the end of the process. Consequently, in a unitary description of the entire measurement process it is expected a continuous transition from complete knowledge of the state of the spin through a decrease during the first state vector collapse through a complete recover of the information at the end of the second vector collapse.

In Figures 6.1 and 6.2 the time evolution of the partial entropy of the object S_O (blue) and the linear entropy (red) are shown for constant and time-dependent modulations, respectively. Due to the maximum value of the partial entropy of the spin, $\log 2$, the binary logarithm $\mathrm{lb} = \log_2$ was used to generate these figures. The variety of the dynamics of both quantities with constant modulations agrees with the diverse behavior of the Bloch vector. For localized simulations, the entropy increases from zero to values around 0.6,

then it decreases to values close to zero. The initial pure state evolves to a mixed state, indicating strong entanglement with the environment and finally arrives to an almost pure state again. This behavior agrees with the expected evolution in a unitary account of the measurement process. For some simulations, the partial entropy exhibits oscillations (Fig. 6.2e) and in others it stabilizes around values different from zero (Fig. 6.2f) signaling the persistence of strong entanglement with the environment.

The behavior of the entropy is much more definite with time-dependent modulations. The gradual switching on of the coupling produces an increase of the entropy to values between 0.1 and 0.2, indicating a moderate entanglement with the environment. Then, it localizes around smaller values and settles down there while the coupling is switched off. The closer the Bloch vector gets to the poles of the Bloch sphere the smaller is residual entropy that remains after the entire interaction. In all the simulations the spin never disentangles from the environment as is pointed out by the fact that entropy does not completely vanish after decoupling the spin from the environment. For simulations evolving towards the center of the Bloch sphere, a completely mixed state of the spin, the entropy reaches its maximum value of 1 bit and remains there, reflecting an undecided result of the measurement protocol.

APPENDIX A

D2-ansatz for the spin-boson model

In this appendix the explicit evaluation of equations (2.38) is presented. A general derivation for Hamiltonians following the time-ordered convention is found in [77]. For the sake of simplicity, we show here the explicit evaluation of these equations for the spin-boson model, the central system in this work.

The dimension of the Hilbert space of the spin is $\dim(\mathcal{H}_{\mathrm{O}}) = 2$. For an environment composed by N modes and a multiplicity of the method M, the number of equations in the D2-ansatz is therefore $M(2+N)$. The explicit form of the equations of motion for the spin-boson model, considering the ansatz (2.39), reads

$$\sum_{l=1}^{M} i \left(X_{l+} + C_{l+} \sum_{n=1}^{N} \gamma_{kn}^{*} \dot{\gamma}_{ln} \right) \langle \boldsymbol{\gamma}_k | \boldsymbol{\gamma}_l \rangle = \langle \boldsymbol{\gamma}_k | \langle +_z | \hat{H} \left| \Psi_{\mathrm{D2}}^{M} \right\rangle , \tag{A.1a}$$

$$\sum_{l=1}^{M} i \left(X_{l-} + C_{l-} \sum_{n=1}^{N} \gamma_{kn}^{*} \dot{\gamma}_{ln} \right) \langle \boldsymbol{\gamma}_k | \boldsymbol{\gamma}_l \rangle = \langle \boldsymbol{\gamma}_k | \langle -_z | \hat{H} \left| \Psi_{\mathrm{D2}}^{M} \right\rangle , \tag{A.1b}$$

$$\begin{aligned} & iC_{k+}^{*} \sum_{l=1}^{M} \left[\gamma_{lr} \left(X_{l+} + C_{l+} \sum_{n=1}^{N} \gamma_{kn}^{*} \dot{\gamma}_{ln} \right) + C_{l+} \dot{\gamma}_{lr} \right] \langle \boldsymbol{\gamma}_k | \boldsymbol{\gamma}_l \rangle \\ & iC_{k-}^{*} \sum_{l=1}^{M} \left[\gamma_{lr} \left(X_{l-} + C_{l-} \sum_{n=1}^{N} \gamma_{kn}^{*} \dot{\gamma}_{ln} \right) + C_{l-} \dot{\gamma}_{lr} \right] \langle \boldsymbol{\gamma}_k | \boldsymbol{\gamma}_l \rangle \\ & = C_{k+}^{*} \langle \boldsymbol{\gamma}_k | \langle +_z | \hat{a}_r \hat{H} \left| \Psi_{\mathrm{D2}}^{M} \right\rangle + C_{k-}^{*} \langle \boldsymbol{\gamma}_k | \langle -_z | \hat{a}_r \hat{H} \left| \Psi_{\mathrm{D2}}^{M} \right\rangle , \end{aligned} \tag{A.1c}$$

where

$$X_{l\pm} = \dot{C}_{l\pm} - \frac{1}{2} C_{l\pm} \sum_{n=1}^{N} \left(\dot{\gamma}_{ln} \gamma_{ln}^{*} + \gamma_{ln} \dot{\gamma}_{ln}^{*} \right) . \tag{A.2}$$

The index $k = 1, \ldots, M$ indicates that the number of equations in (A.1a) and (A.1b) add up to $2M$. The index r runs between 1 and the number of modes N. Therefore, in (A.1c) there are NM equations. Therefore, we get the correct number of equations.

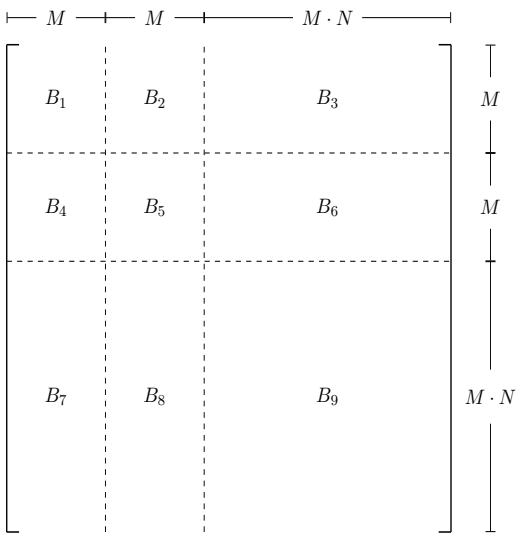

FIGURE A.1. Structure of the square matrix M in Eq. (A.3).

Notice that the left-hand side of equations (A.1) depend only on the parameters of the ansatz. The Hamiltonian enters in the right-hand side of these equations. A different model for a spin interacting with an environment of harmonic oscillators can be easily considered by modifying the Hamiltonian. For instance, slight modifications are needed in order to include the time dependence in the Hamiltonian introduced by the time-dependent modulations.

If a vector of the form $\mathbf{x}^{\mathrm{T}} = \{X_{1+}, \ldots, X_{M+}, X_{1-} \ldots X_{M-}, \dot{\gamma}_{11}, \dot{\gamma}_{12}, \ldots, \dot{\gamma}_{MN}\}$ is defined, the equations of motion can be written as

$$\mathsf{M}\mathbf{x} = \mathbf{B}, \tag{A.3}$$

where $\mathbf{B}$ contains the right-hand side of the equations and the matrix M has the structure depicted in Figure A.1.

The blocks B_2 and B_4 are full of zeros. The matrix elements of the first two diagonal $M \times M$ blocks are

$$B_1 = B_5 = i\mathsf{S} \tag{A.4}$$

with $\mathsf{S}_{lk} = \langle \boldsymbol{\gamma}_k | \boldsymbol{\gamma}_l \rangle$ gives the elements of the overlap matrix. Blocks B_3 and B_6 are $M \times MN$ matrices with matrix elements $iC_{l+}\gamma^*_{kn} \langle \boldsymbol{\gamma}_k | \boldsymbol{\gamma}_l \rangle$ and $iC_{l-}\gamma^*_{kn} \langle \boldsymbol{\gamma}_k | \boldsymbol{\gamma}_l \rangle$, respectively. The relationships $B_7 = B_3^{\mathrm{T}}$ and $B_8 = B_6^{\mathrm{T}}$ relates the elements of these blocks. Finally, the elements of the $MN \times MN$ block B_9 are

$$\begin{cases} i\gamma_{lr}\gamma^*_{kn}(C^*_{k+}C_{k+} + C^*_{k-}C_{k-}) \langle \boldsymbol{\gamma}_k | \boldsymbol{\gamma}_l \rangle & r \neq n, \\ i(\gamma_{lr}\gamma^*_{kn} + 1)(C^*_{k+}C_{k+} + C^*_{k-}C_{k-}) \langle \boldsymbol{\gamma}_k | \boldsymbol{\gamma}_l \rangle & r = n. \end{cases} \tag{A.5}$$

Any numerical ordinary differential equation solver can be used to determine the values of the parameters of the ansatz at each time step. However, due to the form of the $X_{l\pm}$ variables, Eq. (A.2), the matrix form Eq. (A.3) does not represent a system of ordinary differential equations. In order to obtain a proper system of differential equations, the system of linear equations (A.3) must be solved first. Even with a moderate number of

modes, the computational effort is considerable. In fact, this is the most time-consuming task in the propagation algorithm.

The numerical implementation of the D2-ansatz requires two main elements

- An efficient numerical solver of ordinary differential equations. It is recommended an adaptive method with an equilibrium between precision and the intermediate calculations required to achieve a time step. An increasing precision at cost of more intermediate calculations is not convenient because the system of equations A.3 must be solved in each of them. The Runge-Kutta-Fehlberg (4,5) method is a good option meeting this condition.
- A fast linear equation system solver. Methods based on the LU-decomposition are suited for this task.

Conclusions

The present thesis was designed to determine the effect of the environment in the last step of the measurement process when a definite outcome is observed: the second state vector collapse. This was achieved by proposing a model for the entire process that comprehends the preparation of the object and the meter, the establishment of correlations due to their interaction, leading to the first state vector collapse, and finally to the second state vector collapse resulting in a definite outcome of the measurement. The model exploits the benefits of the unitary time evolution of the entire system while circumventing its limitations using the finite bath approach.

Spin measurements were selected as a paradigmatic, yet simple, scenario of randomness in quantum mechanics. For initial states of the spin located on the Equator of the Bloch sphere, there are equal probabilities of obtaining either of the eigenstates of the measured operator $\hat{\sigma}_z$. Following the current description of the measurement process within the decoherence framework, a spin-boson model resulted as a plausible representation of spin measurements. Symmetry considerations allowed to define conditions on the initial states of the spin and the environment to reproduce unbiased measurements.

The optimal region in the space of parameters of the spin-boson model to mimic spin measurements was identified using polarized initial conditions. The first and second state vector collapses can be achieved using an environment in the deep subohmic regime, with moderate adiabaticity and strongly coupled to the spin. The prominent role of the initial displacements of the low-frequency modes was highlighted in simulations with these initial conditions. These results suggest that in the spin-boson model only specific environments lead to a measurement scenario, supporting the idea that only a well-designed meter can measure the desired observable. Every measurement implies an interaction with the meter but not every interaction leads to a measurement.

Initial conditions of the environment compatible with the time propagation method and the restrictions for unbiased measurements were found by sampling the P-function. The result of the measurement was interpreted as the tendency of the Bloch vector to localize towards either pole of the Bloch sphere on long time scales. Different protocols were implemented using the modulation functions of the self-energy and coupling terms. A more realistic simulation of spin measurements is accomplished when there are soft transitions between the preparation, measurement and postmeasurement phases in the protocol. The expected distribution of the measurement outcomes in only two mutually exclusive options is replaced by a continuous bimodal distribution with a shallow plateau between the predominant values around the eigenvalues of the measured operator.

Energy and entropy were used to characterize the measurement process. A register of the process is left in the environment expressed as an increase of its energy; its distribution in the low-frequency modes is evidenced by the energy and coupling density plots. This behavior asserts the crucial role played in the entire process by these modes. Entropy dynamics shows a continuous passage of the initial pure state on the equator of the Bloch sphere through the first state vector collapse, finally reaching either eigenstate of the measured operator in an approximate way in the second. The entire process produces a random number, implying an increase of the entropy that is not reflected by the von Neumann entropy.

Repeatability of quantum measurements is confirmed with the proposed model. The outcome does not change after taking the outcome of a first measurement protocol as the preparation step for a second measurement with a new random preparation for the environment. The result of a spin measurement can be verified by a second measurement of the same operator.

The unitary evolution of the entire system allows us to conclude that fluctuations present in the initial state of the environment manifest as randomness in the final state of the object. As is explained by decoherence, the initial coherent superposition, present at the beginning only in the object, spreads out to the environment due to their interaction. This leads to the observation of a loss of coherence at the level of the object; a consequence of sharing it with the environment. In the same spirit, fluctuations in the environment are evidenced in the state of the object. There is not a spontaneous breaking of the symmetry on the object state; symmetry was already broken by the initial state of the environment, and it is only transferred to the final state of the object during the time evolution.

The superposition principle is compatible with the measurement process if the possibilities of no detections and the register of intermediate outcomes, leading to a continuous distribution, are accepted. Quantization of the possible outcomes in spin measurements would be evidenced by a bimodal distribution with an intermediate plateau. Continuous distributions and predictions of phenomena not expected by the measurement postulate are also observed in detailed and closer descriptions of the Stern–Gerlach experiment including explicitly the magnet [29, 34, 36, 37, 38, 39].

Taken together, these results suggest that essential features of the measurement process, including the first and second state vector collapses, can be reproduced within unitary quantum mechanics. The entire process is then conceived as a continuous transition of the initial state until its projection onto one of the eigenstates of the measured operator.

An important limitation of the model is that it can reproduce the entire measurement process only in an approximate way. As the dynamics of the entropy confirms, a complete loss of coherence is not observed in the first state vector collapse and a complete pure state is never reached in the second. Nevertheless, the model can be refined to provide a closer approximation to this process. Decoherence models show that the irreversible loss of coherence is only effectively achieved, closely related to the infinite dimension of the environment. This suggests that a first improvement can be achieved by increasing the number of modes of the environment.

The vast number of applications of the spin-boson model offers many possibilities of plausible experimental realizations with the optimal parameters found in this model. In particular, the subohmic regime for $s < 0.5$ can be studied in Copper pair boxes [98]. The recovering of the coherence in short time scales is expected in proposed experiments

involving two weakly coupled cavities [117]. The precise monitoring and control of quantum jumps in a recent experiment [118] can provide important insights for experiments of spin measurements as depicted in this work. However, our model is far from an experimental realization because of at least two crucial reasons. In first place, implementation of time-dependent modulations in specific experimental setups can be difficult. In second place, preparation of the environment in initial states corresponding to samples of the P-function seems unfeasible.

To further characterize the simulations of spin measurements, tools borrowed by quantum Darwinism can be used. In particular, the redundancy ratio can be useful to study the information spreading on the environment. The mutual entropy between the object and each mode of the environment is needed to obtain this quantity, a challenging task for many body systems. It is possible to extract the entropy of the whole environment from the state of the entire system in the multi-Davydov ansatz, but numerical convergence of the entropy for each mode is difficult to achieve.

The effect of the environment in the localization of systems in the long term can be studied for continuous variables. The preference for either of the minima of a particle located initially at the top of the barrier of a quartic potential has been studied in [99]. The environment was modeled as a finite number of harmonic oscillators. For a small number of oscillators, the central particle tends to localize in one of the two minima depending on the initial conditions of the oscillators. The quantum analog of this system has been studied in [119]. However, the environment was prepared in the ground state leading to relaxation of the central particle to its ground state. The effect of initial random initial conditions can be explored in this system.

The proposed model is conceived to simulate the main features of a projective measurement of a physical observable with discrete spectrum. It is tempting to explore analogous models able to reproduce measurements of observables with continuous spectrum, for instance, position and momentum. The starting point could be the von Neumann measurement scheme for such observables proposed in [22]. Projective measurements are not the most general measurements in quantum mechanics. With the help of a probing system coupled to the system of interest, POVM measurements on the latter can be considered as projective measurements applied on the former [21]. This opens the possibility to conceive models for these general measurements in the same fashion as was proposed in this work.

How information and entanglement is distributed among the modes composing the environment is essential for the measurement process. This is related to how the system couples with the environment. We have modeled the environment as a set of harmonic oscillators following the Caldeira-Leggett model. It assumes a linear and weakly coupling between both subsystems. Variations of our model could consider strong interactions instead. Recent research indicates that closed but strongly interacting, possibly chaotic, quantum many-body systems do not only relax but even approach thermal equilibrium [120, 121, 122, 123]. Such strong coupling models would allow us to explore how far chaos in the degrees of freedom of the apparatus and the environment affect the exchange of information with the object during the measurement process. These effects can be observed in the quantum randomness of the measurement outcomes.

We have considered measurements applied on a single spin. Independent measurements performed on initially entangled states separated by a long distance, following the EPR experiment, is a challenging and intriguing scenario to explore with extended versions of the model. Such models would include two spins in an initial entangled state interacting

with two independent environments. The dynamics of a spin-boson model constructed in this way have been studied in [124]. A rich dynamical behavior of the correlations between the subsystems included in the model is described in detail in this study. Notably, the establishment of correlations between the environments is produced at the expense of the decreasing of the correlations present in the initial state of the spins, indicating a transfer of the correlations of the spins to the environments. The causal disconnection between measurements is perhaps the most difficult requirement of the EPR experiment to include in this model.

Bibliography

[1] W. Gerlach and O. Stern. Das magnetische moment des silberatoms. *Zeitschrift für Physik*, 9(1):353–355, 1922.

[2] W. Gerlach and O. Stern. Der experimentelle nachweis der richtungsquantelung im magnetfeld. *Zeitschrift für Physik*, 9(1):349–352, 1922.

[3] J. J. Sakurai. *Modern quantum mechanics*. Addison-Wesley, 1994.

[4] H. M. Wiseman and G. J. Milburn. *Quantum measurement and control*. Cambridge university press, 2009.

[5] W. H. Zurek. Pointer basis of quantum apparatus: Into what mixture does the wave packet collapse? *Physical review D*, 24(6):1516, 1981.

[6] W. H. Zurek. Environment-induced superselection rules. *Physical review D*, 26(8): 1862, 1982.

[7] E. Joos and H. D. Zeh. The emergence of classical properties through interaction with the environment. *Zeitschrift für Physik B Condensed Matter*, 59(2):223–243, 1985.

[8] T. Konrad. *Less is more: on the Theory and Application of Weak and Unsharp Measurements in Quantum Mechanics*. PhD thesis, Universität Konstanz, 2003.

[9] C.-M. Goletz, W. Koch, and F. Grossmann. Semiclassical dynamics of open quantum systems: Comparing the finite with the infinite perspective. *Chemical Physics*, 375 (2-3):227–233, 2010.

[10] M. Galiceanu, M. W. Beims, and W. T. Strunz. Quantum energy and coherence exchange with discrete baths. *Physica A: Statistical Mechanics and its Applications*, 415:294–306, 2014.

[11] M. A. Nielsen and I. Chuang. *Quantum computation and quantum information*. Cambridge University press, 2002.

[12] A. Peres. When is a quantum measurement? *American Journal of Physics*, 54(8): 688–692, 1986. ISSN 0002-9505. doi: 10.1119/1.14505.

[13] A. Peres. Quantum Measurements Are Reversible. *American Journal of Physics*, 42 (10):886–891, 1974. ISSN 0002-9505. doi: 10.1119/1.1987884.

[14] N. G. Van Kampen. Ten theorems about quantum mechanical measurements. *Physica A: Statistical Mechanics and its Applications*, 153(1):97–113, 1988. ISSN 03784371. doi: 10.1016/0378-4371(88)90105-7.

[15] J. Von Neumann. *Mathematical foundations of quantum mechanics*. Princeton university press, 1955.

[16] M. Schlosshauer. Decoherence, the measurement problem, and interpretations of quantum mechanics. *Reviews of Modern Physics*, 76(4):1267–1305, 2004. ISSN 00346861. doi: 10.1103/RevModPhys.76.1267.

[17] W. H. Zurek. Decoherence, einselection, and the quantum origins of the classical. *Reviews of Modern Physics*, 75(3):715–775, 2003. ISSN 00346861. doi: 10.1103/RevModPhys.75.715.

[18] M. Schlosshauer. *Decoherence: and the quantum-to-classical transition*. Springer Science & Business Media, 2007.

[19] W. G. Unruh. Analysis of quantum-nondemolition measurement. *Physical Review D*, 18(6):1764–1772, 1978. ISSN 05562821. doi: 10.1103/PhysRevD.18.1764.

[20] S. Weigert. Chaos and quantum-nondemolition measurements. *Physical Review A*, 43(12):6597, 1991.

[21] A. De Pasquale, C. Foti, A. Cuccoli, V. Giovannetti, and P. Verrucchi. Dynamical model for positive-operator-valued measures. *Physical Review A*, 100(1):1–9, 2019. ISSN 24699934. doi: 10.1103/PhysRevA.100.012130.

[22] M. Ozawa. Quantum measuring processes of continuous observables. *Journal of Mathematical Physics*, 25(1):79–87, 1984. ISSN 00222488. doi: 10.1063/1.526000.

[23] O. Pessoa. Can the decoherence approach help to solve the measurement problem? *Synthese*, 113(3):323–346, 1997.

[24] W. H. Zurek. Reduction of the wavepacket: How long does it take? In *Frontiers of Nonequilibrium Statistical Physics*, pages 145–149. Springer, 1986.

[25] R. Horodecki, P. Horodecki, M. Horodecki, and K. Horodecki. Quantum entanglement. *Reviews of modern physics*, 81(2):865, 2009.

[26] A. Einstein, B. Podolsky, and N. Rosen. Can quantum-mechanical description of physical reality be considered complete? *Physical review*, 47(10):777, 1935.

[27] M. D. Reid, P. D. Drummond, W. P. Bowen, E. G. Cavalcanti, P. K. Lam, H. A. Bachor, U. L. Andersen, and G. Leuchs. Colloquium: the Einstein-Podolsky-Rosen paradox: from concepts to applications. *Reviews of Modern Physics*, 81(4):1727, 2009.

[28] N. Brunner, D. Cavalcanti, S. Pironio, V. Scarani, and S. Wehner. Bell nonlocality. *Reviews of Modern Physics*, 86(2):419, 2014.

[29] E. Benítez Rodríguez, E. Piceno Martínez, and L. M. Arévalo Aguilar. A full quantum analysis of the Stern–Gerlach experiment using the evolution operator method: Analyzing current issues in teaching quantum mechanics. *European Journal of Physics*, 38(2):025403, 2017.

[30] A. P. French and E. F. Taylor. *An introduction to quantum physics*. W. W. Norton & Company, 1978.

[31] H. Schmidt-Böcking, L. Schmidt, H. J. Lüdde, W. Trageser, A. Templeton, and T. Sauer. The Stern–Gerlach experiment revisited. *The European Physical Journal H*, 41(4):327–364, 2016.

[32] A. A. Clerk, M. H. Devoret, S. M. Girvin, F. Marquardt, and R. J. Schoelkopf. Introduction to quantum noise, measurement, and amplification. *Reviews of Modern Physics*, 82(2):1155, 2010.

[33] D. E. Platt. A modern analysis of the Stern–Gerlach experiment. *American Journal of Physics*, 60(4):306–308, 1992.

[34] S. Cruz-Barrios and J. Gómez-Camacho. Semiclassical description of Stern–Gerlach experiments. *Physical Review A*, 63(1):012101, 2000.

[35] S. R. Gautam, T. N. Sherry, and E. C. G. Sudarshan. Interaction between classical and quantum systems: A new approach to quantum measurement. iii. illustration. *Physical Review D*, 20(12):3081, 1979.

[36] G. Potel, F. Barranco, S. Cruz-Barrios, and J. Gómez-Camacho. Quantum mechanical description of Stern–Gerlach experiments. *Physical Review A*, 71(5):052106, 2005.

[37] H. Wennerström and P. O. Westlund. A quantum description of the Stern–Gerlach experiment. *Entropy*, 19(5):186, 2017.

[38] A. Venugopalan, D. Kumar, and R. Ghosh. Environment–induced decoherence i. the Stern–Gerlach measurement. *Physica A: Statistical Mechanics and its Applications*, 220(3-4):563–575, 1995.

[39] A. Venugopalan. Decoherence and Schrödinger–cat states in a Stern–Gerlach–type experiment. *Physical Review A*, 56(5):4307, 1997.

[40] P. Gomis and A. Pérez. Decoherence effects in the Stern–Gerlach experiment using matrix Wigner functions. *Physical Review A*, 94(1):012103, 2016.

[41] B. G. Englert, J. Schwinger, and M. O. Scully. Is spin coherence like Humpty-Dumpty? i. simplified treatment. *Foundations of physics*, 18(10):1045–1056, 1988.

[42] E. Benítez Rodríguez, E. Piceno Martínez, and L. M. Arévalo Aguilar. Single-particle steering and nonlocality: The consecutive Stern-Gerlach experiments. *Physical Review A*, 103(4):042217, 2021.

[43] A. Y. Khrennikov. *Probability and randomness: quantum versus classical*. World Scientific, 2016.

[44] T. Jennewein, U. Achleitner, G. Weihs, H. Weinfurter, and A. Zeilinger. A fast and compact quantum random number generator. *Review of Scientific Instruments*, 71 (4):1675–1680, 2000.

[45] P. Diaconis, S. Holmes, and R. Montgomery. Dynamical bias in the coin toss. *SIAM review*, 49(2):211–235, 2007.

[46] A. Nitzan. *Chemical dynamics in condensed phases: relaxation, transfer and reactions in condensed molecular systems*. Oxford university press, 2006.

[47] M. N. Bera, A. Acín, M. Kuś, M. W. Mitchell, and M. Lewenstein. Randomness in quantum mechanics: philosophy, physics and technology. *Reports on Progress in Physics*, 80(12):124001, 2017.

[48] P. Bierhorst, E. Knill, S. Glancy, Y. Zhang, A. Mink, S. Jordan, A. Rommal, Y. K. Liu, B. Christensen, S. W. Nam, et al. Experimentally generated randomness certified by the impossibility of superluminal signals. *Nature*, 556(7700):223–226, 2018.

[49] M. Jofre, M. Curty, F. Steinlechner, G. Anzolin, J. P. Torres, M. W. Mitchell, and V. Pruneri. True random numbers from amplified quantum vacuum. *Optics express*, 19(21):20665–20672, 2011.

[50] P. Grangier and A. Auffeves. What is quantum in quantum randomness? *Philosophical Transactions of the Royal Society A: Mathematical, Physical and Engineering Sciences*, 376(2123):20170322, 2018.

[51] I. V. Volovich. Randomness in classical mechanics and quantum mechanics. *Foundations of Physics*, 41(3):516–528, 2011.

[52] A. Zeilinger. A foundational principle for quantum mechanics. *Foundations of Physics*, 29(4):631–643, 1999.

[53] U. Weiss. *Quantum dissipative systems*. World Scientific, 2012.

[54] R. P. Feynman and F. L. Vernon. The theory of a general quantum system interacting with a linear dissipative system. *Annals of Physics*, 24(C):118–173, 1963. ISSN 1096035X. doi: 10.1016/0003-4916(63)90068-X.

[55] H. -P. Breuer, F. Petruccione, et al. *The theory of open quantum systems*. Oxford University Press on Demand, 2002.

[56] R. Hartmann and W. T. Strunz. Accuracy assessment of perturbative master equations: Embracing nonpositivity. *Physical Review A*, 101(1):012103, 2020.

[57] E. J. Heller. Frozen Gaussians: A very simple semiclassical approximation. *The Journal of Chemical Physics*, 75(6):2923–2931, 1981.

[58] M. F. Herman and E. Kluk. A semiclasical justification for the use of non-spreading wavepackets in dynamics calculations. *Chemical Physics*, 91(1):27–34, 1984.

[59] H. Wang and M. Thoss. Multilayer formulation of the multiconfiguration time-dependent Hartree theory. *The Journal of chemical physics*, 119(3):1289–1299, 2003.

[60] D. V. Shalashilin and I. Burghardt. Gaussian-based techniques for quantum propagation from the time-dependent variational principle: Formulation in terms of trajectories of coupled classical and quantum variables. *The Journal of chemical physics*, 129(8):084104, 2008.

[61] M. Werther, S. L. Choudhury, and F. Grossmann. Coherent state based solutions of the time-dependent Schrödinger equation: hierarchy of approximations to the variational principle. *International Reviews in Physical Chemistry*, 40(1):81–125, 2021.

[62] V. Bargmann, P. Butera, L. Girardello, and J. R. Klauder. On the completeness of the coherent states. *Reports on Mathematical Physics*, 2(4):221–228, 1971.

[63] W. P. Schleich. *Quantum optics in phase space*. John Wiley & Sons, 2011.

[64] A. O. Caldeira and A. J. Leggett. Quantum tunnelling in a dissipative system. *Annals of physics*, 149(2):374–456, 1983.

[65] H. Wang and M. Thoss. From coherent motion to localization: Ii. dynamics of the spin-boson model with sub-Ohmic spectral density at zero temperature. *Chemical Physics*, 370(1-3):78–86, 2010.

[66] S. T. Smith and R. Onofrio. Thermalization in open classical systems with finite heat baths. *The European Physical Journal B*, 61(3):271–275, 2008.

[67] Jane Rosa and Marcus W Beims. Dissipation and transport dynamics in a ratchet coupled to a discrete bath. *Physical Review E*, 78(3):031126, 2008.

[68] F. Q. Potiguar and U. M. S. Costa. Numerical calculation of the energy-relative fluctuation for a system in contact with a finite heat bath. *Physica A: Statistical Mechanics and its Applications*, 342(1-2):145–150, 2004.

[69] H. Hasegawa. Classical small systems coupled to finite baths. *Physical Review E*, 83 (2):021104, 2011.

[70] C. Manchein, J. Rosa, and M. W. Beims. Chaotic motion at the emergence of the time averaged energy decay. *Physica D: Nonlinear Phenomena*, 238(16):1688–1694, 2009.

[71] M. A. Marchiori and M. A. M. de Aguiar. Energy dissipation via coupling with a finite chaotic environment. *Physical Review E*, 83(6):061112, 2011.

[72] A. S. Davydov. The theory of contraction of proteins under their excitation. *Journal of Theoretical Biology*, 38(3):559–569, 1973.

[73] A. S. Davydov and N. I. Kislukha. Solitary excitons in one-dimensional molecular chains. *physica status solidi (b)*, 59(2):465–470, 1973.

[74] A. S. Davydov et al. *Solitons in molecular systems*. Springer, 1985.

[75] M. Werther and F. Grossmann. The Davydov d1. 5 ansatz for the quantum Rabi model. *Physica Scripta*, 93(7):074001, 2018.

[76] J. Frenkel. *Wave mechanics: advanced general theory*, volume 1. Oxford University Press, 1934.

[77] M. Werther. *The multi Davydov-ansatz: Apoptosis of moving Gaussian functions with applications to open quantum system dynamics*. PhD thesis, Technische Universität Dresden, April 2020.

[78] T. Dittrich and R. Graham. Continuous quantum measurements and chaos. *Physical Review A*, 42(8):4647, 1990.

[79] A. J. Leggett, S. Chakravarty, A. T. Dorsey, M. P. A. Fisher, A. Garg, and W. Zwerger. Dynamics of the dissipative two-state system. *Reviews of Modern Physics*, 59 (1):1, 1987.

[80] R. A. Marcus and N. Sutin. Electron transfers in chemistry and biology. *Biochimica et Biophysica Acta (BBA)-Reviews on Bioenergetics*, 811(3):265–322, 1985.

[81] C. Gerry, P. Knight, and P. L. Knight. *Introductory quantum optics*. Cambridge university press, 2005.

[82] H. Wang. Basis set approach to the quantum dissipative dynamics: Application of the multiconfiguration time-dependent Hartree method to the spin-boson problem. *The Journal of Chemical Physics*, 113(22):9948–9956, 2000.

[83] A. Ishizaki, T. R. Calhoun, G. S. Schlau-Cohen, and G. R. Fleming. Quantum coherence and its interplay with protein environments in photosynthetic electronic energy transfer. *Physical Chemistry Chemical Physics*, 12(27):7319–7337, 2010.

[84] B. W. Shore and P. L. Knight. The Jaynes-Cummings model. *Journal of Modern Optics*, 40(7):1195–1238, 1993.

[85] J. Larson. Dynamics of the Jaynes–Cummings and Rabi models: old wine in new bottles. *Physica Scripta*, 76(2):146, 2007.

[86] D. Braak. Integrability of the Rabi model. *Physical Review Letters*, 107(10):100401, 2011.

[87] E. K. Irish. Generalized rotating-wave approximation for arbitrarily large coupling. *Physical review letters*, 99(17):173601, 2007.

[88] E. K. Irish, J. Gea-Banacloche, I. Martin, and K. C. Schwab. Dynamics of a two-level system strongly coupled to a high-frequency quantum oscillator. *Physical Review B*, 72(19):195410, 2005.

[89] T. Werlang, A. V. Dodonov, E. I. Duzzioni, and C. J. Villas-Bôas. Rabi model beyond the rotating-wave approximation: Generation of photons from vacuum through decoherence. *Physical Review A*, 78(5):053805, 2008.

[90] G. A. Finney and J. Gea-Banacloche. Quantum suppression of chaos in the spin-boson model. *Physical Review E*, 54(2):1449, 1996.

[91] J. Gea-Banacloche. Atom-and field-state evolution in the Jaynes-Cummings model for large initial fields. *Physical Review A*, 44(9):5913, 1991.

[92] L. E. Ballentine. States of a dynamically driven spin. i. quantum-mechanical model. *Physical Review A*, 44(7):4126, 1991.

[93] L. E. Ballentine. States of a dynamically driven spin. ii. classical model and the quantum-to-classical limit. *Physical Review A*, 44(7):4133, 1991.

[94] B. Gardas. Exact solution of the Schrödinger equation with the spin-boson Hamiltonian. *Journal of Physics A: Mathematical and Theoretical*, 44(19):195301, 2011.

[95] M. Thoss, H. Wang, and W. H. Miller. Self-consistent hybrid approach for complex systems: Application to the spin-boson model with Debye spectral density. *The Journal of Chemical Physics*, 115(7):2991–3005, 2001.

[96] H. Wang and M. Thoss. From coherent motion to localization: dynamics of the spin-boson model at zero temperature. *New Journal of Physics*, 10(11):115005, 2008.

[97] R. Bulla, N. H. Tong, and M. Vojta. Numerical renormalization group for bosonic systems and application to the sub-ohmic spin-boson model. *Physical review letters*, 91(17):170601, 2003.

[98] D. Kast and J. Ankerhold. Persistence of coherent quantum dynamics at strong dissipation. *Physical review letters*, 110(1):010402, 2013.

[99] T. Dittrich and S. Peña-Martínez. Toppling pencils — macroscopic randomness from microscopic fluctuations. *Entropy*, 22(9):1046, 2020.

[100] R. Hartmann, M. Werther, F. Grossmann, and W. T. Strunz. Exact open quantum system dynamics: Optimal frequency vs time representation of bath correlations. *The Journal of Chemical Physics*, 150(23):234105, 2019.

[101] T. Dittrich. Quantum chaos and quantum randomness: Paradigms of entropy production on the smallest scales. *Entropy*, 21(3):286, 2019.

[102] O. C. Stoica. Quantum measurement and initial conditions. *International Journal of Theoretical Physics*, 55(3):1897–1911, 2016.

[103] C. Gardiner and P. Zoller. *Quantum noise: a handbook of Markovian and non-Markovian quantum stochastic methods with applications to quantum optics*. Springer, 1999.

[104] L. Wang, Y. Fujihashi, L. Chen, and Y. Zhao. Finite-temperature time-dependent variation with multiple davydov states. *The Journal of chemical physics*, 146(12): 124127, 2017.

[105] G. Lindblad. Entropy, information and quantum measurements. *Communications in Mathematical Physics*, 33(4):305–322, 1973.

[106] W. H. Zurek. Information transfer in quantum measurements: Irreversibility and amplification. In *Quantum Optics, Experimental Gravity, and Measurement Theory*, pages 87–116. Springer, 1983.

[107] W. H. Zurek. Einselection and decoherence from an information theory perspective. In *Quantum Communication, Computing, and Measurement 3*, pages 115–125. Springer, 2002.

[108] R. Blume-Kohout and W. H. Zurek. A simple example of "quantum darwinism": Redundant information storage in many-spin environments. *Foundations of Physics*, 35(11):1857–1876, 2005.

[109] R. Blume-Kohout and W. H. Zurek. Quantum darwinism: Entanglement, branches, and the emergent classicality of redundantly stored quantum information. *Physical review A*, 73(6):062310, 2006.

[110] H. Ollivier and W. H. Zurek. Quantum discord: a measure of the quantumness of correlations. *Physical review letters*, 88(1):017901, 2001.

[111] V. Vedral. Foundations of quantum discord. In *Lectures on General Quantum Correlations and their Applications*, pages 3–7. Springer, 2017.

[112] L. Henderson and V. Vedral. Classical, quantum and total correlations. *Journal of physics A: mathematical and general*, 34(35):6899, 2001.

[113] V. Vedral. Classical correlations and entanglement in quantum measurements. *Physical review letters*, 90(5):050401, 2003.

[114] J. Machta. Entropy, information, and computation. *American Journal of Physics*, 67(12):1074–1077, 1999.

[115] V. Vedral. The role of relative entropy in quantum information theory. *Reviews of Modern Physics*, 74(1):197, 2002.

[116] V. Vedral, M. B. Plenio, M. A. Rippin, and P. L. Knight. Quantifying entanglement. *Physical Review Letters*, 78(12):2275, 1997.

[117] J. M. Raimond, M. Brune, and S. Haroche. Reversible decoherence of a mesoscopic superposition of field states. *Physical review letters*, 79(11):1964, 1997.

[118] Z. K. Minev, S. O. Mundhada, S. Shankar, P. Reinhold, R. Gutiérrez-Jáuregui, R. J. Schoelkopf, M. Mirrahimi, H. J. Carmichael, and M. H. Devoret. To catch and reverse a quantum jump mid-flight. *Nature*, 570(7760):200–204, 2019.

[119] S. L. Choudhury and F. Grossmann. Quantum approach to the thermalization of the toppling pencil interacting with a finite bath. *Physical Review A*, 105(2):022201, 2022.

[120] J. Maldacena, S. H. Shenker, and D. Stanford. A bound on chaos. *Journal of High Energy Physics*, 2016(8):1–17, 2016.

[121] D. J. Luitz and Y. B. Lev. Information propagation in isolated quantum systems. *Physical Review B*, 96(2):020406, 2017.

[122] J. Rammensee, J. D. Urbina, and K. Richter. Many-body quantum interference and the saturation of out-of-time-order correlators. *Physical Review Letters*, 121(12): 124101, 2018.

[123] B. Swingle. Unscrambling the physics of out-of-time-order correlators. *Nature Physics*, 14(10):988–990, 2018.

[124] R. C. Ge, M. Gong, C. F. Li, J. S. Xu, and G. C. Guo. Quantum correlation and classical correlation dynamics in the spin-boson model. *Physical Review A*, 81(6): 064103, 2010.

[125] H. Ollivier, D. Poulin, and W. H. Zurek. Environment as a witness: Selective proliferation of information and emergence of objectivity in a quantum universe. *Physical Review A - Atomic, Molecular, and Optical Physics*, 72(4):1–19, 2005. ISSN 10502947. doi: 10.1103/PhysRevA.72.042113.

[126] F. Haake and D. F. Walls. Overdamped and amplifying meters in the quantum theory of measurement. *Physical Review A*, 36(2):730–739, 1987. ISSN 10502947. doi: 10.1103/PhysRevA.36.730.

[127] R. B. Griffiths. What quantum measurements measure. *Physical Review A*, 96(3): 1–20, 2017. ISSN 24699934. doi: 10.1103/PhysRevA.96.032110.

[128] M. Hannout, S. Hoyt, A. Kryowonos, and A. Widom. Quantum measurement theory and the Stern–Gerlach experiment. *American Journal of Physics*, 66(5):377–379, 1998.

[129] M. Werther and F. Grossmann. Apoptosis of moving nonorthogonal basis functions in many-particle quantum dynamics. *Physical Review B*, 101(17):174315, 2020.

[130] C. Duan, Z. Tang, J. Cao, and J. Wu. Zero-temperature localization in a sub-ohmic spin-boson model investigated by an extended hierarchy equation of motion. *Physical Review B*, 95(21):214308, 2017.

[131] Y. Aharonov, D. Z. Albert, and L. Vaidman. How the result of a measurement of a component of the spin of a spin-1/2 particle can turn out to be 100. *Physical review letters*, 60(14):1351, 1988.

[132] C. E. Shannon. A mathematical theory of communication. *The Bell system technical journal*, 27(3):379–423, 1948.

[133] J. Maziero, L. C. Celeri, R. M. Serra, and V. Vedral. Classical and quantum correlations under decoherence. *Physical Review A*, 80(4):044102, 2009.